THE UNIVERSITY OF
WESTERN AUSTRALIA

The Role of Green Surfactants in Microbial Enhanced Oil Recovery

Md. Bashirul Haq

B.Sc. Chemical Engineering; M.Sc. Petroleum Engineering

This thesis is presented for the degree of Doctor of Philosophy

of The University of Western Australia

School of Mechanical and Chemical Engineering

2012

Dedication

This thesis is dedicated to the most important people in my life: my mother Mrs Shahida Begum, father Md. Borhanul Haq and grandfather Abu Taher Joardder.

Acknowledgements

I would like to express my deep respect to coordinating supervisor Prof Jishan Liu, School of Mechanical and Chemical Engineering, UWA, for his careful supervision, constant guidance, constructive comments and enthusiastic encouragement throughout my entire PhD study.

I would also like to express my profound gratitude to supervisor Dr. Keyu Liu, Principal Research Scientist, CSIRO, WA, for his valuable guidance and supervision, and for providing the CSIRO laboratory facilities which were used for the experimental part of this thesis.

I am indebted to Schlumberger for giving an Eclipse license for this study. My special thanks to Vikam Sharma, John Ciccarelli, Esmail Maleki, and Tommi Simpson from Schlumberger for providing technical support for this study.

It was an honour and pleasure to receive two prestigious scholarships: the Western Australian CSIRO-University Postgraduate Scholarship (WACUPS) and the Scholarship for International Research Fees (SIRF) from UWA for this PhD study.

I am thankful for the support of our group members at UWA, specially Jian, Dong, Hongyan and Hamid. I am also grateful to Mohammed Baher and Abdur Rashid at CSIRO for their help in the lab.

I would like to thank to Dr Margaret Johnson of The Book Doctor for professionally editing the thesis and Denzil Dmello of Cognis Australia for providing APG surfactant for this study.

Last but not least, I thank my wife Kamrun and two sons Iash and Isam for their love and patience throughout this PhD journey.

Table of Contents

List of Tables

List of Figures

Nomenclature

List of Abbreviations

APG	Alkyl Polyglucosides
BHPB	BHP Billiton
CMC	Critical Miscible Concentration
CSIRO	Commonwealth Scientific and Industrial Research Organisation
ECL	Exploration Consulted Limited
EOR	Enhanced Oil Recovery
ESSO	Eastern States Standard Oil, (an international trade name for ExxonMobil)
HLB	Hydrophilic/Lipophilic Balance
GEOR	Green Enhanced Oil Recovery
GIMP	GNU Image Manipulation Program
IFT	Interfacial Tension
MEOR	Microbial Enhanced Oil Recovery
OIIP	Oil Initially In Place
OCP	Optimum Concentration Point
OMV	Österreichische Mineralölverwaltung (integrated international oil and gas company)
TOR	Tertiary Oil Recovery
WOR	Water Oil Ratio

Abstract

Microbial Enhance Oil Recovery (MEOR) is a relatively economical method to recover residual oil, but it is difficult to identify optimal conditions for microbe growth rate, activity, or quantity of favourable by-products in the varying conditions of different reservoirs. Many aerobic microorganisms can produce bio-surfactants which are capable of effectively reducing interfacial tensions (IFT) between oil, formation water and the rock matrix. Presently there are few publications on the production of bio-surfactants from anaerobic organisms. Moreover, most of the previous studies deal with single by-product of microbes and single process. The combined effect of bio-surfactant and bio-alcohol, and bio-surfactant, green surfactant and alcohol in the MEOR process, are not well understood yet and require further investigation. This study was conducted to examine the effectiveness of combination of two microbial by-products, bio-surfactant and bio-alcohol, in recovering residual oil within the pores of rock. It also considered whether bio-surfactant capability could be improved by blending it with non-ionic green surfactant. The study consisted of laboratory experiments and simulations.

Three formulations of surfactant and co-surfactant mixtures were selected for core-flood experiments based on phase behaviour study and IFT reduction to examine their potential for enhanced oil recovery (EOR). In the first formulation, JF-2 bio-surfactant was mixed with butanol; it was found that this formulation did not produce a significant quantity of incremental oil (about 1.7% of oil initially in place [OIIP]) after water flooding. This formulation did not perform as expected. In the next formulation, a blend of APG 264 and butanol showed good oil recovery results in a core-flood experiment, with 82% of OIIP recovered. Lastly, a bio-surfactant (anionic) was blended with non-ionic green surfactant alkyl polyglucoside (APG) and butanol; this produced about 25% tertiary oil and 64% OIIP.

A commercial Eclipse simulator was modified to add the option to simulate a MEOR process as this was not available. The modified simulator was used to simulate three core-flood experiments with three formulations. The JF-2 bio-surfactant and butanol solution core-flood test was simulated. The result was slightly higher than the experimental result but compared reasonably well. The simulated tertiary and total

oil recoveries of the APG and Butanol solution were similar to the experimental values: the simulated TOR and total recovery were 41% and 81% respectively, while the core-flooding TOR and total recovery were 41% and 82%. The APG, bio-surfactant and butanol combination core-flood experiment, when simulated, produced an oil recovery curve that was a good match with the experimental curve.

Based on the laboratory and simulation studies, a new method of Green Enhanced Oil Recovery (GEOR) was developed, and its potential for use in Australian oil fields was examined. It was found that this method is applicable to many oil fields, depending on salinity and reservoir temperature. It may also be used in place of MEOR if this is proving slow or inefficient.

Chapter 1 Introduction

Microbiologists and scientists consider that enhanced oil recovery by microbial action is a relatively cheap method of recovering tertiary oil from reservoirs (Donaldson *et al*. 1989). In the microbial enhanced oil recovery (MEOR) method, tertiary oil can be recovered by improving macroscopic sweep efficiency in a number of ways: by microbially modifying the induced permeability profile; by reducing the interfacial tension between oil and water with microbial bio-surfactants to lower the capillary trapping forces; by stimulating the reservoir's porosity and permeability with microbial products such as acids; or by combining all three mechanisms (Donaldson *et al.* 1989). Bio-surfactants produced by an anaerobic microbe, *Bacillus subtilise* strain JF-2, can reduce interfacial tension (IFT) and recover residual oil from a sandstone core (Folmsbee *et al.* 2005; Lin *et al.* 1994). Alkyl Polyglucoside (APG) surfactants are green and work like synthetic surfactants in terms of their oil recovery mechanism. APG surfactants are produced from coconut, palm oil, corn, potato or wheat residues, and are different from conventional enhanced oil recovery (EOR) surfactants because they biodegrade quickly and completely in the environment, and toxicity is very low (Cognis 2009).

This dissertation focuses on the combined effect of bio-surfactants and bio-alcohol produced by microbes in recovering residual oil trapped within the pores of rocks. It also considers the effect of adding green surfactant and/or co-surfactant into the bio-surfactant-based MEOR system.

This chapter offers a brief introduction to EOR and surfactant behaviour, and describes the background of this study. The goals of this dissertation and its contributions to the field are presented, and an overview of experimental and simulation studies on the performance of green surfactants is described. The chapter ends with brief descriptions of the subsequent chapters.

1.1 Background of the study

Oil recovery processes are categorised in three phases: primary, secondary and tertiary. Primary recovery is the first stage, resulting from the displacement energy existing in a reservoir. Secondary recovery is the second stage of the operation,

involving waterflooding, pressure maintenance, or gas injection, and is implemented after primary recovery is no longer feasible. In practice, conventional waterflooding only recovers about 30% of the oil initial in place (OIIP), leaving the rest as unswept and residual oil which is mostly attached to the rock in the reservoir (Curbelo *et al.* 2006). Tertiary oil recovery, known as the enhanced oil recovery (EOR) process, uses miscible gases, thermal energy and chemicals to displace additional oil once the secondary recovery process becomes uneconomical (Green & Willhite 1998) In this stage, injections of microorganisms or chemicals including polymers or surfactants are used to extract approximately 30–60% of the reservoir's OIIP (Hitzman *et al.* 2003).

In chemical EOR processes, the popular chemicals are surfactants, polymers and alkalines. The primary role of the surfactant (or surface active agent) in the EOR process is to reduce IFT between the oil and water molecules to release the oil trapped in the pores of the reservoir rock. Surfactants are usually injected in association with co-solvents and/or co-surfactants (which may be alcohol or another surfactant) to enhance their action (Green & Willhite 1998).

The following section describes the bio-surfactant-based MEOR and green surfactant-based EOR processes and simulation study.

1.1.1 Bio-surfactant based MEOR

MEOR has the potential to compete with other enhanced oil recovery techniques based on thermals, surfactants, and solvents (Leo 1997) because it does not require high energy expenditure or expensive chemicals. The only requirement is the selection of the appropriate nutrients and injection technology to grow indigenous microorganisms under reservoir conditions (temperature, pressure and salinity). Selection of the appropriate microorganisms is the key to MEOR success. Growing microorganisms under reservoir conditions is extremely challenging (Sarkar 1989); the possibility of yielding favourable EOR by-products generally decreases with temperature (Sarkar 1989). It is crucial in MEOR to identify the optimal conditions for the microbe growth rate, activity, and quantity of favourable by-products in reservoirs conditions (e.g. salinity, temperature and pressure, and anaerobic environment) (Ko 1999; Sarkar 1989). If the microbes injected into reservoirs are

inappropriate, they may damage the reservoir rock formation and fluids (Bahar & Liu 2007).

Microbes can produce bio-surfactants which efficiently decrease IFT between oil, formation water and rock matrix; but most of them are aerobic. Little information is available about the anaerobic organisms that produce bio-surfactants. Bacillus mojavensis JF-2 (Mclnerney *et al.* 2003) produces a lipopeptide bio-surfactant that decreases the IFT between oil and water to values of 0.01mN/m. This microbe can grow in anaerobic conditions and at elevated temperatures and salinities. Previous studies (Kawalewski 2006; Lin *et al.* 1994; Maudgalya *et al.* 2005; Sharma *et al.* 1993) have reported that JF-2 bio-surfactants are able to reduce significantly the interfacial tension between oil, formation water and rock matrix, and to remove the residual oil. This JF-2 bio-surfactant (Mulligan *et al.* 1999) is anionic in nature, suggesting that JF-2 behaviour will be similar to well-characterized synthetic anionic surfactants.

The addition of Proteose Peptone to mixed microbial communities obtained from groundwater and inoculated with Bacillus mojavensis JF-2 results in the production of 2,3-butanediol, a fermentation end-product characteristic of Bacillus non-ioncies, and a co-surfactant which may increase the efficiency of the bio-surfactant for oil recovery (Mclnerney *et al.* 2003). Maudgalya *et al.* (2004) conducted a series of experiments to study the ability of Bacillus mojavensis JF-2 bio-surfactant and co-surfactant to mobilize residual oil. Results showed that the co-surfactant 2,3-butanediol helped the surfactant approach optimum IFT at a given salinity.

Most other publications deal with a single by-product and process. In MEOR, microbes produce by-products such as bio-surfactants and bio-alcohol, and work jointly to decrease IFT and increase oil recovery over that achieved by a single surfactant.

It has been documented that reservoirs suitable for MEOR are typically of low temperature and low salinity, with temperatures <90 °C and salinity <10% (Sharma *et al.* 1993; Yakimov *et al.* 1997). The reservoir pressure does not appear to affect the growth of most microorganisms (Sarkar 1989). The key issue in the MEOR process is to determine the temperature and salinity, plus the optimum growth rates,

of microbes that produce bio-surfactants. If bio-surfactant production is not sufficient to recover the optimum residual oil, then two questions arise: (1) how can costs be minimized; and (2) is there any other way to increase recovery?

1.1.2 Green surfactant based EOR

To answer these questions, this study attempts to find a solution. Mixing bio-surfactant (anionic) with a green non-ionic surfactant is a practical approach. Blending anionic and non-ionic surfactants is a technique that has been used in the petroleum industry in EOR for a long time (Green & Willhite 1998). Anionic surfactants have useful properties: they are fairly stable, have low adsorption on reservoir rocks, and are very cheap to produce; non-ionic surfactants are more suitable in high-salinity brine environments (Green & Willhite 1998). Non-ionic surfactants are used primarily as co-surfactants to improve the behaviour of the surfactant system.

Iglauer *et al.* (2009) performed a laboratory study of alkyl polyglycosides (APG) to examine the stability of this non-ionic surfactant for EOR. They found that APG co-surfactant combinations can produce very low IFT with values largely independent of temperature and salinity. Their core flood test using Berea sandstone core and n-octane in oil phase and a selected formulation (Agrimul 2062/ 1-octanol) exhibited oil recovery as high as 85% of OIIP. In 2009 they investigated selected formulations for EOR using core flood tests on Berea sandstone, and also examined the adsorption behaviour of kaolinite clay. All APG formulations were good at Tertiary Oil Recovery (TOR). The solid adsorption of the APG surfactants was dependent on the APG alkyl chain length: a longer chain led to more adsorption. Retention of 40–60 mg/g kaolinite was observed for PG 2062, while negligible retention for PG 2069 was recorded.

In this study, four different Alkyl Polyglucoside (APG) surfactants were selected from the non-ionic group, and one bio-surfactant produced by the microbe *Bacillus mojavensis* (also known as *Bacillus subtilise*) was taken from the anionic group. In addition, different types of alcohol were tested. APG surfactants show low long-term aquatic toxicity for bacteria and are favourable for fish; their effects on Daphnia and

algae are acceptable. Terrestrial toxicity tests reveal no adverse effect in earthworms and plants, even at the highest tested concentrations (Cognis 2009).

Green enhanced oil recovery (GEOR) is a new EOR method of recovering tertiary oil from reservoirs using green chemicals. GEOR can recover tertiary oil by improving macroscopic and microscope displacement efficiency using green surfactants, co-surfactants (mainly alcohols) and polymers. Green surfactants and co-surfactants are environmentally friendly and biodegradable, and work like synthetic surfactants and co-surfactants in terms of the oil recovery mechanism.

Several EOR studies undertaken in the past have not looked at the impact of green surfactants and co-surfactants on MEOR. Green and Willhite (1993) state that anionic and non-ionic surfactants are more suitable for oil recovery applications as they are relatively stable and have low absorption tendencies. Bio-surfactant JF-2 is anionic and APG 264 surfactant is non-ionic; these can be mixed to provide a good EOR slug. MEOR is the only method in which both bio-surfactants and co-surfactants are used, but it is a slow process, complex, and applicable only within a small range of temperatures and salinity. There is a need for a cost effective, environmentally friendly, fast EOR process able to be used in reservoirs with a wide range of temperature and salinity.

1.1.3 Simulation of core flooding experiments

Surfactants' recovery efficiency can be examined using core flood tests. However, conducting core flood experiments with a wide range of formulations is time consuming and laborious. Reservoir simulation has the ability to test different EOR processes under varying conditions without requiring lengthy laboratory experiments. For this study an Eclipse simulator was modified to simulate bio-surfactant and green based core flood tests.

The Eclipse program is designed to use an ASCII text file, usually specified as: *.DATA, in which all the model information is identified (Schlumberger 2009). The *.DATA file, commonly called a "data file" or "data deck", is subdivided into sections: RUNSPEC, GRID, EDIT, PROPS, REGIONS, SOLUTION, SUMMARY, SCHEDULE. Within these sections, the user can use keywords to identify input data, request output data (to various media), and specify condition. Eclipse reads the input

data file section by section and processes each section in turn once that section has been read. Various data and consistency checks are made before proceeding to the next section. The last section is exceptional because it specifies time dependent data and is not read and processed as a whole; instead, the keywords are processed in the order they are presented in the data file.

The first commercial release of the new Eclipse simulator was announced at the SPE NON-ION symposium in San Francisco, in 1983. Eclipse 100 is a Black Oil simulator which was written by Exploration Consulted Limited (ECL). Over the past 30 years, chemical flooding simulators have become more and more complex, but few publications discuss the use of Eclipse in complex EOR processes. Of these, Yu *et al.* (1998) did core flood tests using Eclipse to examine dynamic reservoir parameters and characteristics, using gas and oil injection. Kumur and Shrivastava (2000) studied the effect of gas saturation on the relative permeability and mobility ratio of oil, using Stone I, II and Eclipse default methods; they found that use of Stone II caused serious problems when it created immobile oil saturation around prolific producer wells and as a result the oil's relative permeability became zero. Bedrikovetsky *et al.* (2009) found that Eclipse's constant skin factor model was not able to calculate variable skin factor. Tiamiyu and Boukadi (2011) concluded that surfactants added to steam flooding could not be simulated with the available Eclipse model as it had no option to examine combined effects. In 2012 Shabani-Afrapoli *et al.* found that Eclipse 100 (version 2009) was not a powerful tool for simulating the MIOR process because the bacterial effect on reservoir properties such as relative permeability, capillary pressure and wettability changes could not be not expressed in this simulator.

The main drawbacks of previous studies (EOR and MEOR) can be summarised as follows:

1. Most of the publications concerning the MEOR process deal with a single by-product and process. Many microorganisms are known to produce bio-surfactants in aerobic condition, but only a few of the bio-surfactants produced from bacteria in anaerobic conditions are able significantly to reduce interfacial tension between oil, formation water and rock matrix to the level of moving the residual oil (McInerney,

1990). Microbes produce by-products: bio-surfactants and alcohol; but little information is available on the combined effect of a bio-surfactant and bio-alcohol on EOR.

2. Ionization is vital to the EOR process. The bio-surfactant JF-2 Bacillus is anionic and has a substantial impact on EOR chemistry. The ionic characteristics of this bio-surfactant must to be addressed thoroughly if EOR is to be successful.

3. Many formulations used in surfactant flooding involve blends of surfactants designed to give the best oil recovery efficiency (Koukounis *et al.* 1983). The appropriate surfactant co-surfactant system for a micellar flood to obtain enhanced oil recovery requires careful optimization. Mixing anionic (bio-surfactant) surfactant and non-ionic surfactant (APG) is an area that needs further investigation to get good oil recovery.

4. The combined effect of surfactant and alcohol, oil recovery efficiency, and IFT versus concentration options needs to be added to the Eclipse black oil simulator in order to simulate MEOR and GEOR processes adequately.

1.2 Objectives and scope of this study

The primary objective of this study is to develop a step-wise evaluation approach to the MEOR process that will investigate the combined effects of using the by-products of micro-organisms, bio-surfactants and bio-alcohols, on the reduction of IFT and the improvement of oil recovery. This study will also examine the collective influence of green surfactants, bio-surfactants and co-surfactants on residual oil recovery. The Eclipse simulator will be modified to simulate coreflooding experiments and to predict oil recovery by the by-products of micro-organisms and green surfactants and co-surfactants.

The project aims to

a. document the joint impact of the microbes' by-products, bio-surfactant and bio-alcohol, on decreasing IFT and enhancing residual oil recovery,
b. examine the ionic effect of green surfactants and different blends of surfactants on oil recovery, and
c. modify the Eclipse simulator and simulate the core-flooding experiments.

These objects will be achieved by meeting a number of challenging research milestones, which are the result of several experiments and simulations. These can be summarized as follows:

a. Formulating a green surfactant and co-surfactant slug/mixture that can be used in EOR. This will be achieved by considering reservoir temperature, pressure, oil properties, salinity and ionic environment. This mixture is effective in IFT reduction and is successful in mobilizing trapped oil after water flooding.
b. Formulating a green surfactant, bio-surfactant and co-surfactant slug/mixture suitable for use in MEOR and capable of decreasing IFT and increasing residual oil recovery.
c. Developing a Green enhanced oil recovery (GEOR) method that can be used in a wide range of temperatures and salinity tolerance.
d. Finally, modifying the Eclipse simulator to simulate MEOR and GEOR core flooding experiments.

1.3 Overview of the experimental and simulation work

The goal of thesis is to investigate the role of green surfactants (bio-surfactant and biodegradable surfactant) in MEOR. The performance of surfactant and co-surfactant is mainly evaluated in terms of their oil recovery capability. To fulfil the objectives of this study, the dissertation is divided into two parts. In the first section, a characterization of green surfactant is provided, considering phase behaviour, fluid properties, IFT and ionic behaviour. Laboratory-scale core floods of selected formulations of surfactant and co-surfactant are conducted on Berea sandstone cores. Results are analysed and reported. In the second part of the dissertation, the core flooding experiments are simulated using an Eclipse simulator modified so that it can simulate MEOR and GEOR processes.

1.3.1 Phase behaviour

The phase behaviour of surfactant systems is an important characteristic for EOR, and has been established as a key method for understanding and predicting the performance of surfactant systems. The main aim of most phase behaviour studies is to identify regions of middle phase micro-emulsion. Middle phase micro-emulsion

can be designed to have low Interfacial Tension (IFT), of use in oil recovery processes. The phase behaviour of micro-emulsions is complex and dependent on a number of components, including the types and concentrations of surfactants, co-surfactants, hydrocarbons and brine, and temperature. This study focuses on the effects of anionic and non-ionic surfactant concentrations, types and concentrations of surfactant and co-surfactant, and mixtures of anionic and non-ionic surfactants on middle phase micro-emulsion, using salinity scans.

1.3.2 Fluid properties measurements

Fluid properties including density, viscosity and IFT measurements are described in this section. It is well known that the primary requirement needed to mobilize residual oil saturation is a sufficiently low IFT to give a capillary number large enough to overcome capillary forces and allow oil to flow (Stegemeier 1970). IFT is the force per unit length required to create a new surface area at the interface of two immiscible fluids, it is also the condition of mechanical equilibrium at an interface. The IFT properties of a range of surfactant and co-surfactant systems were measured to determine the optimum formulation for core flood experiments. At the same time density and viscosity measurements of different formulations were conducted.

1.3.3 Ionic effects of surfactant

Ions play a vital role in surfactant performance for EOR. In the effective formulation of micellar fluids (Kremesec *et al.* 1988) for field applications, surfactants should be chosen for their ability to generate very low IFT and to form a micro-emulsion that solubilises large volumes of oil and brine. These design considerations should be examined in an ionic environment as nearly equivalent to that which occurs during the oil-displacement process as possible. This study characterizes some green anionic and non-Ionic surfactants through the determination of the IFT of each group and the combined effect of the surfactants with alcohols on IFT and micro emulsions, determined through laboratory experiments. Four different Alkyl Polyglucosides (APG) which can produce ultra-low IFT were selected from the non-ionic group. Bio-surfactants produced by a microbe called *Bacillus mojavensis* (also known as *Bacillus subtilise*) were taken from the anionic group.

1.3.4 Flooding experiments

Surfactant performance on EOR was determined by coreflooding experiments. This study of EOR techniques not only focused on performance but aimed to develop a green, cost-effective method that would improve profitability. Laboratory development of EOR techniques involves setups that duplicate well and reservoir conditions. Coreflooding experiments are used to test EOR techniques. In this study, three coreflooding experiments were conducted to examine the percentage of oil recovery of three green surfactant and co-surfactant combinations: (1) non-ionic surfactant and alcohol, (2) anionic surfactant and alcohol, and (3) anionic and non-ionic surfactant and alcohol.

1.3.5 Simulation study

Since laboratory core experiments are time-consuming, it is not feasible to conduct them every time a new core flood test is required. For testing and development, an accurate numerical simulator can be a valuable tool for researchers. Simulation provides the ability to test different recovery processes under varying conditions without having to resort to time-consuming laboratory experiments. In this study an Eclipse simulator was modified to simulate MEOR and GEOR processes.

Using reservoir simulators to predict and understand the processes taking place during chemical flooding is currently of interest to the industry because high current oil prices have heightened interest in enhanced oil recovery. As with other simulators, chemical flooding simulators are often used to history match and understand the results of core floods or field performance.

Many widely used reservoir simulators have EOR options. There is no feature available in a commercial simulator in the oil industry to simulate coreflooding experiments that investigate the combined effect of surfactant and alcohol. Eclipse, one of the most popular reservoir simulators, does not have this option.

Three formulations of green surfactants were simulated and the results were used to investigate the effectiveness surfactant mixtures. Three core models for three formulations were simulated to examine the relationship between oil recovery and injected surfactant solutions. In all cases, fresh water was first injected into the core model and then surfactant solutions were injected to see the effect of secondary and

tertiary recoveries. JF-2 bio-surfactant from anionic green surfactants with butanol as a co-surfactant mixture was modelled in the first formulation. The second formulation was a nonionic surfactant APG and butanol mixture; the last was mixture of anionic and non-ionic surfactants with a co-surfactant, in this case, APG and JF-2 bio-surfactant with butanol. APG, bio-surfactant, butanol and brine, and core properties are discussed in chapter V.

The modifications to the Eclipse simulator were to determine (a) the combined effect of surfactant and alcohol, anionic and non-ionic surfactants with alcohol on oil recovery, and (b) the effect of volumetric swift efficiency on recovery.

1.3.6 A new method for EOR - GEOR

Green enhanced oil recovery (GEOR) is a chemical EOR involving the injection of green chemicals (surfactant/alcohol/polymer) that effectively displace oil because of their phase-behaviour properties, and thus decrease the IFT between the displacing liquid and oil. In this process, the primary displacing liquid slug is a complex chemical system called micellar solution. This solution contains green surfactants, co-surfactants, oil, electrolytes and water. Green surfactants are biodegradable and environmental friendly, and are perceived to have great potential for EOR. In GEOR, green polymer or bio-polymer can be used. This study did not conduct any tests for polymer-surfactant flooding, but it has the capacity to be adapted for this purpose.

1.4 Chapter descriptions and summary

This dissertation consists of consists of eight chapters. The introduction to the thesis is presented in Chapter One.

Chapter Two focuses on the phase behaviour of surfactant systems, is a key method for understanding and predicting the performance of surfactant systems. This study uses salinity scans to evaluate the effect of anionic and non-ionic surfactant concentrations, types and concentrations of surfactant and co-surfactant, and mixtures of anionic and non-ionic surfactants on middle phase micro-emulsion.

Fluid properties including density, viscosity and interfacial tension (IFT) and their analysis are described in Chapter Three. Experimental procedures to determine density and viscosity measurements, and the results of the crude oil, brine and

surfactant solution, are presented in the first and second sections. The third section addresses the IFT properties of fluid samples, pressure and temperature effects, the selection of surfactant and co-surfactant, and optimum concentrations of surfactant solutions for coreflooding experiments. Conclusions and recommendations are in the last section.

Chapter Four details the ionic characteristics of biodegradable and environmentally friendly surfactants and co-surfactants. Classification and selection of green surfactants and co-surfactants, and their properties, are presented in the first section. Mixtures of anionic and non-ionic surfactants, and pressure and temperature, are described next, followed by results, conclusions and recommendations.

In Chapter Five details of core floods are presented. Coreflooding experiments are used to test surfactant performance in the EOR process. In this chapter, three coreflooding experiments are discussed: (1) non-ionic surfactant and alcohol, (2) anionic surfactant and alcohol, and (3) anionic and non-ionic surfactant, and alcohol. Methodology, results and discussion, conclusions and recommendations are presented sequentially.

Simulation of MEOR and GEOR is discussed in Chapter Six. Introduction to the GEOR model is contained in the first section of this chapter. Next the modifications to the Eclipse simulator are discussed, then the simulator output is compared with laboratory data to verify the simulator's accuracy. The last section presents the conclusions.

Chapter Seven describes GEOR. The classification of EOR, differences between MEOR and GEOR, environmental factors and design parameters associated with GEOR, theory, methodology, results, conclusions and recommendations are presented here. In addition, the application of this method in Australian oil fields is discussed in this chapter.

Chapter Eight summarizes the study and recommends directions for future studies.

Chapter 2 Phase Behaviour

The phase behaviour of surfactant systems is an important characteristic for enhanced Oil recovery (EOR), and is a key method for understanding and predicting the performance of surfactant systems. The aim of this phase behaviour study is to identify the middle phase of microemulsion, which can be designed to have low interfacial tension (IFT) with oil recovery agents. The phase behaviour of micro-emulsion is complex, and dependent on a number of components, including the types and concentrations of the surfactants, co-surfactants, hydrocarbons and brine, and temperature.

This study focuses on using salinity scans to determine the effect of anionic and non-ionic surfactant concentrations, including different types and concentrations of surfactants and co-surfactants and mixtures of anionic and non-ionic surfactants, on middle phase micro-emulsion.

2.1 Introduction

Microemulsion is a stable, translucent phase that contains oil, electrolytes and one or more amphiphilic compounds (Healy & Reed 1974). It can be further described as swollen micelles that solubilise the immiscible with the solvent (Green & Willhite 1998). There are three type of micro-emulsions: lower phase, upper phase and middle phase, named by Windsor as Type I, Type II and type III respectively (Healy *et al.* 1976). These two terms are used interchangeably throughout this study. Lower phase microemulsion exists when there is an excess upper phase and the lower phase is solubilised in the microemulsion. For the purposes of EOR, the lower phase is usually water and the upper phase oil; so lower phase microemulsion is considered a water external microemulsion. Upper phase microemulsion exists when an oil external micro-emulsion is formed and water is present as the excess phase (Green & Willhite 1998). Middle phase microemulsion is the most important of all three phases, and the main focus of this study. This phase consists of oil and water with no distinct external phase. The importance of this phase is mainly due to its capacity to produce significantly lower IFT than the other two phases (Nelson & Pope 1978). The formation of middle phase microemulsion gives two different IFTs, the oil-microemulsion IFT and the water-microemulsion IFT. Middle phase microemulsion

is used to produce a low IFT between the oil phase and the water phase, and to solubilise the oil. The middle phase microemulsion is only effective when both IFT values are similar (Healy *et al*. 1976; Nelson & Pope 1978).

The objective of this study is to investigate the impact of alcohol and surfactant on middle phase emulsion by examining the effect of different alcohol and surfactant concentrations on the phase behaviour of brine-surfactant-alcohol systems.

2.2 Alcohols and Their Role in Micro-emulsion

Alcohol is used as a co-surfactant because microbes produce alcohol. Microbes can produce propenol, butanol and pentanol from molasses. It has been found that the maximum amount of butanol is produced by bugs from molasses. For this reason, the straight chain 1-butanol is used throughout this study. The terms alcohol and co-surfactant are used interchangeably.

An alcohol used as a co-surfactant may be hydrophobic or hydrophilic. The hydrophobic/hydrophilic properties of the alcohol mainly depend on the number of carbon atoms (Holm & Csaszar 1962; Jones & Dreher 1976).

When the surfactant is mainly water soluble, it is not ideal for middle phase microemulsion formulation because it tends to partition in this phase, forming a lower phase microemulsion. The parameter hydrophilic-lipophilic balance (HLB) is a measure of affinity (Iglauer *et al.* 2009): the higher the HLB, the more water soluble the surfactant. The optimal condition is also defined in term of HLB, and the HLB number defining the middle phase is the optimal HLB (Iglauer *et al.* 2009).

To control the affinity for water, a hydrophobic alcohol is added to the surfactant system. The addition of hydrophobic alcohol brings down the HLB (or makes the surfactant more hydrophobic). This means more surfactant exists in the oil phase. The continuous addition of hydrophobic alcohol will cause the phase transition of II→III→I. The alcohol is usually added until phase three behaviour or a balanced HLB is achieved. This manipulation of phase behaviour using alcohol can be done in reverse using a hydrophilic alcohol.

Alcohol is known to have other effects on the performance of the surfactants. For anionic surfactants, hydrophobic alcohol has been found to decrease the optimal

salinity, and hydrophilic alcohol increases it. Optimal salinity is found where the volume of oil and water solubilized in the middle phase is the same; this is similar to the HLB term. Other uses of alcohol found are to reduce viscosity of the microemulsion, reduce macro-emulsions, and increase equilibration time. The addition of alcohol can also reduce the adsorption of surfactants onto rock and prevent the formation on gels (Dwarakanath *et al.* 2008; Jones & Dreher 1976).

2.3 Methodology

2.3.1 Materials

The study focused on the behaviour of the non-ionic surfactant Alkyl Polyglycoside (APG), the anionic bio-surfactant Bacillus Mojavensis strain JF-2, and the co-surfactant alcohol. The APG 264 surfactant was supplied by the Cognis Corporation Australia. Alcohols of 99% purity and Sodium Chloride of 99.9% purity were purchased from Sigma Aldrich.

2.3.2 Experimental procedure

The experiment was conducted using the concept of salinity scans and followed a number of steps. A fixed surfactant and alcohol concentration combination was prepared and the salinity was varied.

Step 1. Before conducting the experiment the values to be examined for each variable were chosen. The first values to be determined were the concentrations of alcohol, brine and surfactants to be studied. Concentrations of surfactant and co-surfactant were taken based on literature review (Iglauer et al. 2009; Cognis 2009) and salinity scan concept. For this study, weight/volume percentage (w/v%) was used for all concentrations, unless stated otherwise. It was also decided to keep the water–oil ratio (WOR) constant at 1 throughout the study.

Step 2. Volumes for each solution in the sample were fixed at 4.5 ml. The volume of was an essential parameter. All the parameters and their values are tabulated below in Table 2.1.

Table 2.1 Parameters

Parameter	Values
APG 264 concentration (%)	0.5, 1.0, 1.5
Butanol concentration (%)	0.5, 1.0,1.5
NaCl concentration (%)	0, 1, 2, 3, 4, 5, 6, 7, 8
WOR	1.0
Volume of oil in sample (ml)	4.5
Volume of APG 264 solution in sample (ml)	0.7
Volume of butanol solution in sample (ml)	0.3
Volume of NaCl solution in sample (ml)	3.5

Step 3. Each sample consists of an aqueous phase and the oil phase. It was determined that the sample size would be 9ml, given the size of the vials: with WOR=1, there would be 4.5 ml aqueous phases and 4.5 oil phases. The aqueous phase consisted of 3.5 ml brine, 0.7ml surfactant and 0.3ml alcohol.

Step 4: The sample was prepared by first adding 3.5ml of brine, using a 5ml graduated pipette. This was followed by the addition of 0.7 ml of surfactant with a 1ml graduated pipette; then 0.3 ml of alcohol was added using a 0.5 ml graduated pipette. The size of the pipette was chosen to match the selected volumes for surfactant, alcohol and brine, for the best accuracy. Then the total volume was checked to match 4.5ml and sample volumes that did not fall within 0.1ml of the target volumes were discarded.

Step 5: 4.5ml of the oil phase was added to the 4.5ml of the aqueous phase. The volume was checked to ensure it was 9ml. The sample was then shaken vigorously and left to equilibrate. The equilibrium point was determined when there was no change in phase volumes over 24 hours.

Step 6: The data were observed and monitored. The main data observed were the phase volumes, which were monitored and recorded every two days. The changes in phase volumes were used to calculate the solubilised volumes of oil and water, based

on the difference between the initial and final volumes. All monitored data are presented section 2.4 below.

Step 7: Accuracy

3ml graduated syringes were used to add 0.7ml of the 1% APG 264 and 1.5% APG 264 solutions to the samples. For the stag oil 6 ml graduated syringes were used to add 4.5 ml to the sample. The change from pipettes to syringes was required because the APG solutions and stag oil were too viscous for pipettes to handle. All other solutions were added using pipettes.

Some key practices were implemented to increase accuracy when using pipettes and syringes. Before introducing solutions into the vials, the pipettes and syringes were checked to ensure there were no bubbles. Whenever a pipette was used, eyes were kept at the same level as the meniscus to avoid parallax error. Pipettes were read from the bottom of the meniscus.

Step 8: Experimental difficulties

One of the difficulties faced in this stage was the formation of bubbles at the surfactant solution interface/meniscus within the pipette. This made pipetting accurate volumes difficult as the meniscus level was very hard to judge. To overcome this problem, readings were taken from the bottom of the bubbles. Another difficulty encountered was using a syringe to obtain 4.5ml of stag oil. This was difficult because the stag oil was a dark colour similar to the internal rubber of the syringe, and the syringe only had graduations of 0.2ml. This made it very hard to see the volume of stag oil in the syringe accurately. The deviation in the oil phase volume added was estimated to be up to ±0.1ml.

2.4 Observed and Measured Data

Phase volumes were monitored routinely. Data were taken when all phases were stable and had reached equilibrium. Tables 2.2 to 2.4 describe the variation of concentrations both of APG 264 and butanol with concentrations of NaCl varying from 0% to 8%. Table 2.5 presents the APG 264 and bio-surfactant mixture phase behaviour.

Table 2.2 Observed and measure data of varying APG 264 (0.5-1.0 %) and butanol (0.5-1.0 %) concentrations

Sample no	Compositions	Brine con^{n}. (%)	Initial volume (cc)		Final volume (cc)		Middle Phase Emulsion Vol. (cc)
			Oil	Slug	Oil	Slug	
1.7.0	0.5% APG 264 + 0.5% butanol	0	4.5	4.5	0.5	3.5	5
1.7.1	0.5% APG 264 + 0.5% butanol	1	4.55	4.55	0.5	4	4.6
1.7.2	0.5% APG 264 + 0.5% butanol	2	4.55	4.55	3.8	4.3	1
1.7.3	0.5% APG 264 + 0.5% butanol	3	4.55	4.55	4.3	4.4	0.4
1.7.4	0.5% APG 264 + 0.5% butanol	4	4.5	4.5	2	4.3	2.7
1.7.5	0.5% APG 264 + 0.5% butanol	5	4.5	4.5	4.5	4.5	0
1.7.6	0.5% APG 264 + 0.5% butanol	6	4.5	4.5	4.5	4.5	0
1.7.7	0.5% APG 264 + 0.5% butanol	7	4.5	4.5	4.5	4.5	0
1.7.8	0.5% APG 264 + 0.5% butanol	8	4.6	4.6	4.4	4.6	0.2
1.8.0	0.5% APG 264 + 1% butanol	0	4.5	4.5	0.2	3.5	5.3
1.8.1	0.5% APG 264 + 1% butanol	1	4.5	4.5	4.5	4.5	0
1.8.2	0.5% APG 264 + 1% butanol	2	4.5	4.5	4.5	4.5	0
1.8.3	0.5% APG 264 + 1% butanol	3	4.6	4.6	4.2	4.5	0.5
1.8.4	0.5% APG 264 + 1% butanol	4	4.6	4.6	4.6	4.5	0.1
1.8.5	0.5% APG 264 + 1% butanol	5	4.55	4.55	4.5	4.5	0.1
1.8.6	0.5% APG 264 + 1% butanol	6	4.55	4.55	4.5	4.5	0.1
1.8.7	0.5% APG 264 + 1% butanol	7	4.6	4.6	4.6	4.5	0.1
1.8.8	0.5% APG 264 + 1% butanol	8	4.55	4.55	4.5	4.5	0.1
1.9.0	1% APG 264 + 0.5% butanol	0	4.75	4.75	0	4	5.5
1.9.1	1% APG 264 + 0.5% butanol	1	4.55	4.55	1.6	4.1	3.4
1.9.2	1% APG 264 + 0.5% butanol	2	4.65	4.65	3.6	4.5	1.2
1.9.3	1% APG 264 + 0.5% butanol	3	4.6	4.6	3.6	4.5	1.1
1.9.4	1% APG 264 + 0.5% butanol	4	4.6	4.6	2.7	4.5	2
1.9.5	1% APG 264 + 0.5% butanol	5	4.6	4.6	1.1	4.5	3.6
1.9.6	1% APG 264 + 0.5% butanol	6	4.6	4.6	1.8	4.5	2.9
1.9.7	1% APG 264 + 0.5% butanol	7	4.6	4.6	3.2	4.5	1.5

1.9.8	1% APG 264 + 0.5% butanol	8	4.55	4.55	3.55	4.5	1.05
1.10.0	1% APG 264 + 1% butanol	0	4.5	4.5	1	3.8	4.2
1.10.1	1% APG 264 + 1% butanol	1	4.6	4.6	2.7	4.5	2
1.10.2	1% APG 264 + 1% butanol	2	4.6	4.6	2.7	4.5	2
1.10.3	1% APG 264 + 1% butanol	3	4.6	4.6	4.5	4.5	0.2
1.10.4	1% APG 264 + 1% butanol	4	4.6	4.6	3.5	4.5	1.2
1.10.5	1% APG 264 + 1% butanol	5	4.55	4.55	1	4.3	3.8
1.10.6	1% APG 264 + 1% butanol	6	4.55	4.55	1	4.5	3.6
1.10.7	1% APG 264 + 1% butanol	7	4.55	4.55	1	4.5	3.6
1.10.8	1% APG 264 + 1% butanol	8	4.56	4.56	0.1	4.5	4.52

Table 2.3 Observed and measure data of varying APG 264 (0.5-1.5 %) and butanol (0.0-1.0 %) concentrations

Sample no	Compositions	Brine con^{n}. (%)	Initial volume (cc)		Final volume (cc)		Middle Phase Emulsion vol. (cc)
			Oil	Slug	Oil	Slug	
1.11.0	1.5% APG 264 + 0.5% butanol	0	4.75	4.75	0	3.5	6
1.11.1	1.5% APG 264 + 0.5% butanol	1	4.75	4.75	0	3	6.5
1.11.2	1.5% APG 264 + 0.5% butanol	2	4.6	4.6	0.7	4.3	4.2
1.11.3	1.5% APG 264 + 0.5% butanol	3	4.6	4.6	0	4	5.2
1.11.4	1.5% APG 264 + 0.5% butanol	4	4.55	4.55	0	4	5.1
1.11.5	1.5% APG 264 + 0.5% butanol	5	4.55	4.55	0.2	4	4.9
1.11.6	1.5% APG 264 + 0.5% butanol	6	4.6	4.6	0.5	4.2	4.5
1.11.7	1.5% APG 264 + 0.5% butanol	7	4.5	4.5	0.2	4	4.8
1.11.8	1.5% APG 264 + 0.5% butanol	8	4.5	4.5	1	4	4
1.12.0	1.5% APG 264 + 1% butanol	0	4.5	4.5	0	4	5
1.12.1	1.5% APG 264 + 1% butanol	1	4.6	4.6	0	4	5.2
1.12.2	1.5% APG 264 + 1% butanol	2	4.6	4.6	0.1	4	5.1
1.12.3	1.5% APG 264 + 1% butanol	3	4.7	4.7	0	4	5.4
1.12.4	1.5% APG 264 + 1% butanol	4	4.65	4.65	0.1	4	5.2

Sample no	Compositions	Brine con^{n}. (%)	Initial volume (cc)		Final volume (cc)		Middle Phase Emulsion vol. (cc)
1.12.5	1.5% APG 264 + 1% butanol	5	4.6	4.6	0.8	4.2	4.2
1.12.6	1.5% APG 264 + 1% butanol	6	4.55	4.55	0.7	4	4.4
1.12.7	1.5% APG 264 + 1% butanol	7	4.55	4.55	0.7	4.2	4.2
1.12.8	1.5% APG 264 + 1% butanol	8	4.6	4.6	0.6	4.3	4.3
1.13.0	0.5% APG 264 + 0% butanol	0	4.55	4.55	0	3.5	5.6
1.13.1	0.5% APG 264 + 0% butanol	1	4.55	4.55	3.1	4.5	1.5
1.13.2	0.5% APG 264 + 0% butanol	2	4.55	4.55	1	4.3	3.8
1.13.3	0.5% APG 264 + 0% butanol	3	4.55	4.55	3.5	4.5	1.1
1.13.4	0.5% APG 264 + 0% butanol	4	4.5	4.5	1.5	4.4	3.1
1.13.5	0.5% APG 264 + 0% butanol	5	4.55	4.55	3	4.5	1.6
1.13.6	0.5% APG 264 + 0% butanol	6	4.55	4.55	3.55	4.5	1.05
1.13.7	0.5% APG 264 + 0% butanol	7	4.5	4.5	1.5	4.3	3.2
1.13.8	0.5% APG 264 + 0% butanol	8	4.55	4.55	1.5	4.3	3.3
1.14.0	1% APG 264 + 0% butanol	0	4.75	4.75	0	4	5.5
1.14.1	1% APG 264 + 0% butanol	1	4.7	4.7	0.5	4.2	4.7
1.14.2	1% APG 264 + 0% butanol	2	4.65	4.65	1.2	4.5	3.6
1.14.3	1% APG 264 + 0% butanol	3	4.65	4.65	0.3	4.1	4.9
1.14.4	1% APG 264 + 0% butanol	4	4.7	4.7	0.3	4.3	4.8
1.14.5	1% APG 264 + 0% butanol	5	4.75	4.75	0.1	4.2	5.2
1.14.6	1% APG 264 + 0% butanol	6	4.75	4.75	0.2	4.4	4.9
1.14.7	1% APG 264 + 0% butanol	7	4.7	4.7	0.2	4.3	4.9
1.14.8	1% APG 264 + 0% butanol	8	4.6	4.6	0.4	4.2	4.6

Table 2.4 Observed and measure data of varying APG 264 (0.5-1.50 %) and butanol (0.0-1.5 %) concentrations

Sample no	Compositions	Brine con^{n}. (%)	Initial volume (cc)		Final volume (cc)		Middle Phase Emulsion Vol. (cc)
			Oil	Slug	Oil	Slug	
1.15.0	1.5% APG 264 + 0% butanol	0	4.75	4.75	0.1	3.8	5.6
1.15.1	1.5% APG 264 + 0% butanol	1	4.7	4.7	0.1	4.2	5.1
1.15.2	1.5% APG 264 + 0% butanol	2	4.7	4.7	0.2	4.1	5.1
1.15.3	1.5% APG 264 + 0% butanol	3	4.6	4.6	0.1	4	5.1
1.15.4	1.5% APG 264 + 0% butanol	4	4.6	4.6	0.2	4.2	4.8
1.15.5	1.5% APG 264 + 0% butanol	5	4.55	4.55	0.3	4	4.8
1.15.6	1.5% APG 264 + 0% butanol	6	4.7	4.7	0.4	4.1	4.9
1.15.7	1.5% APG 264 + 0% butanol	7	4.6	4.6	0.3	4.2	4.7
1.15.8	1.5% APG 264 + 0% butanol	8	4.55	4.55	0.4	4.1	4.6
1.16.0	0.5% APG 264 + 1.5% butanol	0	4.55	4.55	0.1	3.8	5.2
1.16.1	0.5% APG 264 + 1.5% butanol	1	4.6	4.6	3.6	4.5	1.1
1.16.2	0.5% APG 264 + 1.5% butanol	2	4.5	4.5	4.5	4.5	0
1.16.3	0.5% APG 264 + 1.5% butanol	3	4.6	4.6	4.6	4.5	0.1
1.16.4	0.5% APG 264 + 1.5% butanol	4	4.55	4.55	4.5	4.5	0.1
1.16.5	0.5% APG 264 + 1.5% butanol	5	4.5	4.5	4.5	4.5	0
1.16.6	0.5% APG 264 + 1.5% butanol	6	4.5	4.5	4.5	4.5	0
1.16.7	0.5% APG 264 + 1.5% butanol	7	4.5	4.5	4.5	4.5	0
1.16.8	0.5% APG 264 + 1.5% butanol	8	4.5	4.5	4.5	4.5	0
1.17.0	1.2% APG 264 + 0.8% butanol	0	4.7	4.7	0.6	4	4.8
1.17.1	1.2% APG 264 + 0.8% butanol	1	4.67	4.67	0.7	4.3	4.34
1.17.2	1.2% APG 264 + 0.8% butanol	2	4.5	4.5	0.15	3.8	5.05
1.17.3	1.2% APG 264 + 0.8% butanol	3	4.5	4.5	0.1	4	4.9

Table 2.5 Observed and measure data of bio-surfactant (55mg/l), and APG 264 (0.5%) and varying butanol (0.5-1.0 %) concentrations

Sample No	Composition	Brine con^{n}.	Initial volume (cc)		Final volume (cc)		Middle Phase Microemulsion Volume (cc)
			Oil	Slug	Oil	Slug	
2.1.0	55mg/l BS +.5% butanol	0	5	4.5	4	4.25	1.25
2.1.1	55 mg/l BS +.5% butanol	0.5	4.8	4.5	4.5	4.5	0.3
2.1.2	55 mg/l BS +.5% butanol	1	4.6	4.6	4.6	4.4	0.2
2.1.3	55 mg/l BS +.5% butanol	1.5	4.7	4.7	4.7	4.6	0.1
2.1.4	55 mg/l BS +.5% butanol	2	4.7	4.7	4.7	4.6	0.1
2.1.5	55 mg/l BS +.5% butanol	2.5	4.6	4.6	4.6	4.4	0.2
2.1.6	55 mg/l BS +.5% butanol	3	4.7	4.6	4.6	4.4	0.3
2.1.7	55 mg/l BS +.5% butanol	3.5	4.6	4.6	4.6	4.4	0.2
2.1.8	55 mg/l BS +.5% butanol	4	4.7	4.7	4.7	4.6	0.1
2.2.0	55 mg/l BS +1% butanol	0	4.9	4.6	4.8	4.4	0.3
2.2.1	55 mg/l BS +1% butanol	0.5	5	4.5	4.9	4.4	0.2
2.2.2	55 mg/l BS +1% butanol	1	4.7	4.5	4.7	4.4	0.1
2.2.3	55 mg/l BS +1% butanol	1.5	4.7	4.5	4.7	4.4	0.2
2.2.4	55 mg/l BS +1% butanol	2	4.6	4.5	4.6	4.4	0.5
2.2.5	55 mg/l BS +1% butanol	2.5	4.9	4.5	4.9	4.4	0.1
2.2.6	55 mg/l BS +1% butanol	3	4.9	4.5	4.9	4.4	0.1
2.2.7	55 mg/l BS +1% butanol	3.5	4.7	4.5	4.7	4.3	0.2
2.2.8	55 mg/l BS +1% butanol	4	4.7	4.5	4.7	4.4	0.1
3.1.0	55 mg/l BS +0.5%APG264	0	4.7	4.7	0.1	3.6	5.7
3.1.1	55 mg/l BS +0.5%APG264	0.5	4	4.6	2	4.5	2.1
3.1.2	55 mg/l BS +0.5%APG264	1	4.75	4.75	2.5	4.5	2.5
3.1.3	55 mg/l BS +0.5%APG264	1.5	4.6	4.6	2.7	4.5	2
3.1.4	55 mg/l BS +0.5%APG264	2	4.78	4.7	1.75	4.5	3.23
3.1.5	55 mg/l BS +0.5%APG264	2.5	4.78	4.7	3.75	4.6	1.13
3.1.6	55 mg/l BS +0.5%APG264	3	4.7	4.75	3.4	4.5	1.55
3.1.7	55 mg/l BS +0.5%APG264	3.5	4.75	4.75	3.4	4.5	1.6
3.1.8	55 mg/l BS +0.5%APG264	4	4.7	4.7	1.3	4.6	3.5

2.5 Results and Discussion

Test tube samples were prepared with 4.5 ml of aqueous APG 264/butanol/salt formulations and 4.5 ml of stag oil. After mixing well for several hours, they were set for three weeks to allow the fluids to come to phase equilibrium in ambient conditions. The phase characteristics of each system were recorded. These were: the relative volume of aqueous phase; the middle phase (if present); and the oleic phase. The object of phase behaviour study was to determine the middle phase emulsion. As a general trend, low IFT values appeared when middle phase emulsion formed (Bourrel & Schechter 1988; Healy & Reed 1974). A large middle phase emulsion indicated a low IFT, especially when oil and water were solubilised.

2.5.1 The impact of varying alcohol concentrations on middle phase emulsion

2.5.1.1 Case A: 0.5% APG and 0–1.5% butanol

Four samples of 0.5% APG 264 surfactant and varying butanol concentrations from 0% to 1.5% were made. In all samples the NaCl concentration was constant at 2%. The phase behaviour of the brine-surfactant-alcohol system was recorded; it is presented in Figure 2.1.

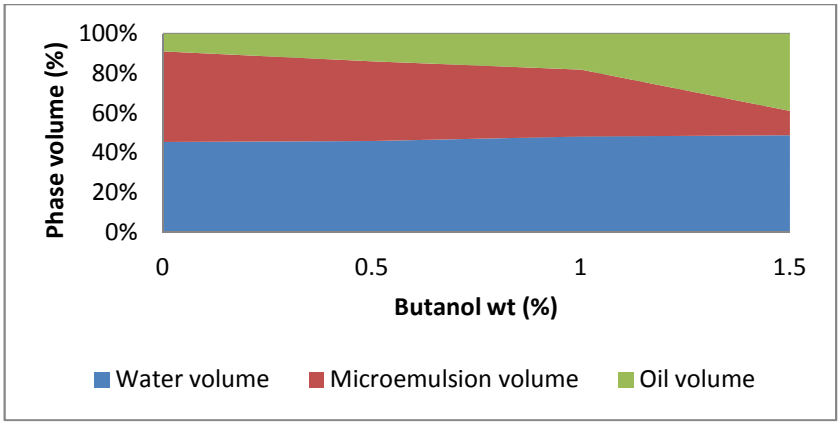

Figure 2.1 Phase diagram of butanol-0.5% APG 264 mixtures

2.5.1.2 Case B: 1% APG and 0–1.5% butanol

In case B, the APG concentration changed to 1.0% and the butanol concentrations varied from 0.5% to 1.5% with a constant 2% NaCl. Results are in Figure 2.2.

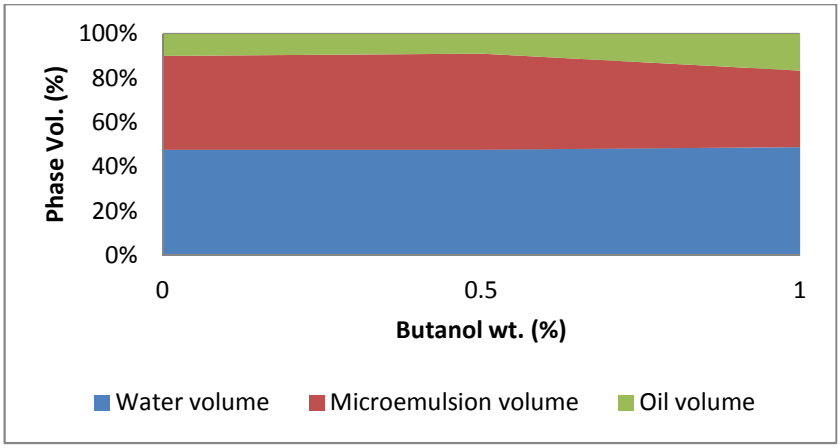

Figure 2.2 Phase diagram of butanol-1 (%) APG 264 mixtures

2.5.1.3 Case C: 1.5% APG and 0–1.5% butanol

Case C represents 1.5% APG, butanol concentrations varying from 0.5% to 1.0%, and 2% NaCl. The phase behaviour characteristics are presented in Figure 2.3.

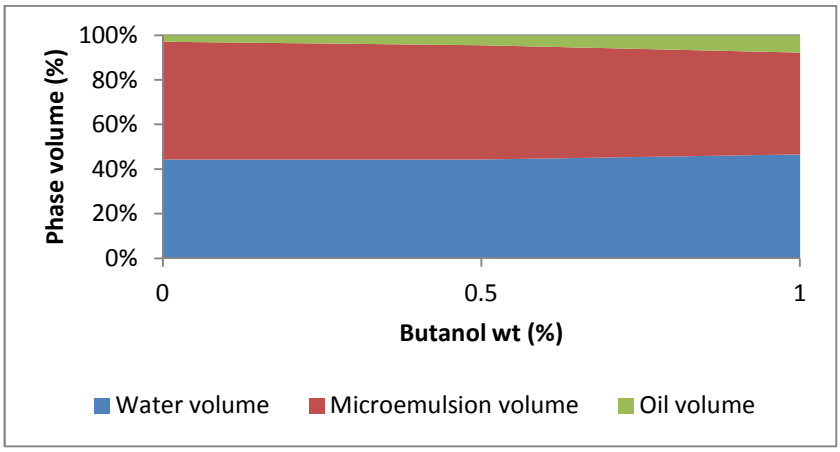

Figure 2.3 Phase diagram of butanol-1.5 (%) APG 264 mixtures

2.5.1.4 Discussion of Figures 2.1–2.3

The three figures above display the effect of different alcohol concentrations on a fixed surfactant concentration. All three figures show the same trend: as alcohol concentrations increase there is a decrease in the microemulsion volume and an increase in oil phase volume. The water phase volume also increases slightly with

the increasing alcohol concentration. The main difference between the three figures is the amount of decrease in the microemulsion volume, which leads to different increases in the oil volumes. This serves as an indicator of the magnitude of the effect of varied alcohol concentrations. Changes in the alcohol concentrations seem to have the biggest effect on 0.5% APG 264.

2.5.1.5 APG 264 (0.5%–1.5%) and butanol (0.5%–1.5%): both concentrations varied

In this case four samples were prepared with varying concentrations of both surfactant and alcohol to make 2% combined concentrations. First was 0.5% APG and 1.5% butanol; second 1% APG and 1% butanol; third 1.2% APG and 0.8% butanol; and last 1.5% APG and 0.5% butanol. NaCl was kept at 2% in all four samples. The recorded results appear in Figure 2.4.

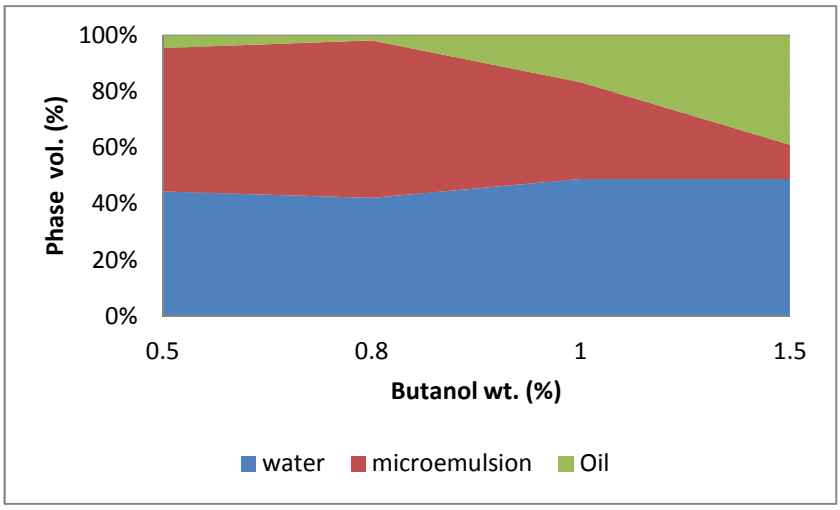

Figure 2.4 Phase diagram of 2% butanol-APG 264 mixtures

The data selected had a total concentration of surfactant and alcohol of 2%. Figure 2.4 shows a decrease in the oil and water phase volume accompanied by an increase in the microemulsion volume, observed at 1.2% APG 264/0.8% butanol. A continuous increase in the oil phase volume is evident after that point.

This indicates that as butanol increases and APG 264 decreases, the amount of microemulsion decreases. Eventually there will be no microemulsion formation for samples with only alcohol; this was found by Iglauer *et al.* (2009) as well. Another perspective on the phase behaviour proposes a fishlike diagram for APG surfactants (Chai *et al.* 2003, Von Rybinski *et al.* 1998); from this point of view, the composition is moving out of the three-phase region into another region. As the solubilised volumes did not indicate a transition into either an upper phase or a lower phase microemulsion, the possibility was raised that the composition was moving into a region of zero microemulsion formation.

2.5.2 The effect of changing surfactant concentrations on middle phase emulsion

2.5.2.1 Case A: APG 264 (0.5% –1.5%) and 0% butanol mixtures

Three samples of varying APG concentrations from 0.5% to 1.5%, with 2% NaCl, were prepared. The phase behaviour of the brine-surfactant system is presented in Figure 2.5.

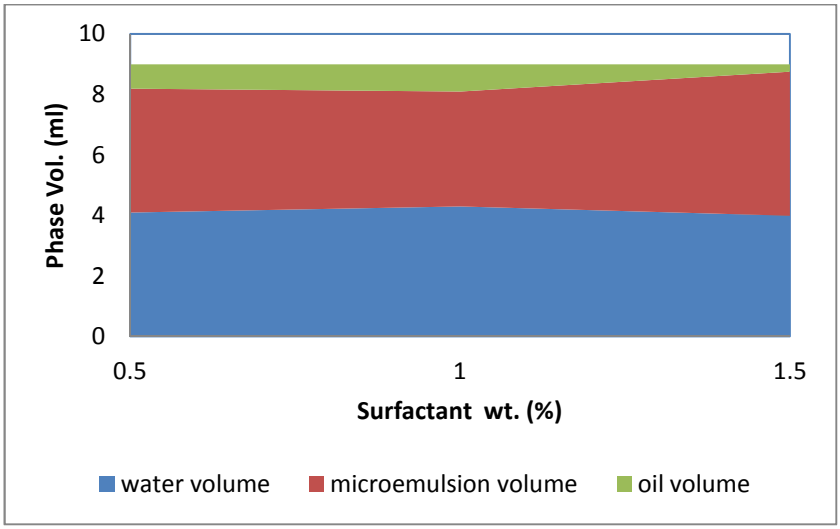

Figure 2.5 Phase diagram of APG 264 (0.5% to 1.5%) and 0% butanol mixtures

2.5.2.2 Case B: APG 264 (0.5% to 1.5%) and 0.5% butanol mixtures

In this case, three samples of varying APG concentrations from 0.5% to 1.5%, and constant butanol concentrations of 0.5% and 2% NaCl were prepared. The results are presented in Figure 2.6.

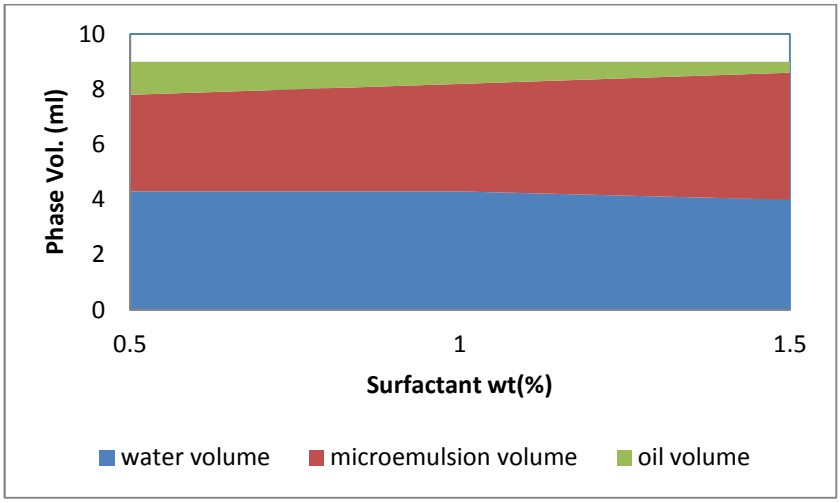

Figure 2.6 Phase diagram of (0.5-1.5%) APG 264 and 0.5% butanol mixtures

2.5.2.3 Case C: APG 264 (0.5% to 1.5%) and 1% butanol mixtures

Three samples were prepared of 1% butanol, varying concentrations from 0.5% to 1.5% of APG and constant NaCl concentrations of 2%. Figure 2.7 shows the recorded phase behaviour of this brine-surfactant system.

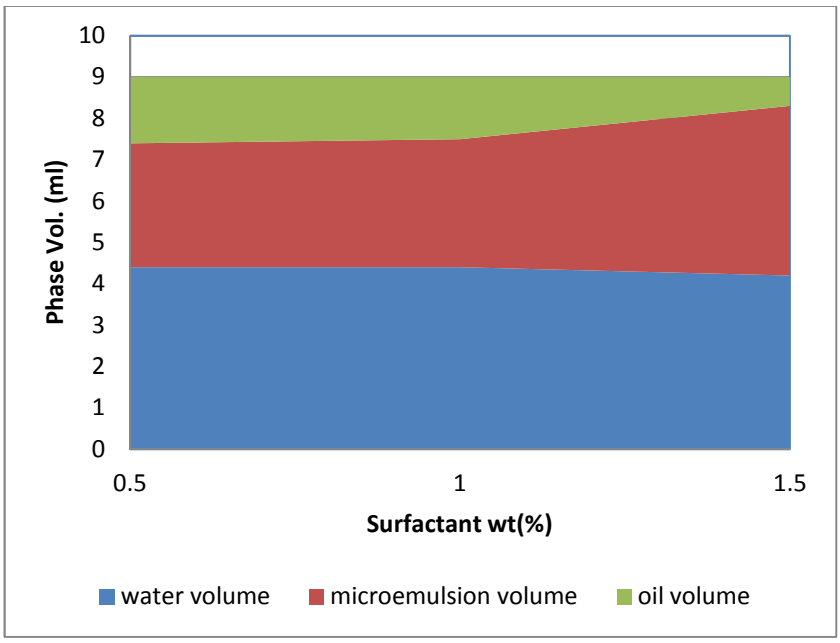

Figure 2.7 Phase diagram of (0.5-1.5%) APG 264 and 1.0% butanol mixtures

2.5.2.4 Discussion of cases A, B, and C

Figures 2.5–2.7 indicate the phase volumes at a fixed alcohol concentration and a fixed salinity of 2% with an increasing surfactant concentration. All the graphs indicate an increasing amount of microemulsion formed with increasing surfactant concentration. It can be observed that the microemulsion volume increases at the expense of the oil phase, implying that the solubilized volume of oil is increasing. The increase in solubilised oil in microemulsion serves as a sign that the composition is moving towards the upper phase region. Based on a fishlike phase behaviour diagram, this trend is expected to produce increasing surfactant concentration while the alcohol concentration is fixed (Chai *et al.* 2003). The diagram also indicates that a certain increase in surfactant concentration will lead to a higher tendency to form an upper phase microemulsion with a higher butanol content.

2.5.3 Effect of anionic and non-ionic surfactants on middle phase emulsion

This investigates the impact of anionic and non-ionic surfactants mixture on the middle phase. APG 264 at a concentration of 0.5% and bio-surfactant at a concentration of 55 mg/l were mixed with NaCl concentrations varying from 0% to 8%. Figure 2.8 indicates a stable middle phase with increasing NaCl concentration.

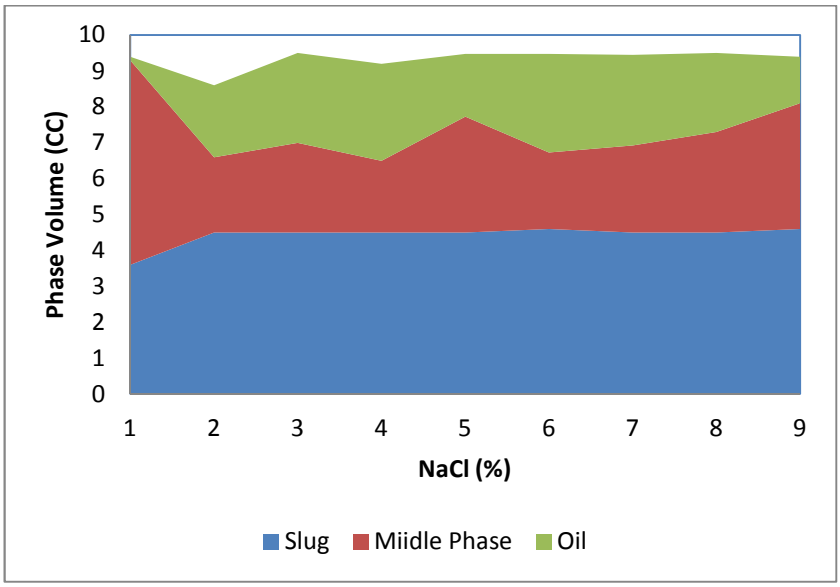

Figure 2.8 Phase diagram of (0.5%) APG 264 and 55mg/l bio-surfactant mixtures

2.6 Conclusions

1. It was found that 0.5% APG and 0.5% to 1.00% of Butanol at 2% NaCl gave stable middle phase micro-emulsion.

2. A combination of bio-surfactant at 55mg/l and 0.5% butanol did not form any middle phase micro-emulsion.

3. Non-ionic (APG 264) and anionic (bio-surfactant) mixtures are able to form stable middle phase micro-emulsion.

2.7 Recommendations

1. It is recommended that graduated pipettes be used for better resolution and measurement of solubilised volumes. This will improve data repeatability. It was found a change of 0.1ml made a significant difference in the calculation of the solubilization ratio. In a small sample of microemulsion, a deviation of 0.1ml in the solubilised volume would cause a large error.

2. It would be useful to narrow any further study to concentrations in the neighbourhood of the optimal combinations. This step will allow a more precise identification of optimal compositions.

Chapter 3 The Measurement of Fluid Properties

The measurement of fluid properties including density, viscosity and interfacial tension (IFT) are described in this chapter.

After a brief introduction, the selection of optimum concentrations is discussed. Procedures used to measure the density and viscosity of the crude oil, brine and surfactant solutions are presented in the third and fourth sections; the fifth and sixth sections contain IFT estimations of the properties of the fluid samples using two methods. Pressure and temperature effects, the selection of surfactants and co-surfactants, and determining the optimum concentrations of surfactant solutions for core-flood experiments are presented in the results and discussions section. Conclusions and recommendations close this chapter.

3.1 Introduction

The magnitude of the density and viscosity of a displacing fluid relative to the displaced fluid are important design variables that affect volumetric displacement efficiency. The tendency for gravity override or underride to occur is determined by the relative densities of the displaced and displacing fluids. Areal and vertical sweep efficiencies are in large measure determined by the mobility ratio in the displacement process, which is inversely proportional to the displacing-fluid viscosity.

Interfacial tension (IFT) is the force per unit length required to create new surface area at the interface between two immiscible fluids. IFT is also a condition of mechanical equilibrium at an interface.

Consider that two immiscible liquids, heptanes and water, are brought into contact. When a surfactant is added to this system, surfactant molecules absorb at the interface, displacing some of the heptane and water molecules there. The surfactant molecules orient themselves such that the hydrophilic part is directed into the water phase and the hydrophobic part into the heptane phase. Accumulation of the surfactant in the interfacial zone disrupts the fluid structure in this region. This is reflected in the rapid decrease in the IFT as the surfactant concentration increases up to critical miscible concentration (CMC).

The IFT between an aqueous surfactant solution and a hydrocarbon phase is a function of salinity, temperature, surfactant concentration, surfactant type and purity, and the nature of the hydrocarbon phase. The general behaviour of IFT between a relatively pure surfactant solution and a hydrocarbon phase is shown in Figure 3.1. The IFT decreases rather sharply as surfactant concentration increases until the CMC is reached. Beyond the CMC, little change in IFT occurs. Surfactant added in excess of the CMC contributes to the formation of micelles and does not increase the concentration at the water/hydrocarbon interface; thus, there is only a small incremental effect on IFT.

The IFT properties of petroleum sulphonate, which are mixtures, generally are similar to those of single-component surfactant systems. There is, however, a difference in that a sharp CMC is not usually observed (Gale & Sandvik 1973). The IFT between an aqueous surfactant system and a hydrocarbon phase may decrease significantly at concentrations well above the CMC, the point of onset of formation of micelles.

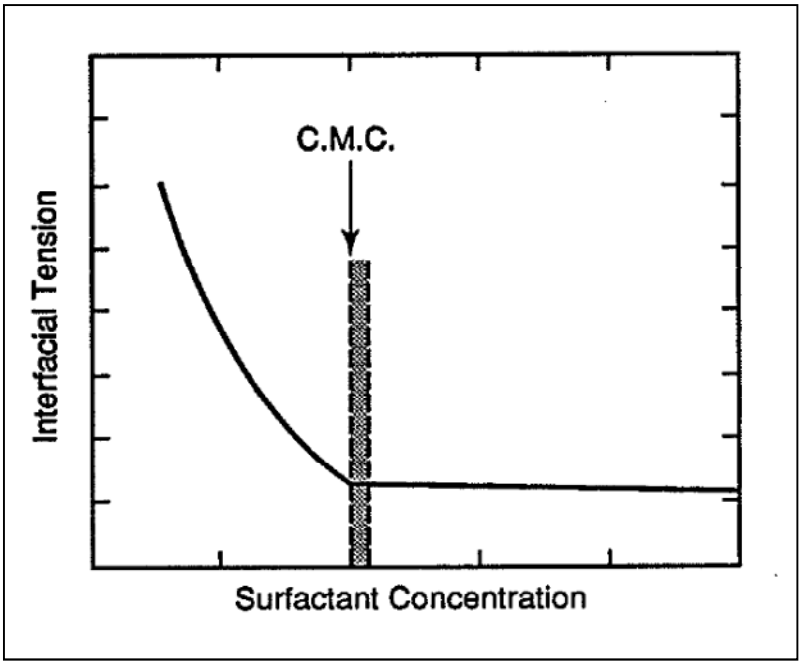

Figure 3.1 IFT as a function of pure single component surfactant concentration (Green & Willhite 1998)

3.1.1 Surfactants and IFTs in an EOR system

Surfactant systems that contain no or limited amounts of alcohol or co-surfactant exhibit ultralow IFT (Gale & Sandvik 1973). Puig *et al*. (1979) and Hall (1980) show that ultralow IFTs observed under these conditions are caused by the presence of a finely dispersed phase at the interface between the oil and brine. This mesophase is liquid crystalline, surfactant-rich, and often exhibits birefringence under polarized light. Puig *et al*. found that ultralow tensions were observed only when the particles were large enough to cause turbidity in the solution. Davis *et al.* (1983) presented a report on measurement of ultralow IFT. These systems have not been used successfully in field applications and are not considered further.

There are about 40 methods that have been used to measure IFT. The most common are: (1) Wilhelmy plate technique, (2) Du Nouy method, (3) Maximum bubble pressure, (4) Capillary rise method, (5) Drop volume or weight method, (6) Spinning drop technique and (7) pendant drop method. In this study, pendant drop and modified captive drop methods were used.

3.1.2 Micelles and critical micelle concentration (CMC)

The properties of surfactants (surface-active agents) indicate that colloidal aggregates are in solution (Rosen 1978). Figure 3.2 shows the formation of these aggregates, which are known as micelles.

At low concentrations of surfactant solution, surfactant molecules are dispersed as monomers. When surfactant concentration increases, the molecules tend to aggregate. After a specific concentration called critical micelle concentration (CMC), is reached, the formation of micelles starts a further addition of surfactant. The concentration of surfactant as monomers essentially remains constant above the CMC; the addition of surfactant after CMC is reached results in the formation of extra micelles but with relatively little change in monomer concentration (Green & Willhite 1998).

In the water based surfactant solution (Green & Willhite 1998), the micelles form with the tail portion directed inward and the head (polar) outward. Water is in the continuous phase, as shown at the lower right in Figure 3.2. In the hydrocarbon-

based surfactant solution, the orientation of the surfactant is reversed, as indicated at the upper right of the figure.

Ottewill (1984) summarizes the structure and properties of micelles, which were first described by Hartlet in 1934:

1. Micelles have a spherical shape. The micelle's radius is about as long as the hydrocarbon chain in the surfactant.

2. Micelles contain about 50 to 100 monomer units.

3. The process of micellization occurs over a very narrow concentration range.

4. For surfactants in an aqueous solution, the interior of the micelle is formed by the association of hydrocarbon chains. They have many of the properties of a liquid hydrocarbon, including the ability to solubilise organic compounds.

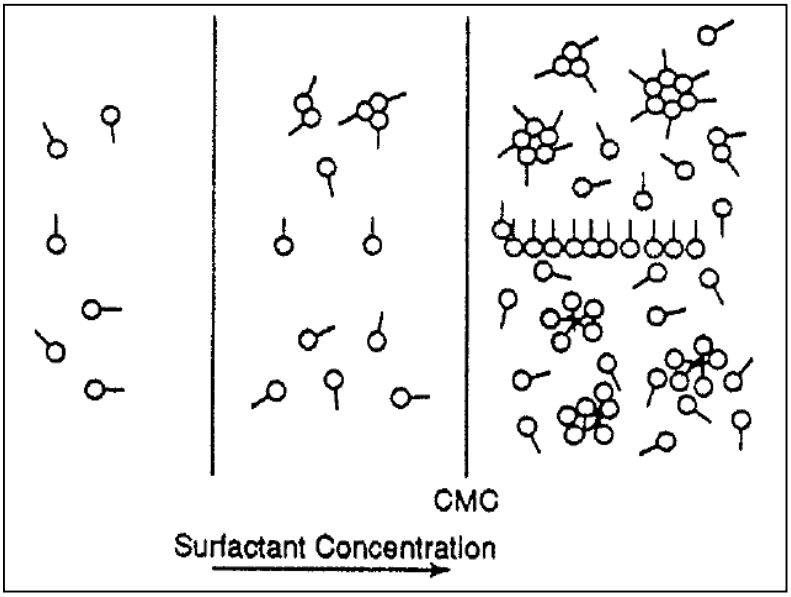

Figure 3.2 Formation of micelles (Green & Willhite 1998)

3.2 Selection of Optimum Concentration

The optimum concentration of a surfactant/co-surfactant in an oil-water-surfactant/co-surfactant system can be defined as the concentration which is just above the lowest IFT value or CMC.

The IFT between an aqueous surfactant solution and a hydrocarbon phase is a function of salinity, temperature, surfactant concentration, surfactant type and purity, and the nature of the hydrocarbon phase. The IFT decreases rather sharply as surfactant concentration increases, until the CMC is reached; beyond this, little change in IFT occurs. Surfactant added in excess of the CMC contributes to the formation of micelles and does not increase the concentration at the water/hydrocarbon interface; thus, there is only a small incremental effect on IFT.

The IFT properties of petroleum sulphonates, which are mixtures, generally are similar to those of single-component surfactant systems. There is, however, a difference in that a sharp CMC is not usually observed by Gale and Sandvik (1973). The IFT between an aqueous surfactant system and a hydrocarbon phase may decrease significantly at concentrations well above the CMC, the point of onset of formation of micelles.

3.3 Density Measurement

A DE40 Delta range density meter at CSIRO laboratory was used to measure fluid densities. This meter works based on the electromagnetically induced oscillation of a U-shaped glass tube.

3.3.1 Methodology

Stepwise procedure:

Step 1: The U-tube was cleaned with n-Hexane followed by water and then acetone to remove trace amounts of water.

Step 2: The DE 40 density meter was calibrated with air and standard water.

Step 3: An injector syringe was used to fill the U-tube with fluid sample to 1.1ml to 1.2 ml. To get a correct value, the tube must be free of air bubbles.

Step 4: The required temperature range was set and then a density measurement was taken.

Figure 3.3 DE40 Delta range density meter

3.4 Viscosity Measurement

A Cambridge viscosity piston-style viscometer was used to measure the viscosity of the fluid sample including oil. It had two magnetic coils inside a stainless steel chamber. The pistons were light stainless steel, placed in the measurement chamber and magnetically moved back and forth in the fluid sample.

3.4.1 Methodology

Stepwise procedure:

Step 1: The viscometer was cleaned with n-Hexane, followed by water and then acetone to remove trace amounts of water.

Step 2: After estimating the range of viscosity of the fluid sample, a piston suitable for that range was selected.

Step 3: The chamber was filled with the required fluid sample to approximately 0.6 ml.

Step 4: The piston was inserted and pushed gently into the chamber.

Step 5: The required temperature range was set using a heating/cooling oil bath system.

Step 6: Measurement was started by selecting the appropriate operating mode; ‘analyse’ and ‘report’ were selected.

Step 7: The viscosity value was taken after the system stabilized.

Figure 3.4 Cambridge piston style viscometer

3.5 IFT measurement

3.5.1 Pendant drop method

A Temco pendant drop interfacial tension cell at CSIRO was used for IFT measurements. A transparent enclosed chamber with temperature and pressure control and optical observation equipment was required. The IFT cell provided an

environment in which the oil drop was in equilibrium with other fluids, in a simulation of in-situ reservoir conditions.

The cell (Temco 2005) can measure pressure up to 10,000 psi and temperature to 175 ^{o}C. This wide range covers most reservoir conditions. The system consists of a high pressure and temperature IFT cell, a hand pump to inject oil and water through the cell, oil and water stock cells, needles, pressure and temperature controllers, a vibration free table, a back pressure regulator, and an imaging system including camera, lamp and software to analyse the captured pictures.

3.5.1.1 Equation for IFT measurement

Oil drop dimensions and fluid densities were required to determine IFT. Figure 3.6 shows the oil drop dimensions and fluid densities required for Eq 3.1. The oil pendant produced by IFT is presented in Figure 3.5.

The following equation (Temco 2005) was used to calculate IFT:

$$\sigma = \frac{\Delta\rho \times g_c \times d_e^2}{H} \tag{3.1}$$

where

$\Delta\rho$ = Difference between fluid densities (g / ml)

σ = Interfacial Tension (IFT), (dyne / cm)

$g_c = 981\,(\mathrm{cm}/\mathrm{sec}^2)$

d_e = Original equatorial diameter of the drop (cm)

$1/H = f\left(d_s/d_e\right) = f(s)$

d_s = Drop diameter with the vertical length (d_e) from the apex of the drop (cm)

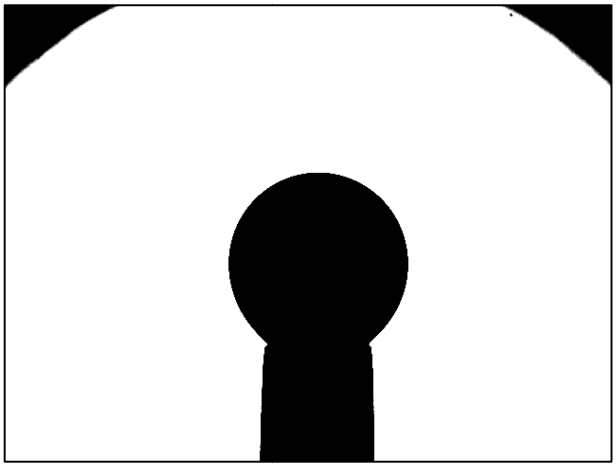

Figure 3.5 Pendant produced from IFT cell

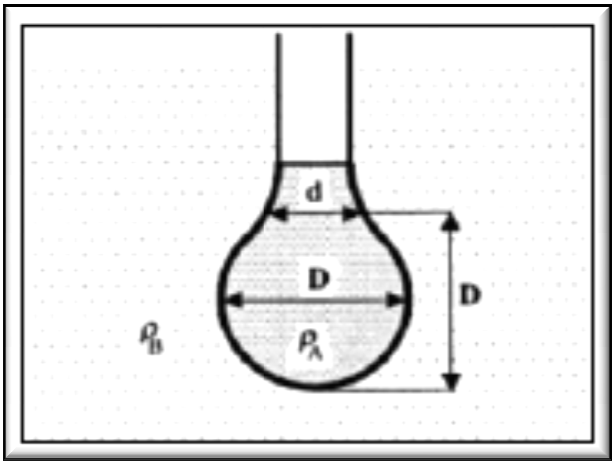

Figure 3.6 Oil drop dimensions and fluid densities

3.5.1.2 Methodology

Stepwise procedure:

Step 1: The IFT cell was calibrated by measuring the IFT of water at 72.2 mN/m at ambient condition.

Step 2: The hand pump was used to fill both transferring cells with relevant fluids.

Step 3: The IFT cell was filled with brine using the hand pump, then the system was calibrated by measuring the needle size while running the software.

Step 4: An oil bubble was formed by pumping crude oil through the needle.

Step 5: Test pressure was set by injecting brine into the cell, and the temperature was set by a thermocouple which surrounded the cell.

Step 6: After reaching the desired pressure and temperature for each measurement, the cell was kept for a period of about 30 minutes in stable conditions to allow the two phases to reach equilibrium; at that point measurement of the IFT was conducted by running the software.

Step 7: The base case was duplicated to verify the results.

Step 8: The IFT cell, lines and cylinder were cleaned first with n-Hexane and then with acetone and water, and dried with air flow.

Step 9: The IFT between brine and crude oil for every temperature and pressure was measured for 100 points, with a 5-second interval to increase accuracy. The software measured the bubble's geometrical properties and IFT values and calculated the standard deviation for data.

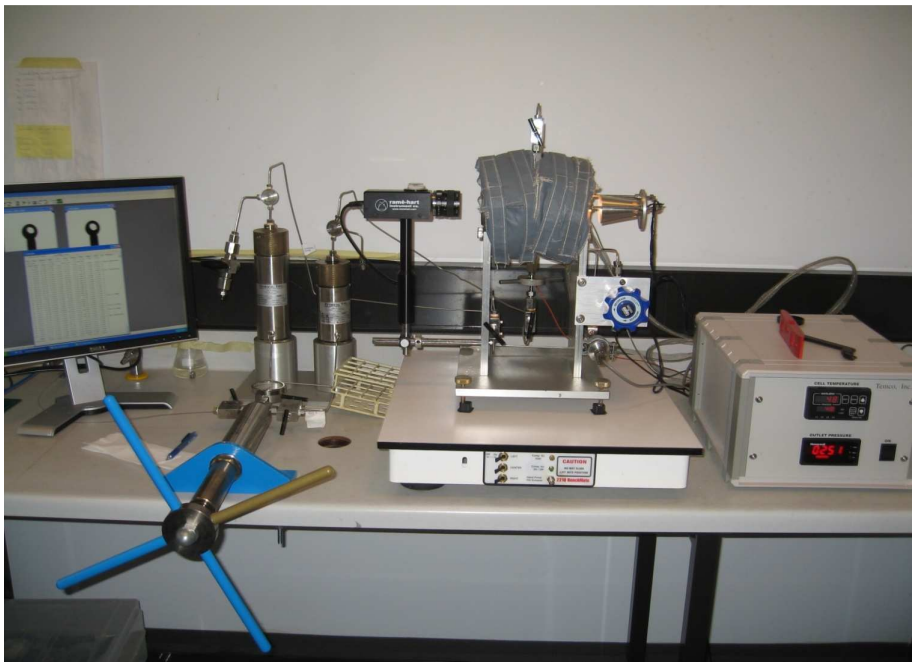

Figure 3**.7 Temco pendant drop IFT cell**

3.5.2 Modified captive drop or single sessile drop

Methods for measuring IFT from the dimensions of a sessile drop have been known for a century. Captive drop cell (Shahri 2012) was modified by Hamid Ahmed Mohammed Ghafram Al Shahri. He is friend of mine. I helped him to buy new camera from my project money and to set up the camera.

The silhouette of a sessile drop submerged in a transparent bulk phase appears to possess a contact angle of 180 with a plane solid support when the drop is separated from the solid surface by a thin film of surrounding fluid.

3.5.2.1 Materials

1. Crude oil; 2. Surfactants, alcohol and brine solution.

3.5.2.2 Apparatus

1. Light source; 2. Droplet chamber; 3. Macro lens; 4. Tube extension; 5. Camera; 6. Macro sliding head; 7. Tri-axial camera base fixed to tripod; 8. Lockable rotating head; 9. Tripod to hold the sliding head; 10. Laptop computer for camera remote control; 11. A syringe; 12. A plastic pipette.

Figure 3.8 Modified captive drop IFT cell

3.5.2.3 Calibration reference

The distance in pixels had to be converted to centimetres as the image processing gave dimensions only in pixels. In order to calculate the IFT the droplet height and median diameter were converted into real distance. The object was moved into the plane of focus in front of the lens; the lens focus was adjusted to infinity or 1:1. The plane of focus of the camera had same distance per pixel scale when the focus was adjusted to infinity.

The distance per pixel in the plane of focus was calibrated against a focused image of the vernier scale. The images were 5184 by 3456 pixels and the scale was 1 mm per division. The horizontal and vertical distances were calibrated. The distance per pixel was found equal to 1.847×10^{-4} cm/pixel and 1.838×10^{-4} cm/pixel for the horizontal and vertical distances respectively.

Figure 3.9 Calibration images of vernier scale for 1:1 lens focus (1 division = 1 mm).

3.5.2.4 Experimental procedure

Stepwise procedure:

Step 1: The lens focus was adjusted to infinity or 1:1 and kept constant during the experiment.

Step 2: The bubble was levelled horizontally, to both the camera and the cell, by adjusting the tripods, tri-axial camera base and lockable rotating head.

Step 3: The platform, which was made of Teflon, was placed close to the front glass window.

Step 4: The Teflon platform was brought into focus in the camera screen by rotating its knobs and by moving the cell bi-directionally using the sliding head.

Step 5: The cell was filled with about 25 ml of oil and left for about 10–15 minutes to settle down.

Step 6: A drop of aqueous solution (surfactant, alcohol and brine mixture) was ejected onto the platform through a syringe and time was monitored.

Step 7: Drop focus was refined by rotating the knobs of the sliding head until the drop was in focus in the centre of the lens.

Step 8: The drop image was taken and the time recorded when the drop was in focus. A plastic pipette was used to suck out the aqueous droplet after each measurement.

3.5.2.5 Equation used for measurement

Malcolm and Elliot (1980) derived an equation to measure IFT for special cases of captive drop. They made two assumptions: (1) that the contact angle was $180^{o;}$ and (2) that the drop was separated from the platform by a thin film of surrounding fluid. Their equation was:

$$\sigma = \Delta\rho \times g_c \left(\frac{h}{G(h/d)} \right)^2 \qquad (3.2)$$

Where

σ = interfacial tension (IFT), (dyne/cm)

$\Delta\rho$ = difference between fluid densities (g/cc)

g_c = local earth gravitational acceleration (cm/sec^2)

d = median diameter of the drop (cm)

h = height of the drop from its base to the apex of the drop (cm)

G (h/d) = fourth order polynomial shape factor = 1.86519 + 2.807066(h/d) – 9.430927(h/d)^2 + 8.669726(h/d)^3 – 3.660622(h/d)^4

3.5.2.6 Methodology

3.5.2.6.1 Image capture and analysis

a. A focused image of the droplet's height and diameter were measured in pixels and then processed by ImageJ and GIMP, both image processing software.

b. An Excel template worksheet was set up to convert these dimensions to distances.

c. IFT was calculated using Equation 3.2 (above).

d. The input parameters were droplet height, maximum horizontal diameter in distance, oil and aqueous densities. The output parameter from this software was IFT.

3.5.2.6.2 Refractive index correction

Light passed through glass (window of the cell), oil (surrounding of the droplet), and air (outside the cell), to the lens. The difference in refractive indices of glass, oil, and air may produce an apparent size of the drop that is different to its actual size.

Shahri (2012) performed an experiment to see the effect of changes to the apparent droplet size induced by differing refractive indices. He found that changes in height and width were very small and could be neglected.

3.5.2.6.3 Contact angle correction

The silhouette of a sessile drop submerged in a transparent bulk phase appears to possess a contact angle of 180 with a plane solid support when the drop is separated from the solid surface by a thin film of surrounding fluid.

The assumptions of a sessile drop are: (1) that the contact angle equals 180^{o} and (2) that the drop is separated from the solid support by a film of bulk fluid of negligible thickness.

The top surface of the Teflon platform was machined to a concave shape and smoothed with abrasive paper. The smoothing process was intended to increase the micro-roughness of the Teflon surface, enhancing its hydrophobicity from a hydrophobic state to a superhydrophobic state (Guo *et al.* 2009). Shahri, (2012) did

contact angle measurements using this cell and found that the surface of the Teflon platform was superhydrophobic to water in the presence of surrounding oil when the contact angle was very close to 180^{o}. He considered that IFT measurements using this cell are an estimation of IFT that provides indicative values of the closest results.

3.6 Results and Discussion

IFT reduction can contribute enormously to oil recovery. The effects of pressure and temperature on IFT were investigated in this study included the pendant drop method, used to measure low concentrations of surfactant and alcohol, because at high concentration it is difficult to produce a stable pendant and estimate IFT. It is almost impossible to measure ultra-low IFT by the pendant drop method. For this reason, the selection of surfactant, the effect of alcohol concentration on IFT, and effects of temperature and pressure on IFT were observed using the pendant drop method. The captive drop method was used to estimate IFT at higher concentrations of surfactant and co-surfactant.

The experiments were conducted to measure IFT between: (1) brine and stag crude oil at different temperatures and pressures; (2) green surfactant and alcohol mixtures and stag oil at low concentration at different temperatures and pressures, and (3) green surfactant and alcohol mixtures and Ondina 68 oil at high concentrations.

3.6.1 Density of fluid

To measure IFT it is necessary to estimate oil and fluid densities and viscosity. Stag oil and Shell Ondina 68 mineral oil densities were measured with a DE40 Delta Range density meter; the results are tabulated in Table 3.1 and plotted in Figure 3.10 below. It was found from both curves that there was a linear relationship between oil density and temperature. Oil densities decrease with increases in temperature.

Table 3.1 Oil densities

	Stag oil	Ondina 68
Temperature (^oC)	Density (gm/cc)	Density (gm/cc)
20	0.9412	0.8638
30	0.9347	0.8576
40	0.9282	0.8515
50	0.9216	0.8452
60	0.9151	0.8391

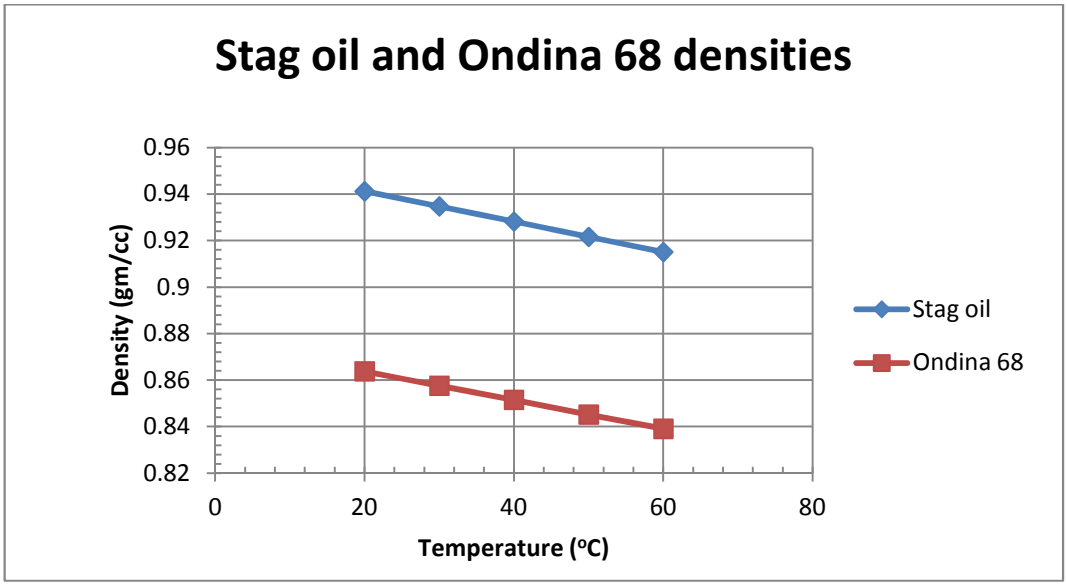

Figure 3.10 Stag oil and Ondina 68 densities change with temperature

Surfactant, alcohol and brine solution densities were measured; results are shown in the tables below. Table 3.2 contains APG 264, 0.8% Octanol and 2% NaCl density values at a temperature range of 20^{o}C to 60^{o}C. APG 264 concentrations varied from 0.5% to 3%. Table 3.3 presents APG 8166, Pentanol and NaCl solution densities at 20^{o}C and 50^{o}C. Both tables show that solution density decreases with temperature. Bio-surfactant and butanol, and bio-surfactant and Pentanol density data, at 20^{o}C and 50^{o}C, are shown in Table 3.4. APG 264, 8105, 8105, and 8166, surfactant solutions' densities are compared in Table 3.5.

Table 3.2 APG 264, Octanol and NaCl formulation densities

Sample No	Formation composition							
		Temp (^oC)	20	25	30	40	50	60
1	0.5 % APG, 0.8% Octanol and 2% NaCl	Density (gm/cc)	1.0123	1.0108	1.0094	1.0058	1.0014	0.9964
2	1.0 % APG, 0.8% Octanol and 2% NaCl	Density (gm/cc)	1.0128	1.01155	1.0099	1.0063	1.0019	0.9970
3	1.5 % APG, 0.8% Octanol and 2% NaCl	Density (gm/cc)	1.0130	1.0115	1.0100	1.0064	1.0020	0.9972
4	2.0 % APG, 0.8% Octanol and 2% NaCl	Density (gm/cc)	1.0132	1.0117	1.0102	1.0065	1.0021	0.9973
5	2.5% APG, 0.8% Octanol and 2% NaCl	Density (gm/cc)	1.0135	1.012	1.0105	1.0068	1.0023	0.9975
6	3 % APG, 0.8% Octanol and 2% NaCl	Density (gm/cc)	1.0141	1.0126	1.0111	1.0074	1.0029	0.9981
7	Base Case (2% NaCl)	Density (gm/cc)	1.0122	1.0107	1.0093	1.0058	1.0014	0.9966

Table 3.3 APG 8166, Pentanol and NaCl formulation densities

Sample No	Formation composition			
		Temp (^{o}C)	20	50
1	10 mg/l APG, and 2% NaCl	Density (gm/cc)	1.0123	0.9935
2	30 mg/l APG, and 2% NaCl	Density (gm/cc)	1.0122	1.0007
3	40 mg/l APG, and 2% NaCl	Density (gm/cc)	1.0123	1.0014
4	50 mg/l APG, and 2% NaCl	Density (gm/cc)	1.0123	1.0008
5	10 mg/l APG, 15 mg/l Pentanol and 2% NaCl	Density (gm/cc)	1.0129	1.0017
6	10 mg/l APG, 30 mg/l Pentanol and 2% NaCl	Density (gm/cc)	1.0125	0.9968
7	10 mg/l APG, 60 mg/l Pentanol and 2% NaCl	Density (gm/cc)	1.0126	1.0018
8	10 mg/l APG, 120 mg/l Pentanol and 2% NaCl	Density (gm/cc)	1.0122	1.0022

Table 3.4 Bio-surfactant, Butanol, Pentanol and NaCl formulation densities

Sample No	Formation composition			
		Temp (^{o}C)	20	50
1	10 mg/l Bio-surfactant and 2% NaCl	Density (gm/cc)	1.0124	1.0018
2	3 mg/l Bio-surfactant and 2% NaCl	Density (gm/cc)	1.0125	1.0019
3	6 mg/l Bio-surfactant and 2% NaCl	Density (gm/cc)	1.0124	1.0017
4	3 mg/l Bio-surfactant 0.5% Butanol and 2% NaCl	Density (gm/cc)	1.0117	1.0010
5	3 mg/l Bio-surfactant 0.5% Pentanol and 2% NaCl	Density (gm/cc)	1.0124	1.0017

Table 3.5 APG 264, 8105, 8105, and 8166, and NaCl formulation densities

Sample No	Formation composition			
		Temp (^{o}C)	20	50
1	3 mg/l APG 264 and 2% NaCl	Density (gm/cc)	1.0124	1.0018
2	3 mg/l APG 8105 and 2% NaCl	Density (gm/cc)	1.0123	1.0013
3	3 mg/l APG 8107 and 2% NaCl	Density (gm/cc)	1.0123	1.0016
4	3 mg/l APG 8166 and 2% NaCl	Density (gm/cc)	1.0123	1.0017

3.6.2 Viscosity of fluid

Stag oil viscosity at temperatures between 20^{o}C and 60^{o}C were measured with a Cambridge viscometer; results are shown in Table 3.6 and plotted in Figure. 3.10. It was found that oil viscosity decreases with an increase of temperature.

Table 3.6 Stag oil viscosity

	Stag oil
Temperature (^{o}C)	Viscosity (cP)
21	126.10
30	65.57
41	35.75
50	23.46
60	15.62

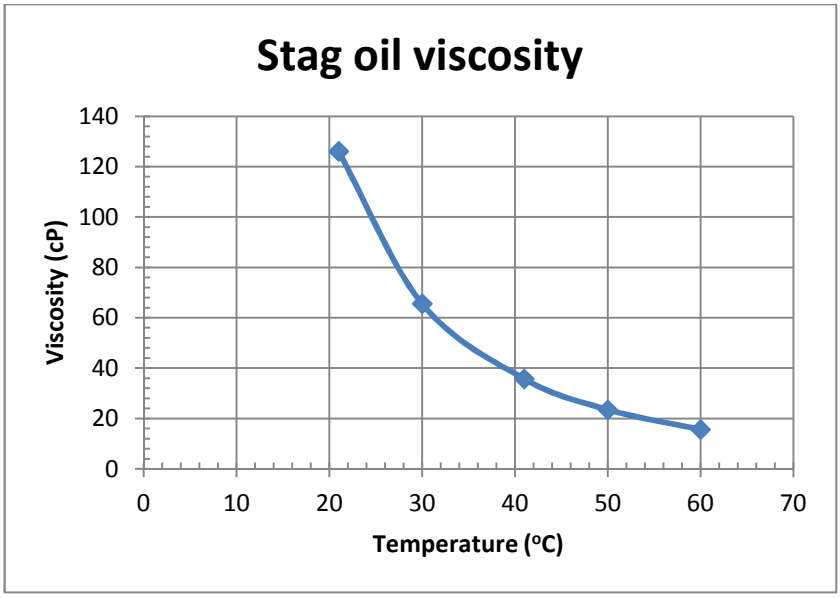

Figure 3.11 Stag oil viscosity change with temperature

3.6.3 Selection of surfactant

In this study, IFT measurements were taken at a constant concentration of surfactants of 3 mg/l and salinity of 2% NaCl in laboratory conditions (temperature 20^{o}C and ambient pressure). The IFT values are tabulated in Table 3.7 and plotted against the anionic and non-ionic surfactants in Figure 3.12. Four non-ionic surfactants (APG 8166, APG 8105, APG 8107, and APG 264) and one anionic surfactant (JF-2 bio-surfactant) were taken into consideration. Alkyl group carbon number, actives in percentage (%), and hydrophilic/lipophilic balance (HLB) values were supplied by Cognis; they are shown in Table 3.7. HLB is the balance between the hydrophilic and hydrophobic parts of a surfactant that gives it the characteristics associated with a surface-active agent. HLB is an empirical number that has sometimes been used to characterize surfactants (Garret 1972); it indicates the relative tendency to solubilise in-oil or oil-in-water emulsions. Low HLB numbers are assigned to surfactants that tend to be more soluble in oil and to form water-in-oil emulsions and give lower IFT values.

IFT measurements were made to select surfactants from the non-ionic group. It was found that APG 264 gave the lowest IFT value in the non-ionic group. The lowest IFT value shown in Figure 3.12 is 1.63 dyne/cm. APG 8166 did not show promising

IFT reduction although it had a low HLB value. IFT values of APG 8105 and APG 8107 were 5.59 dyne/cm and 2.93 dyne/cm.

Bio-surfactants reduced IFT from 12.65 dyne/cm to 2.53 dyne/cm. In this study, we got only JF-2 bio-surfactant from the anionic group. For this reason it was selected.

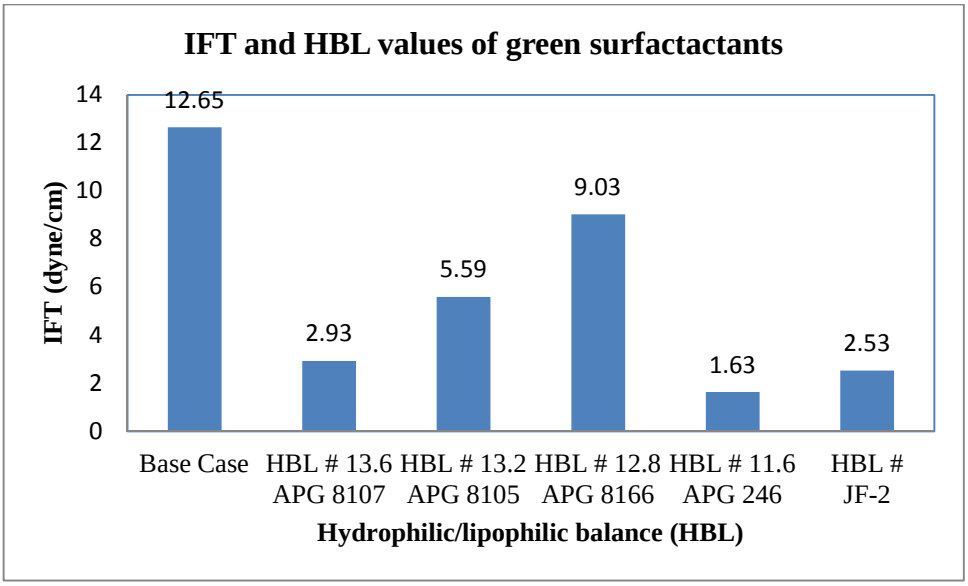

Figure 3.12 Comparison of IFT and HBL values of anionic and non-ionic green surfactants under laboratory conditions (20^{o}C and ambient pressure)

Table 3.7 APG surfactant properties

Property	APG Type				Bio-surfactant
	8105	8107	8166	264	JF-2
Alkyl Group [a] (Carbons)	8 - 10	8 - 10	8 - 16	12 - 14	
Actives % [a]	60	70	50	50	
HLB [a]	13.2	13.6	12.8	11.6	
IFT (dyne/cm)[b]	5.59	2.93	9.03	1.63	2.53
a. Values supplied by Cognis b Values measured under laboratory conditions (3mg/l surfactant, 2% NaCl)					

3.6.4 Effect of temperature on combinations of green surfactant and alcohol

The object of the study was to examine the effect of alcohols (butanol and pentanol), in combination with bio-surfactants, on IFT under laboratory and reservoir conditions.

The CSIRO MEOR group performed an experiment to produce bio-products by petroleum microbe population after anaerobic cultivation on molasses for two weeks at 50^{o}C. It was found that about 174500 (ng/ml) of 1-proponal, 64000 (ng/ml) 1-butanol, 124500 (ng/ml) of 2,3-methyl butanol, and 14000 (ng/ml) of 1-Pentanol of aliphatic alcohol were produced. Butanol production was higher that of pentanol. The value of butanol was 188500 (ng/ml).

In this study, three samples were prepared to measure IFT. First was 3 mg/l bio-surfactant and 2% NaCl; the second was 3 mg/l bio-surfactant, 0.5% butanol and 2% NaCl; and the third was 3 mg/l bio-surfactant, 0.5% pentanol and 2% NaCl. Results are presented in Figure 3.13. A formulation of APG 8166 surfactant at a concentration of 3 mg/l and pentanol at a concentration of 0.5% was taken into consideration because APG 8166 has low HLB value. IFT values are presented in Table 3.8. It was found butanol was more active in reducing IFT than pentanol under laboratory conditions. Based on this result, butanol was taken into consideration for the core-flooding experiment.

Table 3.8 Bio-surfactant, Butanol, Pentanol and NaCl formulation IFT

S/L	Formulations	IFT	
		Laboratory (T 20 ^{o}C & P amb)	Reservoir T 50^{o}C & T 1000 psi
	2% NaCl	12.65	
	3 mg/l Bio-surfactant and 2% NaCl	2.53	2.56
	3 mg/l Bio-surfactant 0.5% Butanol and 2% NaCl	1.75	2.75
	3 mg/l Bio-surfactant 0.5% Pentanol and 2% NaCl	2.4	
	10 mg/l APG 8166 and 2% NaCl	3.96	5.55
	10 mg/l APG 8166, 0.5% Pentanol and 2% NaCl	5.63	5.56

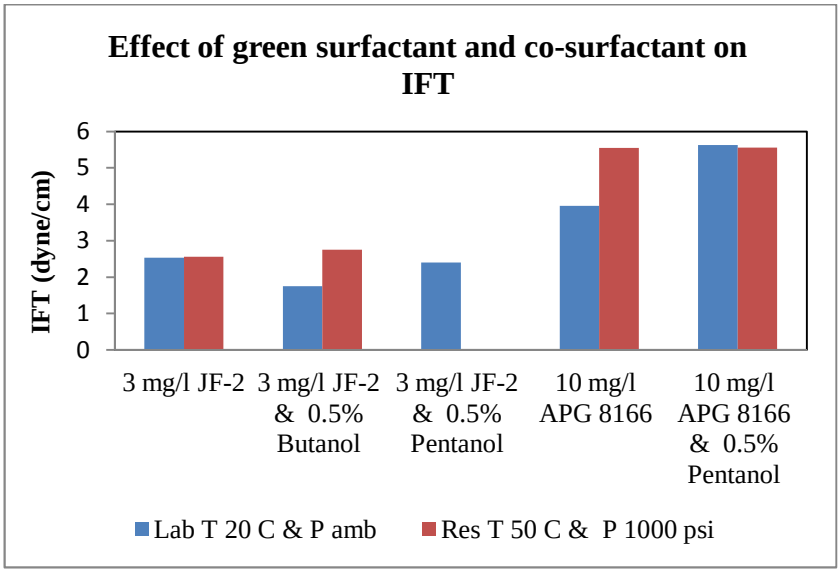

Figure 3.13 Effect of green surfactant and co-surfactant on IFT under laboratory conditions (20^{o}C and ambient pressure) and reservoir conditions (50^{o}C and 1000 psi)

3.6.5 Selection of optimum bio-surfactant concentration

Six samples of JF-2 bio-surfactant at concentrations from 10mg/l to 60mg/l at a constant concentration of 0.5% butanol and salinity of 2% NaCl were prepared, and IFT values were measured by the captive drop method, described previously. The Ondina Oil 68 (Shell) and Ondina Oil 15 (Shell) were from the Shell Company of Australia Ltd. The IFT values are tabulated in Table 3.9 and plotted against the bio-surfactant concentration in Figure 3.14. The first value on the plot is 0.00mg/l of bio-surfactant concentration, equal to 27 dyne/cm. The IFT decreased to 1.833 dyne/cm as the bio-surfactant concentration increased to 20 mg/l. Between 20 mg/l and 60mg/l, IFT remained steady and close to 1.8 dyne/cm. It was conservatively estimated that at concentrations above 50mg/l it remained unchanged.

An oil-brine IFT equal to 27 dyne/cm is within the normal range of IFT for different oil-water systems (Donaldson *et al.* 1969). At 20mg/l the IFT was 1.83 dyne/cm. The CMC of synthetically purified JF-2 bio-surfactant was close to 10mg/l (Rosen 1978). The IFT remained unchanged until the bio-surfactant reached 40mg/l, at which point it decreased again to 1.787 dyne/cm. It is believed that that a third phase containing

oil, water and a microemulsion with very low IFTs had formed in this concentration range.

Two low concentrations were identified from these data: 40mg/l and 60mg/l; they were selected for the core-flooding experiment.

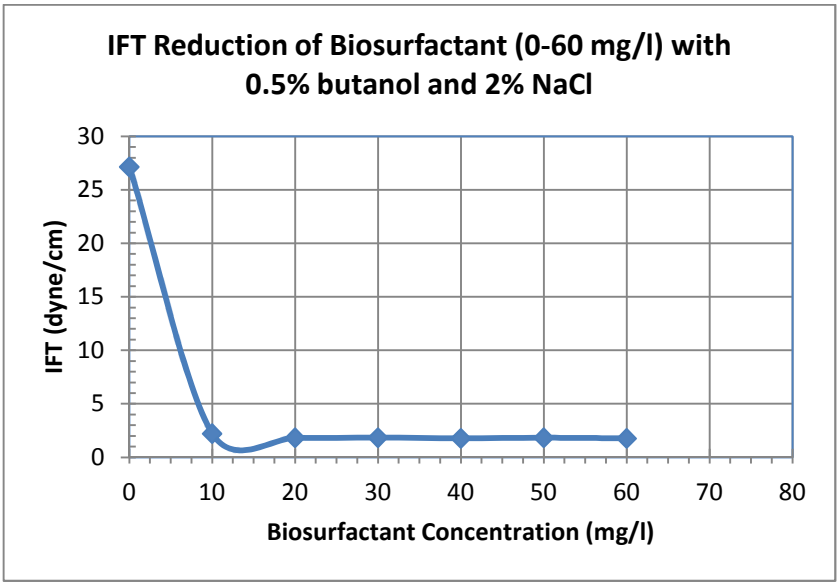

Figure 3.14 IFT reductions in JF-2 bio-surfactant at concentrations from 0mg/l to 60 mg/l with 2% NaCl under laboratory conditions

Table 3.9 IFT values of bio-surfactant at various concentrations and butanol at constant (0.5%) concentration

JF-2 bio-surfactant concentration (mg/l)	IFT dyne/cm
0	27.1520
10	2.2230
20	1.8330
30	1.8520
40	1.7870
50	1.8350
60	1.7730

3.6.6 Selection of optimum APG 264 concentration

Nine samples of APG 264 surfactant at concentrations from 0.2% to 2.0% and a constant salinity of 2% NaCl were prepared, and IFT values measured by the captive drop method described previously. The Ondina Oil 68 (Shell) and Ondina Oil 15 (Shell) came from the Shell Company of Australia Ltd. The IFT values are tabulated in Table 3.10 and plotted against the bio-surfactant concentration in Figure 3.15.

The IFT value dropped sharply from 27 dyne/cm to 1.3 dyne/cm with the increase of APG concentration to 0.2%. After that it rose slightly 1.3dyne/cm to 1.4 dyne/cm between concentrations 0.2% and 1.8% and then fell to 1.3 dyne/cm at 2% APG surfactant. At concentrations greater than the CMC, micelle formation stops or greatly slows the decrease in IFT (Rosen 1978). It was found that APG concentrations beyond 0.4% brought no reduction of IFT; The APG concentration 0.5% was therefore selected for the core-flooding experiment.

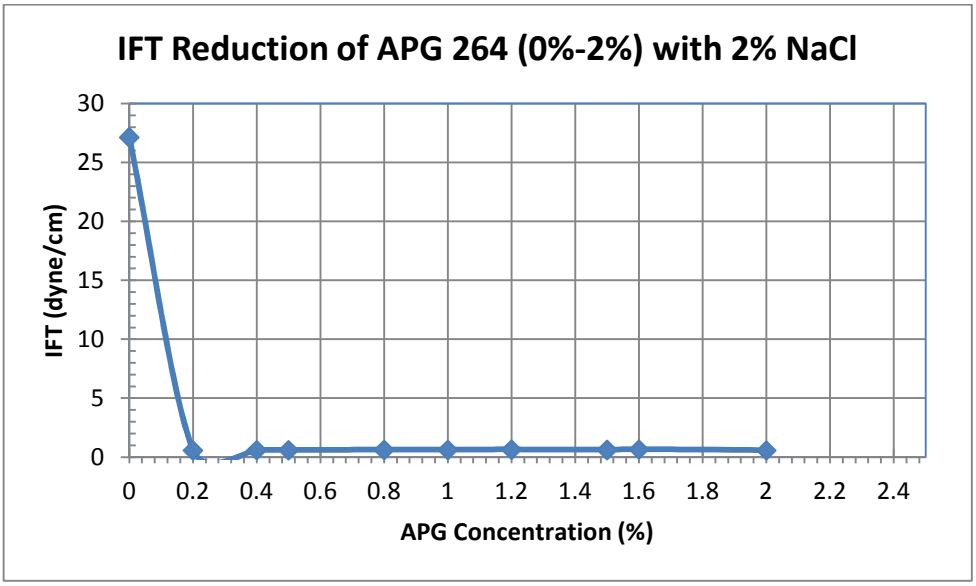

Figure 3.15 IFT reduction APG 264 surfactant at concentration from 0% to 2% with 2% NaCl under laboratory conditions

Table 3.10 IFT values of APG 264 surfactant at different concentrations

APG 264-surfactant concentration (%)	IFT dyne/cm
Base case	27.1520
0.20	0.5798
0.40	0.6121
0.50	0.6057
0.80	0.6225
1.00	0.6317
1.20	0.6451
1.50	0.6247
1.60	0.6613
2.00	0.5850

3.6.7 Selection of the optimum combined concentration of APG 264 and butanol

To analyse the effect of Butanol combined with APG 264 on IFT, measurements were taken of a constant APG 264 concentration with butanol concentrations ranging from 0.4% to 2.0%. Salinity of 2% NaCl was used for all samples in this set of experiments. IFT data for different butanol concentrations are shown in Table 3.11; IFT data are plotted against co-surfactant concentrations in Figure 3.16.

The first IFT value on the plot is at 0.0% of butanol concentration, and is equal to 27 dyne/cm. After that IFT went down to 1.211 dyne/cm at a butanol concentration of 0.4%, then maintained the same level of 1.2 dyne/cm between 0.4% and 1.0 % before falling slowly to 1.1 dyne/cm at 1.05%.

The two lowest IFTs were 1.211 dyne/cm between 0.4% and 1.0%, and 1.05 dyne at 1.5%. To be on the safe side, butanol concentrations greater than 0.4% can be taken for core-flooding as in concentrations greater than the CMC, micelle formation stops, or greatly slows, the decrease in IFT (Rosen 1978).

Butanol concentration 0.5% with 0.5% APG 264 was selected for the core-flooding experiment.

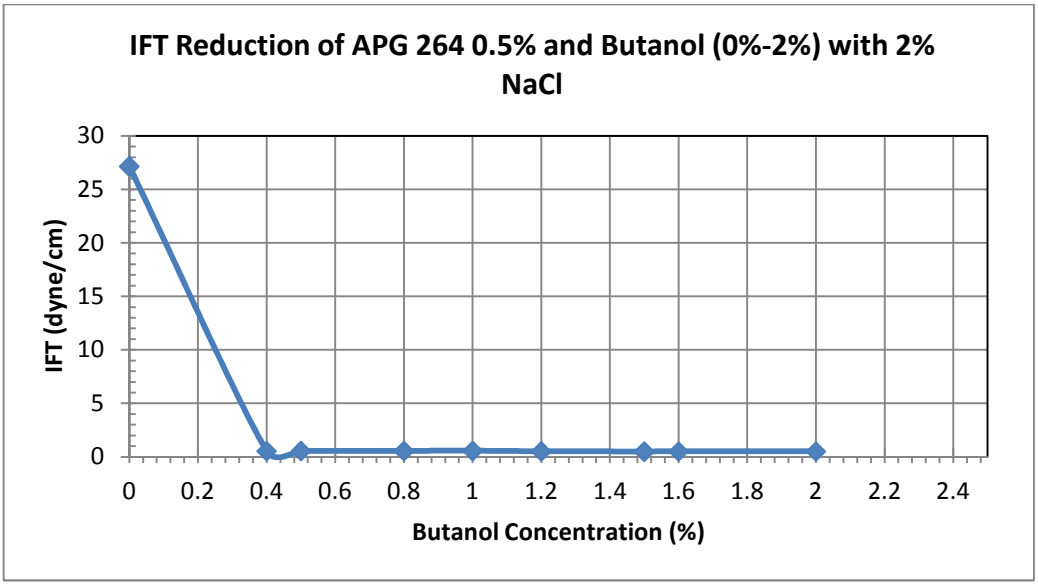

Figure 3.16 IFT reduction APG 264 surfactant at concentration 0.5% and butanol concentrations from 0.4% to 2%, with 2 % NaCl, under laboratory conditions

Table 3.11 IFT values of APG 264 0.5% and butanol at concentrations from 0.4 5 to 0.2%

Formulations	IFT dyne/cm
Base case	27.1520
APG 0.5% + B'ol 0.4%	0.5380
APG 0.5% + B'ol 0.5%	0.5520
APG 0.5% + B'ol 0.8%	0.5510
APG 0.5% + B'ol 1.0%	0.5610
APG 0.5% + B'ol 1.2%	0.5150
APG 0.5% + B'ol 1.5%	0.4930
APG 0.5% + B'ol 1.6%	0.5080
APG 0.5% + B'ol 2.0%	0.5060

3.6.8 Selection of optimum combined concentration of APG 264 and bio-surfactant

In this stage, the effect of anionic and non-ionic surfactant mixtures on IFT reduction was examined. The optimum concentration of APG 264 was already determined, based on the lowest IFT value, as 0.5%. Here the optimum concentration of bio-surfactant was examined.

Eleven samples of bio-surfactant in concentrations from 10mg/l to 57mg/l with a constant concentration of 0.5% APG 264 were prepared. IFT values were measured and are shown in Figure 3.17 and Table 3.12.

IFT decreased substantially about 25 dyne/cm from 27 dyne/cm to 1.33dyne/cm at the beginning of bio-surfactant concentration. It reduced gradually to 1.17 dyne/cm at 45mg/l of bio-surfactant concentration. After that it increased slowly and remained steady. It was found that there was no further reduction of IFT after 45mg/l. In conclusion, based on the figure optimum concentration can be selected as 45pmm.

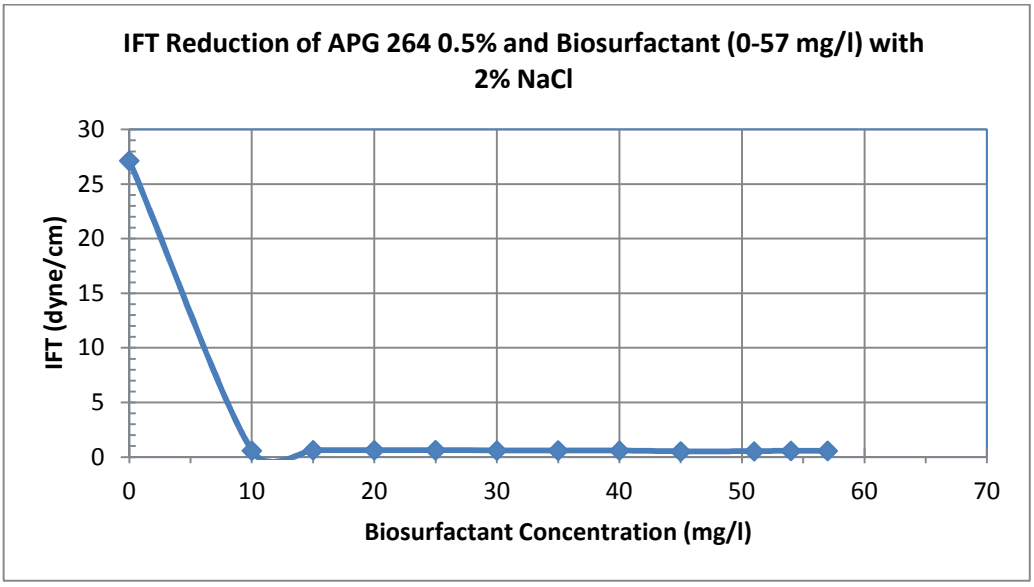

Figure 3.17 IFT reduction APG 264 0.5% and bio-surfactant at concentrations from 0 mg/l to 57 mg/l with 2% NaCl, under laboratory conditions

Table 3.12 IFT values of solutions of APG 0.5%, bio-surfactant (0-57mg/l) and 2% NaCl

Formulations	IFT dyne/cm
Base case	27.1520
APG 0.5% +BS 10mg/l	0.5940
APG 0.5% +BS 15mg/l	0.6380
APG 0.5% +BS 20mg/l	0.6400
APG 0.5% +BS 25mg/l	0.6380
APG 0.5% +BS 30mg/l	0.6080
APG 0.5% +BS 35mg/l	0.6100
APG 0.5% +BS 40mg/l	0.5990
APG 0.5% +BS 45mg/l	0.5210
APG 0.5% +BS 51mg/l	0.5380
APG 0.5% +BS 54mg/l	0.5790
APG 0.5% +BS 57mg/l	0.5810

3.6.9 Selection of optimum combined concentration of APG 264, bio-surfactant and Butanol

This study was conducted to select the optimum concentration of co-surfactant with blending of non-ionic and anionic surfactants. 0.5% APG 264 and 45 mg/l of bio-surfactant were mixed with 0.4% to 1.2% butanol. Measured IFT data are presented in Figure 3.18 and Table 3.13.

Between concentrations 0.4% and 1.2%, IFT went down 0.12 dyne/cm, from .0.91 dyne/cm to 0.79 dyne/cm. IFT rose slightly to 0.85 dyne/cm at 1.2% butanol concentration. The lowest IFT value in this system was 0.71 dyne/cm at 1.2%. It is the most likely optimum concentration for the micelle system.

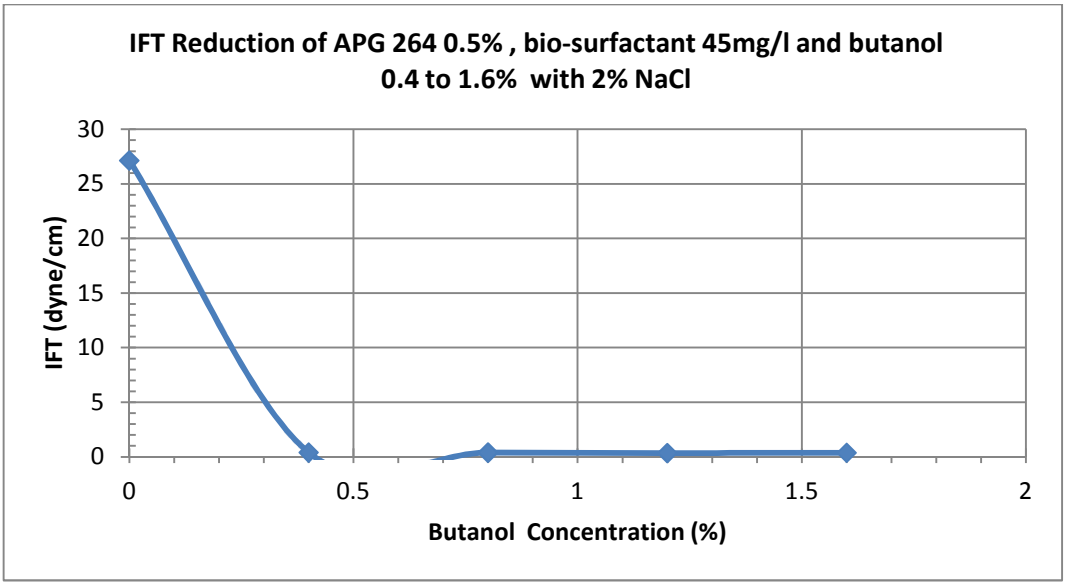

Figure 3.18 IFT reduction APG 264 at 0.5% and bio-surfactant at 45 mg/l and butanol at concentrations from 0.4% to 1.6%, with 2 % NaCl, under laboratory conditions

Table 3.13 IFT reduction of APG at 0.5%, bio-surfactant at 45mg/l and butanol from 0.4% to 1.6%

Formulation	IFT dyne/cm
Base case	27.1520
APG 0.5% +BS 45mg/l+0.4%Butanol	0.4060
APG 0.5% +BS 45mg/l+0.8%Butanol	0.3960
APG 0.5% +BS 45mg/l+1.2%Butanol	0.3520
APG 0.5% +BS 45mg/l+1.6%Butanol	0.3790

3.7 Conclusions

1. Based on IFT reduction, two low concentrations (40mg/l and 60mg/l) of bio-surfactant were identified where IFT values were low. Any value above 40 mg/l can be selected; as 45 mg/l bio-surfactant and 0.5% butanol produced a low IFT value it can be used for the core-flooding experiment.

2. The optimum concentration of APG 264 was 0.5% and of butanol was 0.5%. The combined optimum concentration was 0.5% APG 264 and 0.5% butanol' this can be used for the core-flooding experiment.

3. The optimum concentration of APG 264, bio-surfactant and butanol was 0.5%, 45mg/l and 0.5%. This combination can be selected for the core-flooding experiment.

3.8 Recommendations

1. IFT measurement at reservoir conditions should be conducted, as temperature has an impact on IFT.

2. IFT at higher concentrations should be estimated by the spinning drop method to achieve results that are more reproducible.

Chapter 4 Ionic Effect of Green Surfactants

The ionic environment of the reservoir is one of low salinity but a relatively high divalent-ion (hardness) concentration in the presence of a high cation exchange capacity (CEC). In this environment the injection of a micellar fluid encourages the development of large hardness gradients. In a highly variable ionic environment, the required tolerance of the micellar fluid should be balanced with respect to the IFT required to displace residual oil effectively.

In this chapter, bio-surfactants, biodegradable and environmental friendly surfactants and co-surfactant ionic characteristics are discussed. After an introduction, the background, classification and selection of green and co-surfactant and their properties are presented. Mixing anionic and non-ionic surfactants, and pressure and temperature, are addressed next. Results, conclusions and recommendations comprise the last three sections.

4.1 Introduction

Ions play a vital role in surfactant chemistry for enhanced oil recovery (EOR). Phase behaviour, IFT measurements, fractionation studies and core-floods are used to formulate green-surfactant-alcohol micellar fluids for application in a changing ionic environment that attains a relatively high hardness concentration as a result of ion exchange. For the effective formulation of micellar fluids for field applications, surfactants should be chosen based on their ability to generate very low IFT and to form a micro-emulsion that solubilises large volumes of both oil and brine. Initial design considerations should be examined in an ionic environment equivalent to that which occurs during the oil displacement process. Other design considerations also must be considered, such as the mobility of the micellar fluid, adsorption loss, and the possible chromatographic separation of the micellar fluid's components. Divalent ions and cation exchange have a significant impact on EOR. For this reason these two parameters are discussed below.

4.1.1 Effect of divalent ions

Brine contains divalent ions and has an impact on IFT. Divalent ions in brine, for example Ca^{++} and Mg^{++}, contribute to the hardness of brine: the tendency to

precipitate and an increased incompatibility with surfactant. There are divalent ions in the porous matrices of reservoir rocks. The divalent-ion in the surfactant system may change as it passes through the reservoir rock. The surfactants are less compatible with divalent ions in the aqueous phase. The divalent ions tend to drive the system towards an upper-phase system and the IFT of a surfactant system at optimum salinity increase as the salinity reduces (Green & Willhite 1998). The depletion of divalent cations from the equilibrium brine phase is a consequence of the association of the divalent cations with the surfactant (Glover *et.al.* 1979).

4.1.2 Effect of cation exchange

Ion exchange (Green & Willhite 1998) is a reaction between an electrolyte in solution and electrolyte attached to a solid surface. A general reaction involving cations may be expressed as

$$M^{-}A^{+} + B^{+} = M^{-}B^{+} + A^{+} \qquad (4.1)$$

where

M = solid materials such as clay

A^{+} and B^{+} = Cations

Clays found in reservoir rocks have the interesting property that through an ion-replacement process involving Al^{+++}, the clay acquires a negative charge during diagnosis. To preserve electroneutrality, cations from the associated fluid are incorporated within the clay structure. When this clay later comes into contact with a different liquid, as occurs during a displacement process, cations within the clay structure are available for exchange with cations in the contacting liquid (Amphlett 1964). The cation-exchange process can result in a significant change in the composition of a displacing fluid.

The ionic effects of green surfactants are not yet well characterized. Green surfactants are biodegradable and environmental friendly, and are perceived to have great potential for EOR. This study characterizes some green anionic and non-ionic surfactants through the determination of the IFT of each group and the combined effect of the surfactants with alcohols on IFT and micro-emulsions through laboratory experiments. Four different alkyl polyglucosides (APG) which can

produce ultra low IFT were selected from the non-ionic group. APG surfactants are produced from coconut, palm oil, corn, potato or wheat residues, and are completely and quickly biodegradable. They show low long-term aquatic toxicity for bacteria, favourable effects for fish and acceptable effects on Daphnia and algae. Bio-surfactants produced by the microbe *Bacillus mojavensis* (also known as *Bacillus subtilise*) were taken from the anionic group.

4.2 Background

Many formulations used in surfactant flooding involve blends of surfactants designed to give the most efficient oil recovery (Koukounis *et al.* 1983). The appropriate surfactant–cosurfactant system for a micellar flood that achieves best oil recovery requires careful optimization. Carlin *et al.* (1978) and Kalfoglu (1977) indicate that mixtures of anionic surfactants and non-ionic surfactants may be capable of producing low IFT and middle phase micro-emulsion in a high divalent ion environment. Koukounis *et al.* (1983) studied the phase partitioning of anionic and non-ionic surfactant mixtures, varying the composition of oil/water/surfactant equilibrated systems and passing into the optimal formulation region. They found that anionic and non-ionic surfactant mixtures cannot be assumed to be pseudocomponents in ternary phase representations. The partitioning of anionic surfactants into oil in Type I and Type III phase systems was minor. The concentration of non-ionics partitioned into the oil phase exhibits no discontinuity when shifting from a Type I to a Type III system. Graciaa *et al* (1987) studied the partitioning of non-ionic and anionic surfactant mixtures between oil, microemulsion and water phases, and developed and tested a new theory of surfactant partitioning between phases. They found that critical micelle concentrations (CMCs) of surfactant mixtures in water and the partition coefficients of the surfactant between oil and water measured at total surfactant concentrations less than the CMC. Another conclusion of this study (Graciaa *et al* 1987) was that mixtures of anionic and non-ionic surfactant were expected to exhibit a smaller degree of chromatographic separation than polydispersed non-ionic surfactants do when used without anionic surfactant. Surfactants used in these studies were not oil field surfactants and are not green. The ionic effect of green surfactant is not well understood yet, and its impact on EOR needs to be thoroughly investigated.

4.3 Classification of Surfactants and Co-surfactants

4.3.1 Classification of surfactants

According to the ionic charge of the head group, surfactants can be classified into four different types: anionic, non-ionic, cationic and zwitterionic (Ottewill 1984). Anionic surfactants have negative charges in their head group because the molecule ionizes in the aqueous solution. Similarly cationic surfactants cause the head group to be positively charged when the ionization of molecules occurs. Non-ionic surfactants have a larger head group than the tail group, but the molecules do not ionize; therefore, no ions exist in the head group. Zwitterionic surfactants have two groups of opposite charges. This research primarily focuses on green anionic and non-ionic surfactants as these types of surfactant are believed to have good potential in EOR. Anionic surfactants have good surfactant properties: they are fairly stable, have low adsorption on reservoir rocks, and are cheap to produce; non-ionic surfactants are more suitable for high-salinity brine environment (Green & Willhite 1998).

4.3.2 Classification of alcohols

Alcohol can be categorised into two types: hydrophobic and hydrophilic. The hydrophobic/hydrophilic properties of an alcohol mainly depend on the number of carbon atoms (Holm & Csaszar 1962; Jones & Dreher 1976), but alcohols can have various different structures and the most common variation is in the branching. The relation between branched and straight chain alcohol has been studied before and has determined that a single-branched alcohol behaves like a straight chain alcohol with one less carbon (Jones & Dreher 1976).

When the surfactant is mainly water soluble, it is not ideal for middle phase microemulsion formulation. This is because the surfactant partitions mainly in the water phase, hence forming lower phase microemulsion. The parameter hydrophilic-lipophilic balance (HLB) is the measure of affinity for water phase of oil phase (Iglauer *et al.* 2009): the higher the HLB value the more water-soluble the surfactant. The optimal condition is also defined in terms of HLB: the HLB number produced in the middle phase is the optimal HLB (Iglauer *et al.* 2009).

To control the affinity for water phase, a hydrophobic alcohol is added to the surfactant system. The addition of hydrophobic alcohol brings down the HLB, or makes the surfactant more hydrophobic. This means more surfactant exists in the oil phase. The continuous addition of hydrophobic alcohol will cause the phase transition II→III→I. The alcohol is usually added until the third phase behaviour, or a balanced HLB, is achieved. This manipulation of phase behaviour using alcohol can be done inversely using a hydrophilic alcohol.

Alcohol is also known to have other effects on the performance of surfactants. For anionic surfactants, hydrophobic alcohol decreases the optimal salinity and hydrophilic alcohol increases it. Optimal salinity is defined as that where the volume of oil and water solubilized in the middle phase is the same – which is similar to the HLB term. Other uses of alcohol are to reduce the viscosity of the microemulsion, reduce macro-emulsions, and increase equilibration time. The addition of alcohol may also reduce adsorption of surfactant onto rock and prevent the formation of gels (Dwarakanath *et al.* 2008; Jones & Dreher 1976).

In this study, butanol, Pentanol and Octanol were examined to determine their effect on IFT when combined with anionic and non-ionic surfactants.

4.4 Surfactant Structure

Surfactants are surface-active materials which possess one or more hydrophilic and one or more hydrophobic (lipophilic) groups in individual molecules. The hydrophilic polar (ionic) portion is called the head and the non-polar hydrophobic/lipophilic part (usually in the form of hydrocarbon chain) is called the tail. The tail portion of surfactants can be either a straight chain or a branched chain (Green & Willhite 1998). Figure 4.1 is a simplified sketch of a surfactant molecule. Hydrophilic and hydrophobic features of surfactants make it possible for the head of the surfactants to form a strong attachment with the surrounding water molecules while at the same time the tail attaches to oil particles inside the reservoir. The molecular structures of APG 264 and JF-2 bio-surfactants are showed in Figures 4.2 and 4.3.

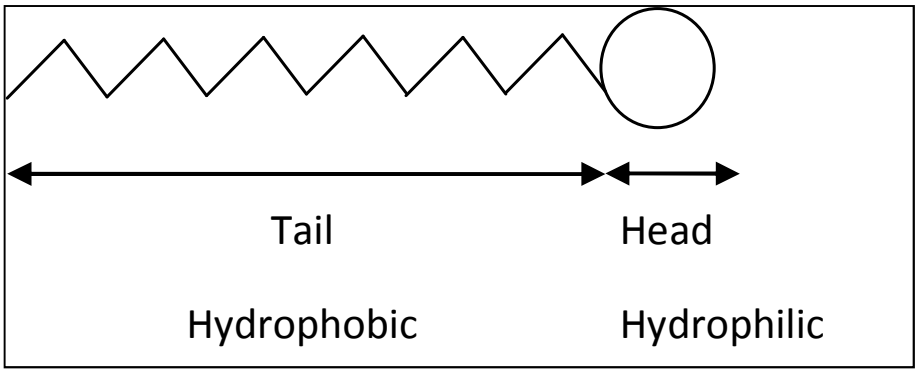

Figure 4.1 Schematic of surfactant (Ottewill 1984)

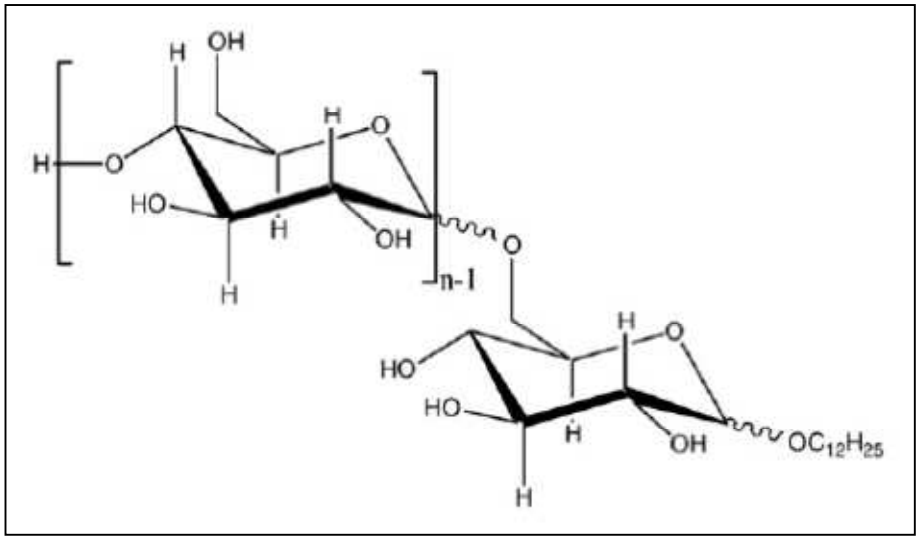

Figure 4.2 Molecular structure of APG 264 (Hill *et al.* 1997)

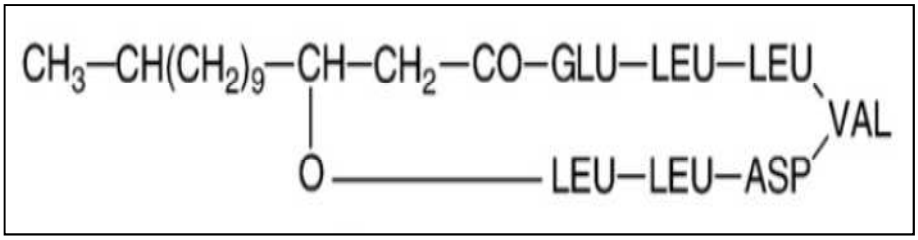

Figure 4.3 Molecular structure of JF-2 Bio-surfactant (Anne-Marie *et al.* 2010)

4.5 Mixing Surfactants

Many studies have demonstrated that solutions properly balanced between the aqueous and oleic phases of a surfactant-cosurfactant system reduce IFT dramatically in reservoir conditions. This balance is sensitive to the equivalent weight (Morgan *et al.* 1977) as well as the structure of the surfactant (Doe *et al.* 1977 a&b). The concentration and type of alcohol cosurfactant used (Salager *et al.*1979; Salter 1977), the ionic nature of the brine (Glover et al 1979; Nelson & Pope 1978) and the composition of the oil (Cash *et al.* 1977; Cayias *et al.* 1976) are all important.

4.5.1 Mixing rule

Wade et al (1976) demonstrated that a surfactant mixture behaves like a linear average of its components, so that the alkane of minimum tension (n_{min}) of a mixture is the sum of the products of the mole fraction of each component and its individual $n_{min.}$ For given surfactant components, this allows a simple calculation of the composition that gives the lowest interfacial tension against a particular alkane or crude oil. The alkane of minimum tension of surfactants mixture is given by:

$$(n_{\min})_M = \sum_i (n_{\min})_i \times x_i$$

where

(n_{min}) = the alkane of minimum tension

$(n_{min})_M$ = the alkane of minimum tension of a mixture of surfactants

x_i = the mole fraction of the ith component of the surfactant mixture

The results obtained also help clarify the roles of surfactant molecular weight and structure in the production of low interfacial tensions.

Anionic and non-ionic surfactants have been used in the petroleum industry for EOR process for long time. Anionic surfactants are relatively stable and exhibit relatively low adsorption on reservoir rock (Green & Willhite 1998). Non-ionic surfactants are used primarily as co-surfactants to improve the behaviour of the surfactant system.

Non-ionics do not reduce IFT as well as anionics but are much more tolerant of high-salinity brine. Cationic surfactants are not normally used for EOR because they absorb strongly on reservoir rocks.

4.5.2 Mixing rule using IFT screening

The optimum concentration point (OCP) is a limit or point just above the lowest IFT and the start of a steady IFT value. The OCP can be determined by IFT screening.

First we found the OCP of one surfactant by varying the concentration then added other surfactants and found the mixture's OCP. Anionic and non-ionic surfactants were mixed based on the OCP.

The optimum brine concentration is first selected. For this study 2% NaCl was chosen as the OCP. A series of surfactant samples of varying concentrations were prepared and IFT values were measured and plotted against the concentrations; then the OCP was selected. The example below shows how this was determined for APG 264.

Example of OCP selection: APG 264

Nine samples of APG 264 surfactant at concentrations from 0.2% to 2.0% at a constant salinity of 2% NaCl were prepared, and IFT values were measured using the captive drop method described in 3.5.2. Ondina Oil 68 and Ondina Oil 15 were supplied by the Shell Company of Australia Ltd. The IFT values are tabulated in Table 3.10 and plotted against the bio-surfactant concentration in Figure 3.15.

The IFT value dropped sharply from 27 dyne/cm to 1.3 dyne/cm with the increase of the APG concentration to 0.2%. After that it rose slightly 1.3dyne/cm to 1.4 dyne/cm between concentrations 0.2% and 1.8%, then fell to 1.3 dyne/cm at 2% APG. At concentrations greater than the CMC, micelle formation stops or greatly slows the decrease in IFT (Rosen 1978). Figure 3.15 indicates that the APG concentration after 0.4%, showed no reduction of IFT. As a result, an APG concentration of 0.5% can be selected for the core-flooding experiment.

4.6 Selection of surfactants

We selected four non-ionic green surfactants from the APG group: APG 8105, APG 8107, APG 8166 and APG 264; plus the *Bacillus* bio-surfactant from the anionic group, to measure IFT by the pendant drop method. At the same time we tested the effect of butanol and pentanol as co-surfactants on IFT under laboratory conditions (20^oC and ambient pressure) and reservoir conditions (50^oC and 1000 psi) using Stag Crude. The initial reservoir pressure and temperature of the Stag Oil Field are 1045 psi @ 2230 ft sub-sea and 52^oC (McDiarmid *et al* 2001)

4.6.1 Pressure and temperature effects

An increase in temperature causes an increase in the IFT and shifts the optimal salinity for a given system to a higher value. As temperature is increased for a system at a specified concentration, the phase shifts from upper to middle to lower-phase environments.

Normally the pressure effect on phase behaviour is small. Nelson (1983) studied the effect of live crude on phase behaviour and the oil recovery efficiency of surfactant flood systems and reported that the effect of pressure alone was negligible. Skange and Fotland (1990) examined the effect of pressure and temperature on the phase behaviour of micro-emulsions and found that the effect of pressure alone was negligible. They also reported that optimal salinity increased as pressure increased for a given system.

4.7 Methodology

The Temco pendant drop interfacial tension cell was used to measure IFT; it is capable of measuring up to 10,000 psi and 175^oC. First the IFT equipment was calibrated using distilled water, air and dodocane, then oil was transferred to the oil cylinder and brine was transferred to the brine cylinder using a hand pump. Next the IFT cell was filled with brine using the hand pump, and the system was calibrated by measuring the outer diameter of the needle. An oil pendant was produced through the needle using the hand pump. Pressure and temperature were set and the cell was left to reach equilibrium. Finally IFT was measured using software, and calculated using equation (Alotaibi & Nasr-El-Din 2009). Details of the pendant drop method are presented in 3.5.1.

4.8 Results and Discussion

4.8.1 Effect of alkyl group in non-ionic surfactant

Four non-ionic green surfactants based on alkyl groups (carbon) were tested to evaluate the different effects of the alkyl group on the IFT on crude oil (Stag oil) and surfactant-brine. A 2% NaCl solution was the base case, kept constant throughout the experiment. A concentration of 3mg/l surfactant was used to get a stable pendant, as the pendant drop method cannot measure ultra-low IFT. The alkyl group carbons of PG 8105, PG 8507, PG 8166 and PG 264 are 8-10, 8-10, 8-16 and 12-14, respectively. It was found that the IFT value decreased by increasing the lower limit alkyl group carbon number. The lowest IFT value of PG 264 (alkyl group carbon no 12-14) was 1.63 dyne/cm a decrease from 12.65 dyne/cm to 1.63 dyne/cm. However, increasing the upper limit carbon number did not reduce IFT significantly: for example, the PG 8166 (alkyl carbon no 8-16) only reduced the IFT value from 12.65 dyne/cm to 9.03 dyne/cm.

APG 264 was selected from the non-ionic group as it has the best IFT reduction capacity. A commercially available bio-surfactant was selected from the anionic group. APG 264 reduced IFT by 11.02 dyne/cm, from 12.65 dyne/cm to 1.65 dyne/cm. The bio-surfactant reduced IFT by 10.12 dyne/cm, from 12.65 dyne/cm to 2.53 dyne/cm. Figure 4.5 compares the IFT values of anionic and non-ionic surfactants under laboratory conditions.

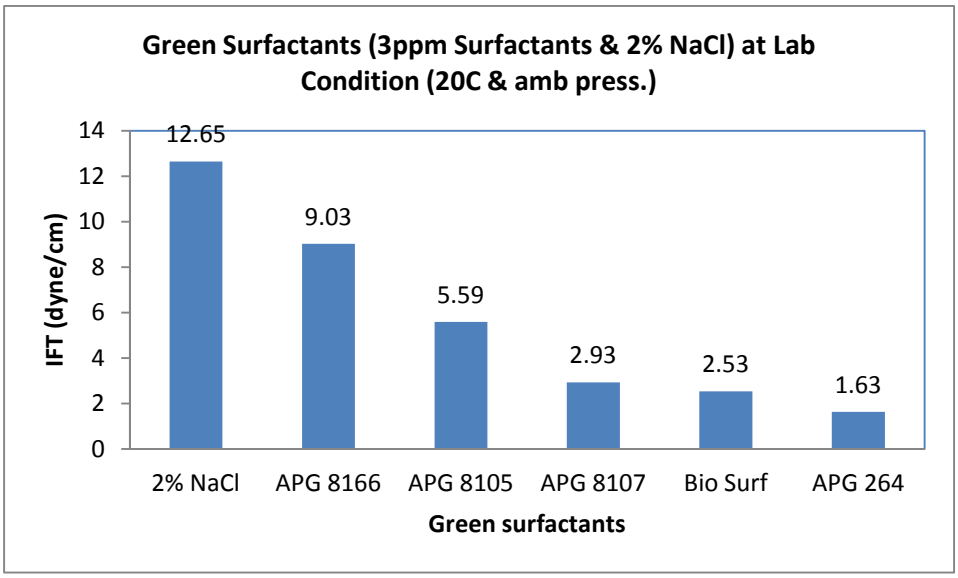

Figure 4.4 Comparison of anionic and non-ionic green surfactants under laboratory conditions (20^{o}C and ambient pressure)

4.8.2 Effect of co-surfactant on anionic surfactant

To investigate the effect of a co-surfactant on IFT, two alcohols, butanol and pentanol, were selected. Three samples were prepared. Sample 1 contained 3mg/l bio-surfactant and 2% NaCl; Sample 2 contained 3mg/l bio-surfactant and 2% NaCl and 0.5% butanol; and Sample 3 contained 3mg/l bio-surfactant and 2% NaCl and 0.5% pentanol. IFT values were measured under laboratory conditions (20^{o}C and ambient pressure). It was found that only the bio-surfactant decreased IFT significantly, by 10.12 dyne/cm, from 12.65 to 2.53 dyne/cm. Adding 0.5% butanol to Sample 1 reduced IFT by only 0.78 dyne/cm, from 2.53 dyne/cm to 1.75 dyne/cm. In the pentanol–bio-surfactant system, IFT was reduced by 0.13 dynes/cm, from 2.53 dyne/cm to 2.40 dyne/cm. The butanol-bio-surfactant system performs better than the pentanol-bio-surfactant system, reducing IFT by 65%. Figure 4.6 shows the effect of alcohol as a co surfactant on IFT, in both laboratory and reservoir conditions. A stable pendant was not produced in the bio-surfactant (BS) and 0.5% pentanol solution, and is thus not shown on the plot. 1-Pentanol and 1-Butanol can be produced by microbes when cultured in molasses (Hendry *et al.* 2010). We found that both pentanol and butanol could reduce oil density to almost the same magnitude with increasing alcohol concentrations. For this reason, pentanol and butanol were taken as co-surfactants to investigate their effect on EOR.

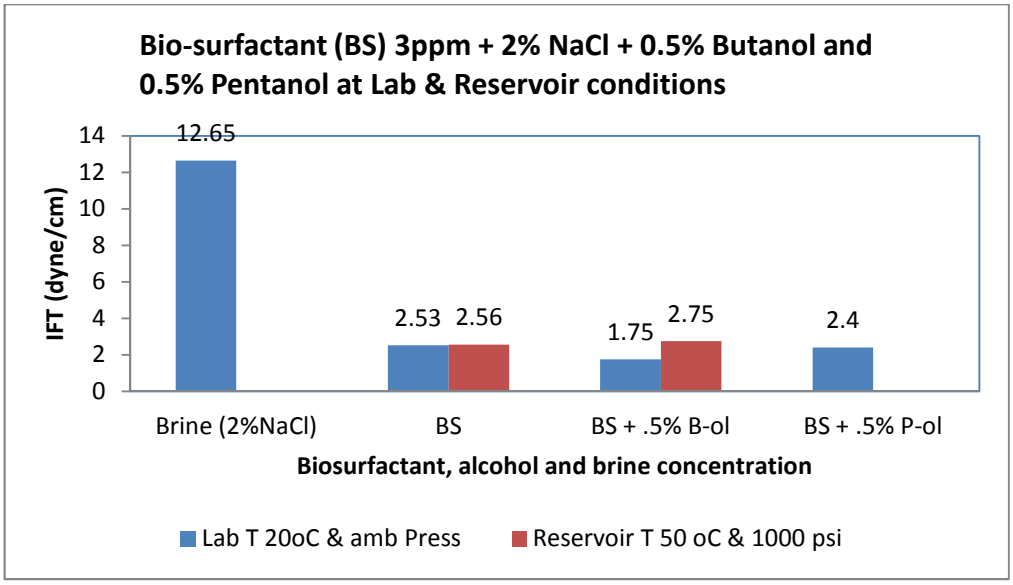

Figure 4.5 Effect of alcohols on anionic green surfactant IFT values in laboratory condition (20^{o}C and ambient pressure) and reservoir condition (50^{o}C and 1000 psi)

4.8.3 Effect of pentanol concentrations on non-ionic surfactants

Four samples were prepared with APG 8166 10mg/l, 2% NaCl and varying (15, 30, 60, and 120mg/l) pentanol concentrations, to evaluate the effect on IFT. It was found that there was no reduction of IFT value with increasing pentanol concentrations from 15 mg/l to 120mg/l. Figure 4.7 shows effect of pentanol concentration as a co-surfactant with a non-ionic green surfactant APG 8166.

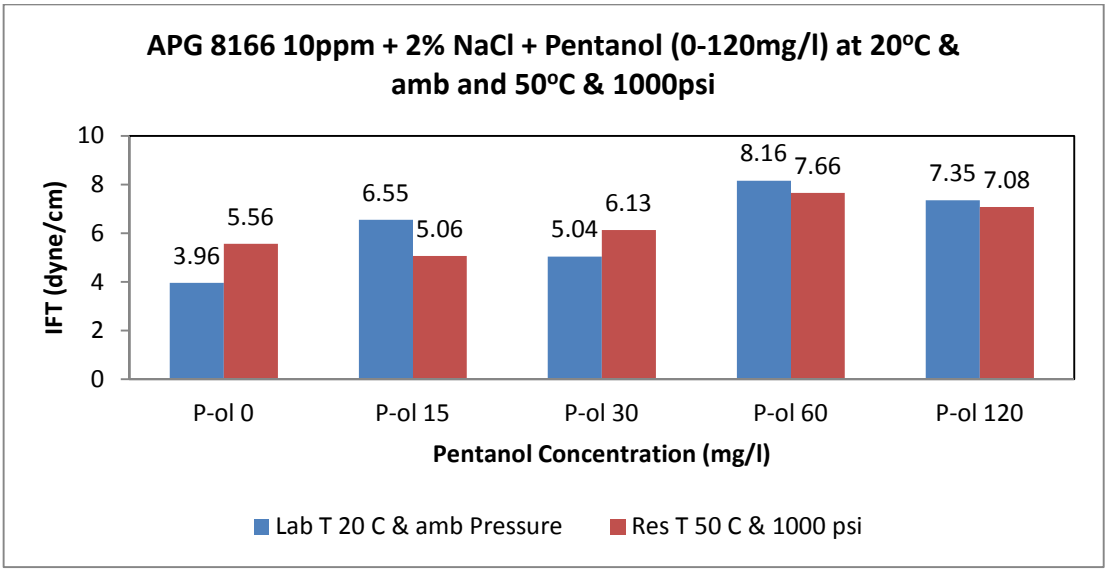

Figure 4.6 Effect of Pentanol concentrations on non-ionic green surfactant APG 8166 at laboratory condition (20°C & ambient pressure) and reservoir condition (50°C & 1000 psi)

4.8.4 Temperature and pressure effects of a non-ionic surfactant on IFT

We tested the pressure and temperature of APG 8166 10mg/l and 2% NaCl and a crude oil sample from the Stag field. A series of experiments with varying pressures and temperatures were carried out to evaluate the effect on IFT. Pressure and temperature varied from 500psi to 3000psi and from 20°C to 60°C. There were minor fluctuations in IFT values with increasing pressure and temperature. We found that APG can be used at a temperature range of 40°C to 60°C and a pressure range of 500psi to 3000psi. Table 4.2 presents the temperature and pressure effect on the IFT of APG 8166 at 10mg/l, 2% NaCl and Stag Crude.

Table 4.1 Effect of temperature and pressure on IFT between APG 8166 10mg/l and 2% NaCl

Pressure	Ambient	1000 psi	2000 psi	3000 psi
Temperature (^{o}C)	IFT dyne/cm	IFT dyne/cm	IFT dyne/cm	IFT dyne/cm
20	3.96	4.43	4.93	4.76
30	4.45	3.87	3.87	3.66
40	4.6	5.71	5.83	5.77
50	5.63	5.56	5.31	4.9
60	5.74	5.44	5.06	4.76

4.9 Conclusions

1. Our laboratory experiments confirm that the non-ionic surfactant APG 264 at 3mg/l and 2% NaCl concentration decreases IFT 11 dyne/cm, from 12.65 dyne/cm to 1.65 dyne/cm. In contrast, an anionic bio-surfactant of similar concentration reduces IFT 10.12 dyne/cm, from 12.65 dyne/cm to 2.53 dyne/cm. Non-ionic green surfactant is more active in the reduction of IFT than anionic surfactant.

2. There is no significant reduction in IFT values when the APG 8166 at 10 mg/l is combined with pentanol at concentrations of 15 mg/l to 120 mg/l.

3. Temperature appears to have little effect on the IFT of APG 8166.

4. APG 8166 is effective to use in the temperature range 20^{o}C to 60^{o}C and the pressure range 500psi to 3000psi.

4.10 Recommendations

1. Surfactant loss due to precipitation should be examined, because the presence of multivalent ions can lead to surfactant precipitation as a result of phase separation of surfactant and co-surfactant (Mayer & Salter 1981).

2. The effect of divalent ions on IFT should be investigated as their presence shifts the optimum salinity to a lower value.

3. The adsorption of surfactant on reservoir rock depends on the ionic nature of the reservoir materials and surfactant type. Investigation of surfactant adsorption is recommended.

Chapter 5 Core-flooding Experiments

Core-flooding experiments can duplicate reservoir conditions well and test the EOR performance of surfactant systems. The aim of these core tests is to determine the percentage of oil recovery using green surfactant and co-surfactant formulations. To do this, three core-flood experiments have been conducted to test the EOR capability of three green surfactant and co-surfactant mixtures. The three formulations are: bio-surfactant (anionic) and alcohol; APG 264 (non-ionic) surfactant and alcohol; and bio-surfactant and APG 264 surfactant, and alcohol.

In this chapter, an introduction to core-flooding tests is presented first. Methodology and observed and measured data are described in the second and third sections. The results of each formulation are discussed and compared in section four. Conclusions and recommendations conclude the chapter.

5.1 Introduction

The life of an oil well goes through three phases, primary, secondary and tertiary; in each, various techniques are employed to maintain crude oil production at maximum levels. The primary aim of these techniques is to force oil into the wellhead, from whence it can be pumped to the surface. In primary recovery, oil is forced out by the pressure generated from the gas present in the oil; but this typically produces only a small fraction of a reservoir's total oil capacity. In secondary recovery, the reservoir is subjected to water flooding or gas injection to maintain a pressure that will continue to move oil to the surface. Secondary recovery techniques can increase productivity to a third or more than primary techniques. Tertiary recovery, also known as enhanced oil recovery (EOR), introduces fluids that reduce viscosity and improve flow. These fluids may consist of gases that are miscible with oil (typically carbon dioxide), steam, air or oxygen, polymer solutions, gels, surfactant-polymer formulations, alkaline-surfactant-polymer formulations, or microorganism formulations. Techniques employed at the EOR phase can substantially improve extraction efficiency. Tertiary oil recovery (TOR) enables producers to extract up to over half of a reservoir's original oil content, depending on the reservoir and the EOR process applied.

Chemical flooding mainly consists of using surface active chemicals to reduce interfacial tension (IFT) between the residual oil phase and the displacing fluid (Green & Willhite 1998). One of the chemical systems used is micellar flooding: it consists of components such as surfactants, co-surfactants, hydrocarbons, water and electrolytes (Green & Willhite 1998). The performance of micellar flooding is judged on its ability to reduce IFT. To date, only 10% to 40% of initial oil in place has been recovered from oil fields. The rest of the oil is still trapped in the reservoir even after secondary recovery techniques such as water flooding, pressure maintenance and gas injections have been conducted. This trapped oil is commonly known as residual oil. It generally cannot be removed by conventional methods, mainly because of high IFT between the residual oil and the water flood. To achieve a large mobilization of residual oil, IFT values should be in the order of 10^{-3} dyne/cm (Willhite *et al.* 1980), although a reduction to the order of 10^{-2} dyne /cm is sufficient to mobilize a significant amount of the trapped oil (Green & Willhite 1998).

In this study, three core-flooding experiments have been conducted to examine the percentage of oil recovery obtained using three green surfactant and co-surfactant combinations: JF-2 bio-surfactant and butanol; APG 264 surfactant and butanol; and JF-e bio-surfactant, APG 264 and butanol.

5.2 Methodology

Core-flooding experiments were carried out in the Core-flooding Laboratory at Curtin University. The core-flooding equipment, manufactured by Sanchez Technologies, is shown in Figure 5.1. This equipment has four injection and three collection pumps, which are accurate and capable of working at low flow rates. The system is equipped with a temperature control chamber in order to simulate the required reservoir temperature for core-flooding. All injection and collection vessels, separator and core holder are placed in the enclosed chamber so that they all remain at the same temperature. The overburden pressure is applied on the core using a manual hydraulic pump, which is connected to two synthetic oil vessels to stabilize the pressure before the core inlet. Three injection cylinders contain crude oil, water and gas through the core, and several valves control the fluid flooding. Detailed flooding steps are given below. All observed and measured data are given in Tables

5.1–5.7 in data section. All formulae used to calculate required parameters are also given in Appendix A.

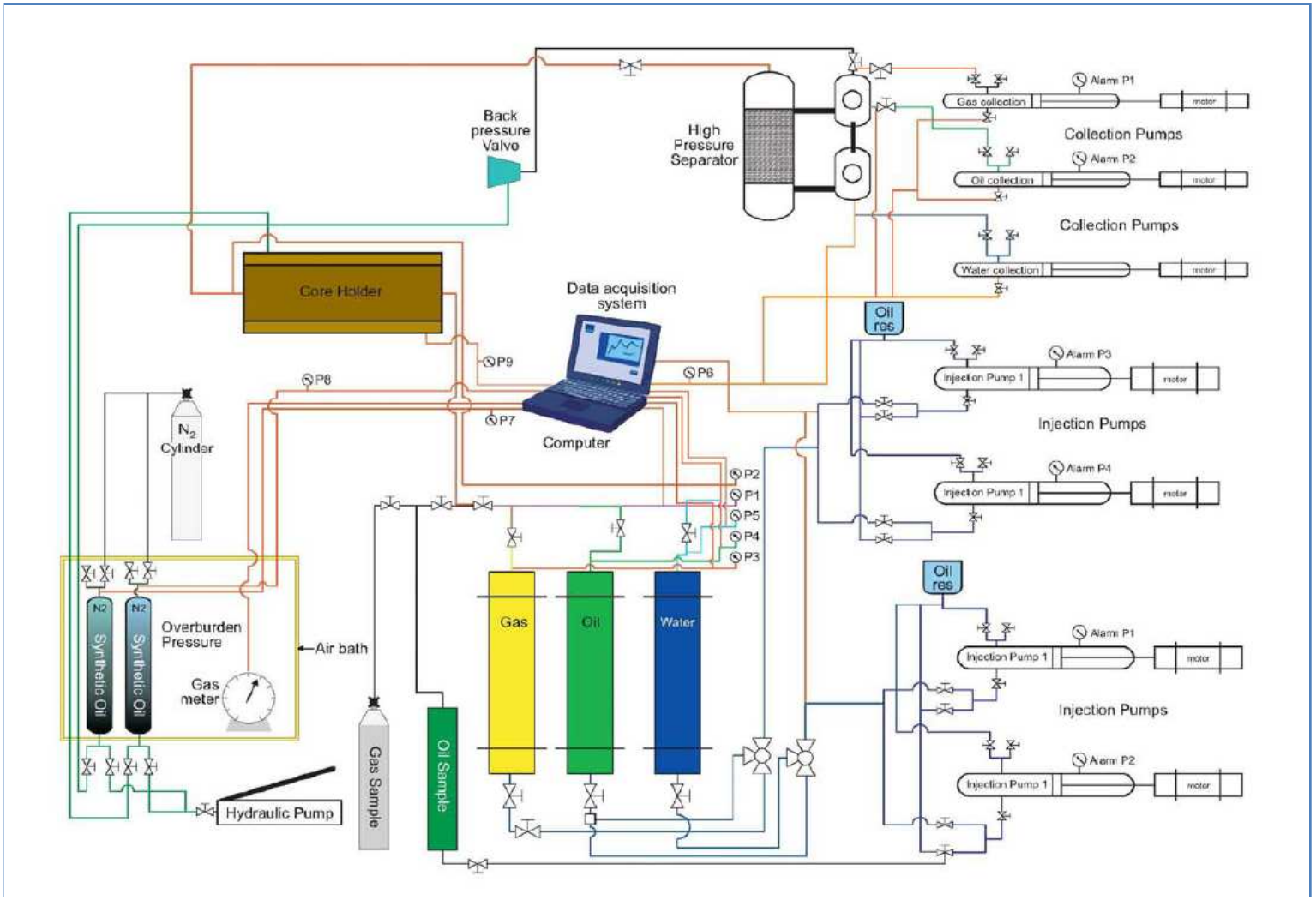

Figure 5.1 Core-flooding set-up

5.2.1 Cut and dry the core

a. Berea sandstone cores were selected for the experiments because of the homogenous nature of their permeability and porosity.
b. Three 1.5 inch (3.81cm) diameter and 6 inch (15.24cm) length cores were cut from a block of Berea sandstone.
c. The wet cores were oven dried at 50–60 ^{o}C for a week.
d. Each dried core was weighed and its length and diameter measured. The results are tabulated in Table 5.1.
e. The porosity and permeability of the core plugs were measured using an automated permeability-porosimeter (Model AP-608, manufactured by Coretest Systems). Porosity and permeability of sample #1 were measured at different confined pressures to find accurate values. Sample # 2 and 3 were taken from the same homogeneous Berea Sandstone core. Porosity and permeability are assumed to be same as sample #1. The results are tabulated in Table 5.1. In addition, the core plugs had to be as dry and clean as possible to measure the value precisely. The absolute permeability of core to water was calculated by Darcy's Law, Eq 5.1. When the core was saturated by synthetic reservoir brine, it was flooded at a known flow rate to reach a stable condition; then Darcy's Law was applied to find the core absolute permeability:

$$K_{abs} = \frac{Q_{Brine} \times \mu_{Brine} \times L_{Core}}{A_{Core} \times \Delta P} \qquad (5.1)$$

where

K_{abs} = Absolute permeability of core to brine at 100% saturation, Darcy

μ_{Brine} = Brine viscosity, cP

ΔP = Pressure drop across the core, atm

L_{core} = Length of core, cm

A_{core} = Area of cross-section of core, cm^2

Q_{Brine} = Brine flow rate, cm^3/sec

5.2.2 Core placement in the core holder

a. The core plug was placed inside a rubber sleeve, and both were inserted into the core holder. The sleeve grips and squeezes the core when a confining pressure is applied. This confining pressure is similar to the overburden pressure, and forces any injected liquid to flow through the core and not around it. The sleeve dimensions are engineered to fit the core holder and the core, leaving only a small gap between the outer wall and the core holder's inner surface.

b. One end plate of the core holder is a fixed plate; the other is floating. Once the core and the sleeve were inserted into the core holder, the cap was screwed into place. After ensuring that the core rested firmly against the fixed plate, the other cap of the holder with the floating plate was screwed into plate so that the core fitted tightly between the two end plates. This floating arrangement allows the end plate to adjust its position to the length of the core.

c. The overburden pressure was applied on the core using a manual hydraulic pump connected to two synthetic oil vessels in order to stabilize the pressure in the core holder.

Figure 5.2 Core Holder

d. Once the overburden /confining pressure was at the desired value, the inlet and outlet valves were closed and the core was ready for evacuation.

5.2.3 Evacuation

a. A vacuum was created to remove air trapped within the core, to reduce error in the pressure reading. A carbon dioxide gas flush was used because it dissolves readily in water and can be removed from the core.
b. With the core holder inlet valve closed, a vacuum was applied on the core from the discharge end and maintained for twenty-four hours. Following this, the discharge valve was closed before disconnecting the vacuum line.
c. Carbon dioxide flushing was started by first charging the inlet side tubing of the core holder with gas before opening the inlet valve to allow gas into the core. This kept air from the core. The outlet valve was opened so the gas could flow through the core. The gas flush was maintained for fifteen minutes and the inlet and outlet valves closed.
d. A vacuum was again applied. As recommended, the gas flush-vacuum cycle was carried out three times to remove all traces of air from the core. The last step was a vacuum before brine injection.
e. The valves were closed and the core isolated. The core was now ready for the flood experiment.

5.2.4 Brine preparation and filling the brine and crude oil transfer cylinders

a. The required amount of NaCl for 2% bt wt (20000mg/l) solution was added to de-ionized water. The brine was placed under vacuum in a desiccator (Figure 5.3) for twenty-four hours to remove oxygen dissolved in the solution.
b. The brine and crude oil densities and viscosities were measured.
c. Cylinders were cleaned and dried before filling with crude oil and brine.
d. Brine, oil and surfactant/co-surfactant mixtures were transferred into the oil, brine and surfactant cylinders.

Figure 5**.3 Desiccator**

5.2.5 Brine injection

a. The brine injection rate was set at a constant flow rate with a Ruska pump. Keeping the core holder isolated from the rest of the system, the inlet tubing was flushed with brine. The pump was started, and the flow rate at a tap on the inlet tubing was measured to ensure that it was equal to the set flow rate. Once that was achieved the flow was stopped and the system was ready for injecting brine into the core.
b. The volumetric reading on the pump was noted before starting the pump.
c. Brine was injected at a low rate initially, because the core permeability was unknown. A high flow rate through a core with low permeability will damage the tubing and equipment. The flow rate can be changed at any time during the injection.
d. The inlet valve remained closed after starting the pump until the inlet pressure gauge showed a reading of 35 psi. A transducer connected to the gauge displayed the pressure on a monitor. When the pressure reading displayed 35 psi, the inlet valve was opened to allow brine to flow into the core. The pressure decreased as the valve was opened, and as brine entered the core, which was under a vacuum. The core outlet valve was kept closed.
e. The outlet valve was opened when the inlet pressure gauge displayed 20 psi. The pressure was built up to dissolve any carbon dioxide gas

remaining in the core in the brine solution and to prevent any vapour phase to develop in the dry core.

f. The brine produced from the core was collected in a measuring flask.
g. About four (4) pore volumes of brine were injected into a core.
h. The injection pressure was recorded to determine the absolute permeability of the core to brine. Since the discharge valve of the core holder opened into atmospheric pressure, the injection pressure was sufficient for calculating the pressure drop across a core. A back pressure system could be fixed at the discharge to simulate conditions in a producing well.
i. The final volumetric reading minus the sum of the initial reading, the volume of brine collected and the dead volume inside the tubing, was the core pore volume. An underlying assumption was that the core was 100% saturated.

5.2.6 Crude oil saturation

a. With the inlet and discharge valves closed, the inlet tubing was connected to the oil accumulated with a three-way valve. The Ruska pump was started at the required flow rate and the inlet tubing of the core holder flushed with crude oil to remove the brine through the tap on the inlet tubing. The tap was closed after the crude oil filled the tubing.
b. The injection pump was started and the outlet and inlet valves of the core holder were opened to inject crude oil into the core. Brine and oil produced from the core were collected in measuring flasks.
c. Crude oil injection was continued until less than 1.00 cc of brine was produced for every 20 cc of crude oil. At this point the core was close to residual water saturation. The injection pressure was recorded to calculate the effective oil permeability at residual water saturation.
d. Oil injection was stopped and the inlet and outlet valves closed.
e. The volume of brine collected minus the tubing holdup volume was used to determine the residual water saturation.
f. The oil was injected to displace water and to reach the connate water condition. This process was continued until no more water was produced.

Core-flooding experiments are faced with viscous discontinuity at both ends of the core, known as end effect. To reduce end effect, it is necessary to have a sufficiently high flow rate and /or core length to meet the Rapoport and Leas scaling coefficient. For this reason, the oil flooding was conducted at 100 cc/hr to minimize the end effects. In addition, all data from collection and injection sides, including pressure, temperature and flow rate, were automatically recorded.

5.2.7 Water flooding

a. With the inlet valve closed, the inlet tubing was connected to the brine accumulator. The Ruska pump was set to the waterflood rate and started. The inlet side tubing was flushed with brine to remove the crude oil. Once the tubing was free of oil, the pump was stopped and the tap on the inlet closed.
b. The pump was restarted and the inlet and outlet valves of the core holder were opened. The oil and water produced from the core were measured.
c. The waterflood was continued until negligible oil was produced. This was determined by observing the effluent stream. The core was determined by observing the effluent stream. If there was no oil, the core was at residual oil saturation and waterflooding could be stopped.
d. After completion of the aging of the core, the core was flooded by synthetic brine. The flow rate was again set at 100cc/hr to satisfy the Rapoport and Leas coefficient. The water flooding was carried on until the produced oil was negligible and the water recovery curve flattened.
e. The injection pressure was recorded to determine the effective brine permeability of the core at residual oil saturation. Differential pressure between inlet and outlet of core was maintained constant at 1050 psi as Stag reservoir pressure is 1050 psi.
f. The inlet and outlet valves were closed and the tubing inlet flushed and filled with the surfactant solution to prepare the core for surfactant injection.

g. The volume of oil recovered from the core minus the tubing holdup volume provided the residual oil saturation and the target oil volume for tertiary recovery.

5.2.8 Surfactant flooding

a. In this step, three surfactant and co-surfactant combination solutions were flooded to reach residual oil saturation. Solutions were injected into the core at the same rate as the original brine (100cc/hr) in order to be comparable with the secondary recovery. The volume of produced fluids was measured at the separator. The fluid recoveries were calculated by material balance analysis, and recovery graphs were obtained. Step by step details are given below.
b. With the inlet valve of the core holder closed, the inlet tubing was connected to the surfactant accumulator. The Ruska pump was set to the injection rate and started. The inlet side tubing was flushed. When only surfactant flowed, the pump was stopped and the tap on the inlet tubing was closed.
c. The pump was again started and the inlet and outlet valves opened. The oil, brine, and surfactant that flowed from the core were collected into 25 cc measuring flasks.
d. Depending on the experimental protocol, the specified volume of surfactant was injected and the pump stopped.
e. The injection pressure was recorded continuously during the surfactant injection to determine the permeability reduction factor at the end of the experiment.
f. The volume of oil recovered was used to calculate the tertiary oil recovery.
g. In flow experiments where a brine postflush was injected, the core inlet valve was closed before connecting the tubing to the brine transfer vessel. The tubing was then flushed before brine was injected into the core.

5.3 Observed and Measured Data

Table 5.1 Core Properties

Core plug	Length (cm)	Diameter (cm)	Pore Volume (CC)	Dry Weight (gm)	Porosity (%)	Permeability (mD) Ka
1	8.129	3.850	19.35	196.72	20.45	470.8601
2	8.018	3.842	18.98	194.07	20.45	470.8601
3	8.090	3.823	18.95	194.43	20.45	470.8601

Table 5.2 Observed and measured data of formulation 1 (JF-2 bio-surfactant and butanol)

Step No.	Phases	Water/Surf Injection		Vol. Injected	Water/Surf Collection		Vol. Collected	Remainder	Q
		Start	End		Start	End			
		cc	cc	cc	cc	cc	cc	cc	(cc/hr)
1	Oil Inj	0.00	0.00	0.00	52.02	81.56	29.55	15.55	100
2	Water Inj	6.61	167.57	160.95	81.54	225.02	143.49	5.88	100
3	Surf. Inj	16.26	199.93	183.67	225.02	410.64	185.63	0.80	100

Table 5.3 Observed and measured data of formulation 1 (JF-2 bio-surfactant and butanol)

Step No.	Phases	Oil Injection		Vol. Injected	Oil Collection		Vol. Collected	Remainder	Sample PV	Sw
		Start	End		Start	End				
		cc	cc	cc	cc	cc	cc	cc	cc	(%)
1	Oil Inj	105.85	287.45	181.60	19.43	176.38	156.95	13.37	18.99	18.14
2	Water Inj	0.00	0.00	0.00	176.38	196.73	20.35	6.35	18.99	49.12
3	Surf. Inj				196.74	197.93	1.19	1.19	18.99	53.35

Table 5.4 Observed and measured data of formulation 2 (APG 264 surfactant and butanol)

Step No.	Phases	Water/Surf Injection		Vol. Injected	Water/Surf Collection		Vol. Collected	Remainder	Q
		Start	End		Start	End			
		cc	cc	cc	cc	cc	cc	cc	(cc/hr)
1	Oil Inj	0.000	0.000	0.000	53.752	83.375	29.623	15.123	100
2	Water Inj	38.634	235.636	197.002	83.3130	263.0550	179.7420	6.215	100
3	Surf Inj	98.493	140.260	41.767	139.7800	176.0000	36.2200	6.174	100

Table 5.5 Observed and measured data of formulation 2 (APG 264 surfactant and butanol)

Step No.	Phases	Oil Injection		Vol. Injected	Oil Collection		Vol. Collected	Remainder	Sample PV	Sw
		Start	End		Start	End				
		cc	cc	cc	cc	cc	cc	cc	cc	(%)
1	Oil Inj	30.34	266.7	236.36	43.49	259.00	215.51	12.26	19.35	21.84
2	Water Inj	0.00	0.0	0.0	182.14	203.76	21.62	7.62	19.35	53.96
3	Surf Inj	0.00	0.0	0.0	203.79	209.18	5.39	5.39	19.35	85.87

Table 5.6 Observed and measured data of formulation 3 (APG 264, bio-surfactant and butanol)

Step No.	Phases	Water/Surf Injection		Vol. Injected	Water/Surf Collection		Vol. Collected	Remainder	Q
		Start	End		Start	End			
		cc	cc	cc	cc	cc	cc	cc	(cc/hr)
1	Oil Inj	0.000	0.000	0.000	64.21	93.970	29.760	15.760	100
2	Water Inj	8.618	172.48	163.87	94.00	240.24	146.24	6.085	100
3	Surf Inj	6.475	29.80	23.33	240.24	262.42	22.180	1.500	100
3b	Post Flood (Brine)	172.24	207.15	34.91	262.39	295.43	33.035	2.397	100

Table 5.7 Observed and measured data of formulation 3 (APG 264, bio-surfactant and butanol)

Step No.	Phases	Oil Injection		Vol. Injected	Oil Collection		Vol. Collected	Remainder	Sample PV	Sw
		Start	End		Start	End				
		cc	cc	cc	cc	cc	cc	cc	cc	Fraction
1	Oil Inj	26.26	174.87	148.60	18.48	140.06	121.58	15.25	19	0.17
2	Water Inj	0	0	0	140.09	161.56	21.47	7.47	19	0.49
3	Surf Inj	0	0	0	161.43	162.99	1.56	1.56	19	0.57
3b	Post Flood (Brine)	0	0	0	162.99	165.4	2.41	2.41	19	0.70

5.4 Results and Discussion

In this study, three core-flood experiments have been conducted to test the EOR capability of three green surfactant and co-surfactant mixtures. The first experiment was carried out to see how a combined bio-surfactant and bio-alcohol increased the TOR. The objective of the second experiment was to find effective alternatives to bio-surfactants that would work in the MEOR process. APG 264 surfactant and a bio-alcohol like a butanol mixture were flooded to see the TOR effect. The aim of the last core-flood test was to observe how a mixture of anionic and non-ionic green surfactants affected the TOR in the MEOR process. To find the TOR, APG 264, bio-surfactant and butanol were mixed together and flooded. Detailed results are given below.

5.4.1 Experiment 1(Formulation 1: JF-2 Bio-surfactant and butanol)

A 8.126 cm long and 3.85 cm diameter Berea sandstone core was oven dried at 60^{o}C for four days, and then the core was measured and placed in the core holder and overburden pressure applied. A vacuum was applied to the core for twenty-four

hours to remove any air. The core was saturated with 2% NaCl brine and then flooded with 19^{o} API Stag crude oil until the core reached residual water saturation; the oil-saturated core was then flooded with 2% NaCl brine until it was near residual oil saturation and ready for surfactant treatment. Typically, brine flooding was stopped when only a trace of oil was being produced or 10 pore volumes (PVs) of brine had been injected through the core. The surfactant was a solution of 45mg/l JF-2 bio-surfactant with 0.5% butanol as co-surfactant. Interfacial tension between oil and brine was measured and tabled in section 3.6.5. Results of this core-flood are presented in Table 5.8.

At the end of the oil flood, residual water saturation (S_{wr}) was measured at 18.14 %. In the water flooding stage, residual oil saturation (S_{or})was 50.88 % and secondary oil recovery 37.8 % of oil initially in place (OIIP). About three pore volumes of surfactant were injected into the core but only 0.265cc of oil was produced. Incremental oil recovery was 1.7 % of OIIP and total oil recovery was 39.5 % of OIIP. Figure 5.4 displays the measured tertiary oil production for the Berea sandstone core, which was subjected to waterflood residual oil conditions (waterflood S_{or} = 50.88 %) and surfactant slug injection. A very low amount of additional oil was produced, less than 10 % tertiary oil recovery. Figure 5.5 shows total recovery calculated after brine, and bio-surfactant and butanol mixture flooding.

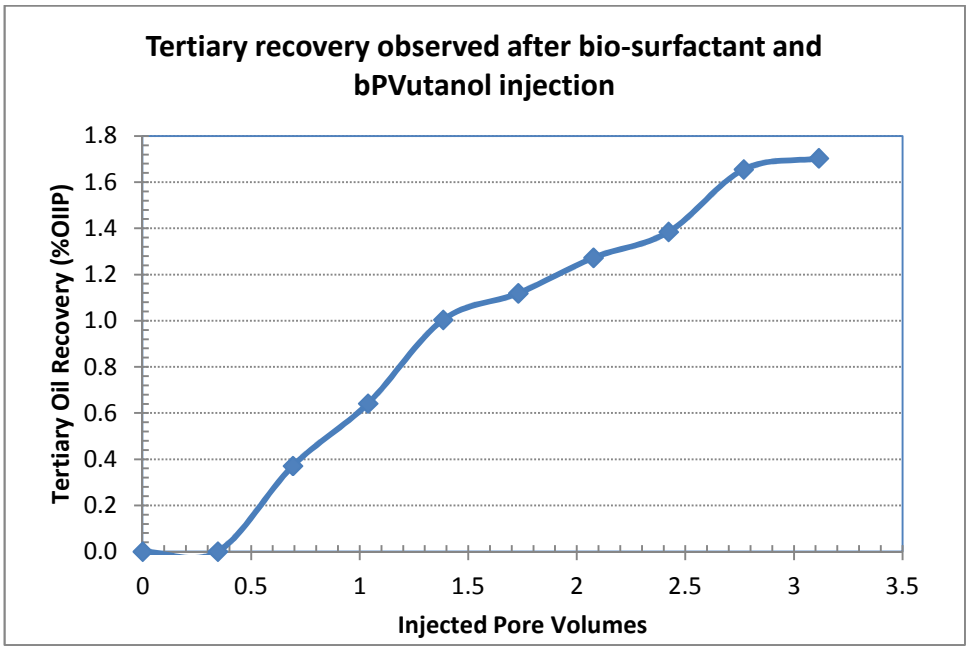

Figure 5.4 TOR versus PVs plot of bio-surfactant and butanol injection

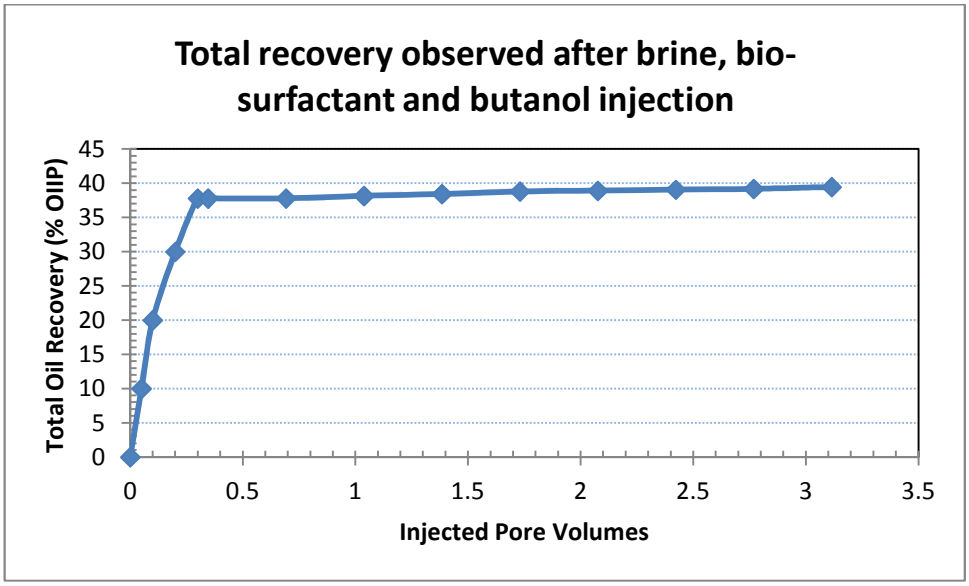

Figure 5.5 Total recovery observed after water and surfactant flooding

The low oil recovery from this core even after 3 PVs of surfactant injection was caused either by insufficient bio-surfactant or inefficient sweep by the surfactant due to viscous fingering. Viscous fingering was unlikely because the mobility ratio between the oil and surfactant was less than one and favourable. Surfactant adsorption is the primary cause for surfactant degradation in porous media. For JF-2 this could only be confirmed by studies to determine adsorption losses. Capillary end effect was not an issue because the displacing aqueous phase flowed from the core without any abnormal injection pressure increase. The experiment was classified an immiscible displacement process because the crude oil–brine IFT measured prior to the experiment was 2.5 dyne/cm: for miscible displacement the IFT has to be zero dyne/cm. The passage of oil at this flow rate thorough the core was likely further aided by gravity segregation between the heavier surfactant and the displaced oil.

Table 5.8 Core-flooding experimental results of formulation 1(JF-2 Bio-surfactant and butanol)

Phases	Descriptions	Values
Oil Flood	Residual water saturation at the end of oil flooding, Swr (%)	18.14
	Maximum oil saturation at the end of oil flooding, So (%)	81.86
Water Flood	Residual oil saturation at the end of water flooding, Sor (%)	50.88
	Oil Recovery, % of OIIP	37.8
Surfactant Flood	Oil produced, CC	0.265
	Incremental oil recovery, % of OIIP	1.7
	Final oil recovery, % of OIIP	39.5

5.4.2 Experiment 2 (Formulation 2: APG 264 surfactant and butanol)

The effectiveness of APG 264 surfactant as an alternative to bio-surfactant in oil recovery was studied in this experiment. A 8.126 cm long and 3.85 cm diameter Berea sandstone core was vacuumed and saturated with 2% NaCl brine, then flooded with 19^{o} API Stag crude oil until the core reached residual water saturation. After that the core was waterflooded with 2% NaCl brine to residual oil saturation prior to surfactant injection. The surfactant contained

0.5% of APG 264 and 0.5 % butanol as co-surfactant. The IFT between the crude oil and surfactant solution was 0.55 dyne/cm. The surfactant was injected at a rate of 100cc/hr.

The results of this core-flooding test are displayed in figs 6-7 and table 5.9. Fig5.6 presents tertiary oil recovery measured for the APG 264 and butanol formulation. The core was conditioned to waterflood residual oil condition prior to surfactant slug injection. At the end of waterflood the residual oil saturation Sor was 46.06 %. Tertiary oil recovery of this formulation amounted to 40.8%. This is significant amount of addition oil recovery. The total oil recovery of this formulation is 81.9%

of OIIP. Figure 5.7 shows total oil recovery of the core-flood test. This proofed the effectiveness of the surfactant formulation in terms of enhancing oil recovery. In addition, APG 264 surfactant can be added with bio-alcohol like butanol and may give good oil recovery.

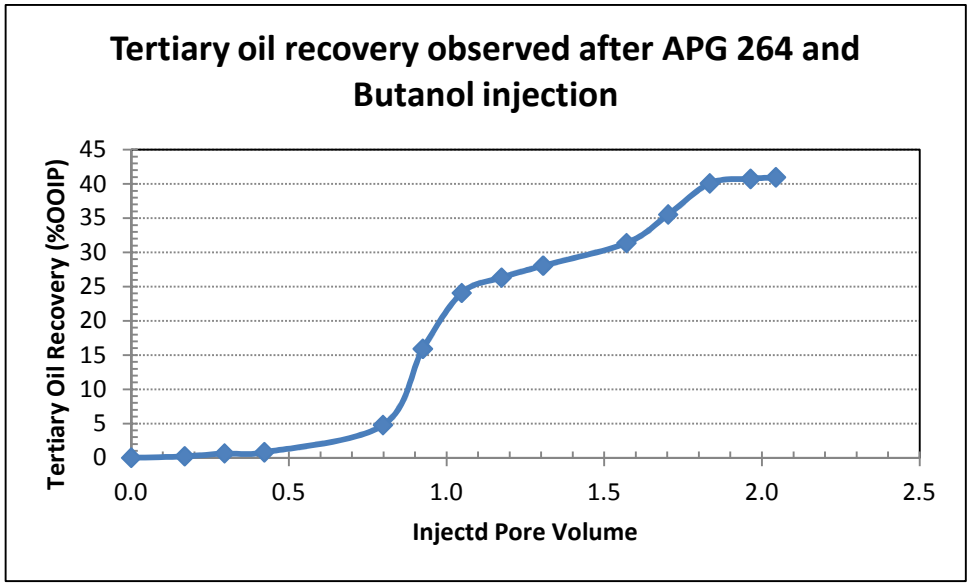

Figure 5.6 Tertiary oil recovery observed after APG 264 and Butanol injection

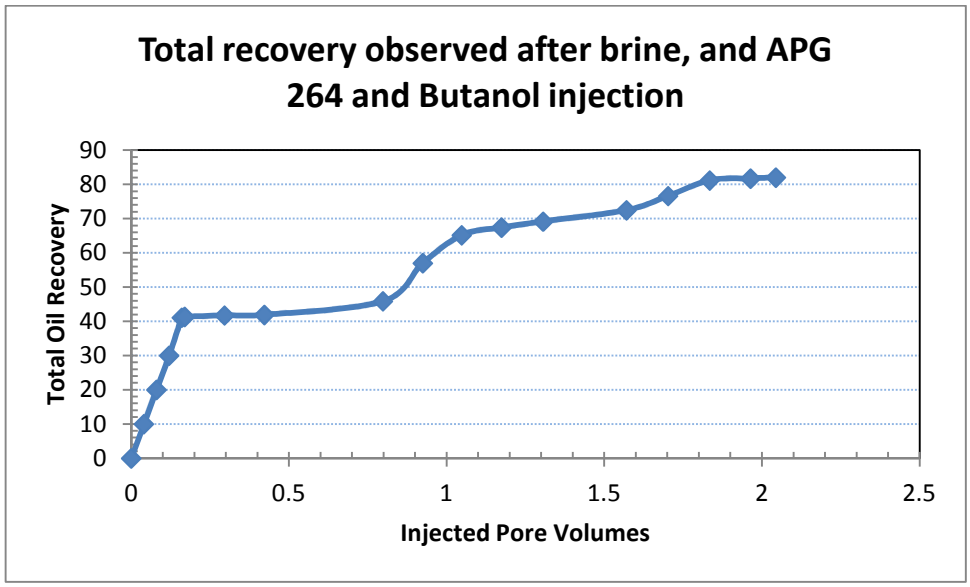

Figure 5.7 Total oil recovery observed after water and APG 264 and Butanol flooding

Table 5.9 Core-flooding experimental results of formulation 2(APG 264 surfactant and butanol)

Phases	Descriptions	Values
Oil Flood	Residual water saturation at the end of oil flooding, Swr (%)	21.84
	Maximum oil saturation at the end of oil flooding, So (%)	78.16
Water Flood	Residual oil saturation at the end of water flooding, Sor (%)	46.04
	Oil Recovery , % of OIIP	41.1
Surfactant Flood	Oil produced, CC	6.174
	Incremental oil recovery , % of OIIP	40.8
	Final oil recover, % of OIIP	81.9

5.4.3 Experiment 3 (Formulation 3: APG 264, bio-surfactant and butanol)

The impact of anionic and non-ionic surfactants mixture together with alcohol on oil recovery was studied in the experiment. In this formulation 3, non-ionic surfactant APG 264 of 0.5 % and anionic bio-surfactant of 45mg/l were mixed with 0.5% butanol. Results of this formulation are presented in table 5.10 and Figures 5.8–5.9.

The core was saturated with 2% NaCl brine and then flooded with 19^{o} API Stag crude oil until the core reached residual water saturation (Swr = 17.05%). The oil-saturated core was then flooded with 2% NaCl brine until it was near residual oil saturation and ready for surfactant treatment. Typically, brine flooding was stopped when only a trace of oil was being produced.

In water flooding stage, residual oil saturation Sor was 50.92% and secondary oil recovery was 38.6 % of Oil Initially in Place (OIIP). In surfactant flooding, there was 3.89 cc oil production after 1.2 PVs of surfactant injection. Tertiary oil recovery was 24.7%. Figure 8 displays tertiary oil recovery measured for the APG 264, bio-surfactant and butanol formulation. At the end of surfactant flooding, the total oil

recovery was 63.34%. Figure 9 exhibits total recovery calculated after water flood and surfactant flood (APG 264, and bio-surfactant and butanol mixture).

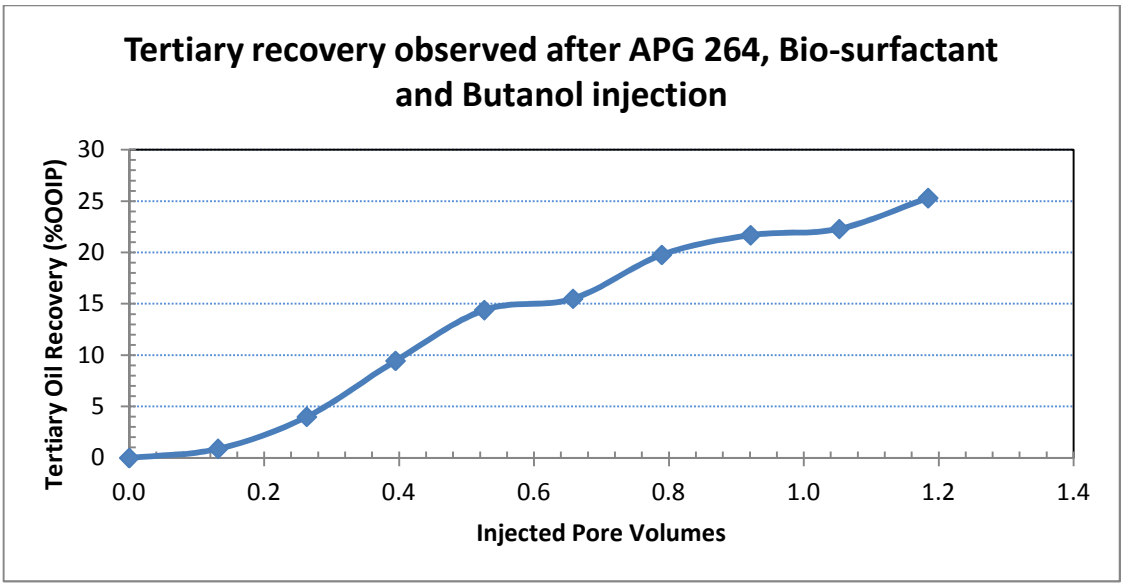

Figure 5.8 Tertiary oil recovery observed after APG 264, Bio-surfactant and butanol mixture injection

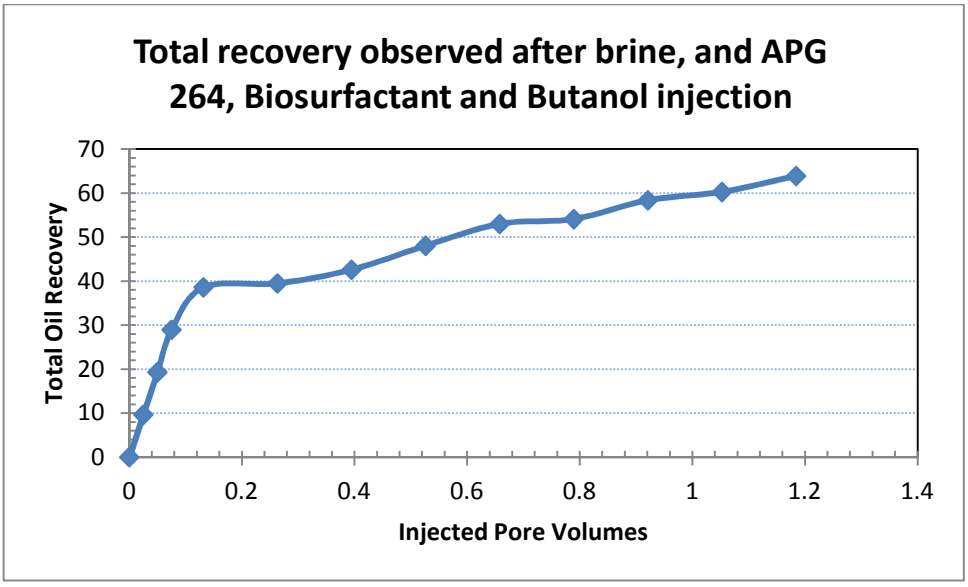

Figure 5.9 Total oil recovery observed after water and anionic and non-ionic surfactants mixture flooding

Table 5.10 Core-flooding experimental results of formulation 1(APG 264, bio-surfactant and butanol)

Phases	Descriptions	Values
Oil Flood	Residual water saturation at the end of oil flooding, Swr (%)	17.05
	Maximum oil saturation at the end of oil flooding, So (%)	82.95
Water Flood	Residual oil saturation at the end of water flooding, Sor (%)	50.92
	Oil recovery, % of OIIP	38.6
Surfactant Flood	Oil produced, CC	3.9
	Incremental oil recovery, % of OIIP	24.71
	Final oil recovery, % of OIIP	63.34

5.4.4 Comparison of three formulations

The summary of three formulation results is shown in Table 5.11 and Figure 5.10. Comparing three formulations, APG formulation is efficient. In Formulation 2 (APG 264 and Butanol), TOR is 40.8%. On the other hand TOR in Formulation 1 (Bio-surfactant and Butanol) is 1.7%. Formulation 1 is not capable to produce sufficient additional oil in core-flood experiment. Anionic and non-ionic surfactants mixture shows 24.7% TOR and this formulation is effective to additional recover oil.

Table 5.11 Summary of three formulations EOR

Expt. No	Core No	Formulations	S_{wi} (%)	Secondary Oil Recovery (%)	Tertiary Oil Recovery (%)	Total Recovery (%)
1	1	Bio-surfactant and butanol	18.14	37.8	1.7	39.5
2	2	APG 264 and Butanol	21.84	41.1	40.8	81.9
3	3	APG 264, bio-surfactant and butanol	17.05	38.6	24.7	63.3

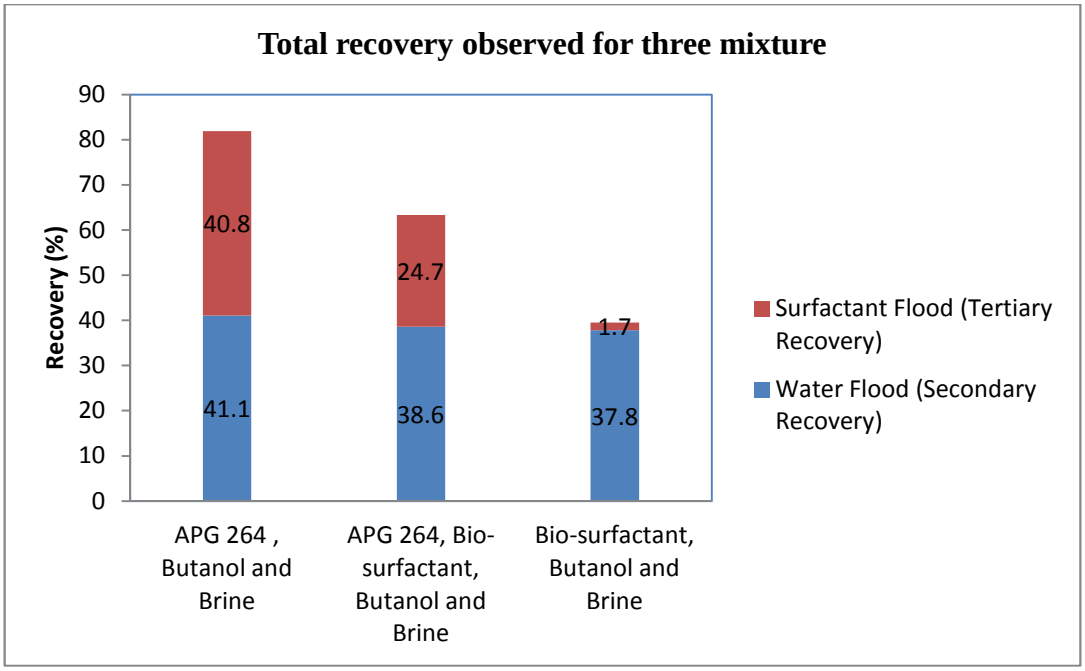

Figure 5.10 Total oil recovery observed for three formulations

5.5 Conclusions

1. APG 264 and butanol formulation showed good oil recovery results in a core-flood experiment. This formation recovered 41% of residual oil and 82% of OIIP.

2. The bio-surfactant and butanol formulation was not successful in producing a significant amount of incremental oil (about 1.7% of OIIP) after waterflooding. A total about 39.3 % of OIIP was recovered in a bio-surfactant/butanol flood.

3. The APG 264 and butanol formulation is more likely to be an effective alternative to bio-surfactant in MEOR as it can work when APG 264 is combined with bio-surfactant and alcohol.

4. An anionic bio-surfactant and non-ionic APG 264 surfactant formulation is efficient in terms of recovering additional oil from the core.

5.6 Recommendations

1. Rock wettability changes and end point effective permeability changes during surfactant flooding should be investigated. Understanding such changes is important

to simulate bio-surfactant and mobilized oil flows accurately in reservoirs and to predict oil recovery.

2. Adsorption of surfactants onto reservoir rock should be examined as it is a function of the surfactant type, equivalent weight, concentration, rock minerals, temperature, clay content, redox condition and flow rate of the solution (Green & Willhite 1998).

3. Field flow and frontal advance rates should be maintained during core-flood tests to replicate field conditions (e.g. field tests).

Chapter 6 Simulation Study

Green enhanced oil recovery (GEOR) is an EOR technique that is cheap and environmentally friendly. In this method a green surfactant and alcohol mixture is used to reduce IFT and enhance oil production. MEOR is a GEOR process where bio-products are combined to reduce IFT and increase oil recovery.

The simulation of core flood is-flooding was used in this study to understand, optimize, interpret and design the GEOR flooding process. When GEOR was successfully simulated and tested in the laboratory, it was found that it was capable of recovering more tertiary oil than a standard MEOR process.

The simulation of GEOR is discussed in this chapter. An introduction to GEOR opens the chapter, followed by a discussion of the modifications made to the Eclipse simulator, as it did not include GEOR and MEOR options. The simulator output is then compared with laboratory data to verify the simulator's accuracy before the conclusions close the chapter.

6.1 Introduction to GEOR

Using reservoir simulators to predict and understand the processes taking place during chemical flooding is currently of renewed interest to the industry given high current oil prices, which have greatly increased the interest in enhanced oil recovery. As with other simulators, chemical flooding simulators are often used to history match and understand the results of core-floods in field performance.

Many widely used reservoir simulators include an EOR option, but there is no feature available in a commercial simulator in the oil industry that simulates core-flooding to enable the investigation of the combined effect of surfactants and alcohols. Eclipse, one of the popular reservoir simulators, does not have this option. In this study the Eclipse reservoir simulator has been modified and used to simulate GEOR core-flooding experiments. The combined effects on oil recovery of anionic surfactants and alcohol, non-ionic surfactants and alcohol, and anionic and non-ionic surfactants blended with alcohol, are examined.

Three formulations of green surfactants were simulated, and the results used to investigate the effectiveness of each surfactant mixture. Three core models for three

formulations were simulated to examine the relationship between oil recovery and injected surfactant solutions. In all cases, fresh water was first injected into the core model and then surfactant solutions were injected to see the effect of secondary and tertiary recoveries. The JF-2 bio-surfactant from anionic green surfactants with butanol as a co-surfactant was modelled in the first formulation. The second formulation was the nonionic surfactant APG with butanol. The final one was a mixture of anionic and non-ionic surfactants with a co-surfactant, in this case APG and JF-2 bio-surfactant blended with butanol. APG, bio-surfactant, butanol and brine, and core properties, were discussed in Chapter Five.

The modifications to the Eclipse simulator were: (a) the combined effect of surfactant and alcohol, anionic and non-ionic surfactants with alcohol on oil recovery, and (b) the effect of volumetric swift efficiency on recovery.

6.2 Background to the study

In the past 30 years, chemical flooding simulators have become more and more complex. The need for accurate chemical flooding prediction has become more important as enhanced oil recovery projects have received more attention. Nelson and Pope (1978), Todd and Chase (1979), Dongu *et al.* (1984), and Scott *et al.* (1987) were among the first to publish papers on chemical flooding simulators.

Eclipse was developed by Exploration Consulted Limited (ECL) in the late 1970s. Its first commercial release was announced at the SPE in San Francisco, in 1983. Eclipse 100 is a Black Oil simulator, which computes the flow of fluids like oil, water and gas through porous media in reservoirs on the assumption that the oil and gas are homogeneous fluids and that the oil is allowed to dissolve in the gas and vice versa. The reservoir is discretised into grid blocks and the flow is computed using Darcy's law. In the early years Gjerde *et al.* (1988) proposed parallelization in the linear solver of black oil simulators based on isolated geologic structures. They succeeded in creating parallelized sections that took into account the possible number of phases present in each reservoir: in the old version, if three phases were present in a reservoir, then all reservoirs were treated as 3-phase. Gjerde *et al.* offered a model whereby if any reservoir had two phases, it could be treated as a

two-phase reservoir. This reduced the number of equations to be solved for the two-phase case by a factor of four ninths.

Yu *et al* (1998) used Eclipse to simulate core-flood experiments and to match simulated data with experimental results. The core-flood experiments were performed using live pre-equilibrated oil and gas phases at reservoir conditions by separating liquid samples and excess gas. The core-flood conditions were designed prior to the physical experimental, using the reservoir simulator. The basis for history matching was the CT in-situ saturation measurements of oil and gas in six cross sections along the length axis of the core versus pore volume (PV) of the equilibrium gas injected; oil and gas production volumes versus PV injected; and the differential pressure recordings across the core during the injection experiments. The results identified the most important dynamic reservoir parameters and characteristics that controlled the recovery mechanism during each displacement sequence of the experiments. Yu *et al* (1998) also investigated hysteresis functions in the two-phase gas-oil injection sequences.

Kumur and Shrivastava (2000) studied the effect of gas saturation on oil's relative permeability and mobility ratio using Stone I, II and Eclipse default methods. They found that use of Stone II caused serious problems when it created immobile oil saturation around the prolific producer wells; as a result the relative permeability of the oil came to zero. The Eclipse default method gave significantly higher values of relative permeability and very low values of mobility ratio in comparison with both Stone I and Stone II.

Salimi and Bruining (2008) carried out simulations of waterflooding in fractured media and formulated a numerical 3D model for the boundary condition (BC) approach. The results from this model were compared with those from Eclipse, which was based on the Warren and Root (WR) approach of an empirical transfer function between the fracture and matrix block. The comparison showed that the cumulative oil and water production for both the Homogenized model and Eclipse were the same at lower Péclet numbers, but at higher Péclet numbers the Homogenized model predicted a higher oil production in the early stages than Eclipse. Afterwards, the predicted rate of oil production of Eclipse became higher

than the rate of oil production predicted by the Homogenized model, and gradually the cumulative oil and water production of Eclipse reached the value of the cumulative oil and water production of the Homogenized model. One of the most important reasons for the discrepancy between the Homogenized and Eclipse models was that three-dimensional matrix block subgridding was not available in Eclipse.

The skin factor in horizontal injection wells caused by the injection of particulated water monotonically increases with time. Bedrikovetsky *et al*. (2009) investigated the effects of injected water quality on waterflooding using the Eclipse 100 reservoir simulator and found that the option of water injection with a constant skin factor was already available in the Eclipse model, but it was not able to calculate variable skin factors. They designed an analytical model for injectivity decline, accounting for particle capture and a low permeability external filter cake formation in the Eclipse simulator, to examine the effect of raw water injection on sweep efficiency during waterflooding. It was shown that sweep efficiency in a heterogeneous formation can increase by up to 5 %, compared with clean water injection, after one pore volume injected.

Tiamiyu and Boukadi (2011) performed a simulation study of surfactant and de-emulsifier blend additives in steam flooding as an EOR technique in heavy oil reservoirs, using Eclipse. This study concluded that surfactant-added steam flooding could not be simulated with the available simulator as it had no option to examine combines effects; however, the simulation of core-flooding runs for water, surfactant solution and steam flooding were successful and confirmed the validity, accuracy and applicability of laboratory results.

Shabani-Afrapoli *et al.* (2012) tried to simulate Microbial Improved Oil Recovery (MIOR) core-flooding using Eclipse and found that there was no option to examine the combined effect of bio-surfactants and bio-alcohol; in MIOR, bio-products work in combination to increase oil recovery. They concluded that Eclipse 100 (version 2009) was not a powerful enough tool to simulate MIOR because the bacterial effect on reservoir properties, particularly relative permeability, capillary pressure and wettability changes, were not expressible in this simulator.

It was found that options to measure the combined effect of surfactant and alcohol, and of oil recovery efficiency, needed to be added to Eclipse to simulate GEOR.

6.3 Model Description

The core-flooding model is a batch process. In Eclipse, the model is created as an ASCII text file, usually specified as: **.DATA* (Schlumberger 2009). This file contains a complete description of the model and a collection of keywords and comments. Each keyword has a specific syntax, although many keywords have similar or identical syntax. The data file is divided into sections by a few specific keywords: RUNSPEC, GRID, EDIT, PROS, REGIONS, SOLUTION, SUMMARY and SCHEDULE. The model reads the input data file section by section and processes each section in turn as it is read. Various data and consistency cheeks are made before proceeding to the next section. The last section is exceptional because it specifies time-dependent data and is not read and processed as a whole; instead, the keywords are processed in the order they are presented in the data file.

The RUNSPEC section allocates memory for general model characteristics. Although the model is dynamically dimensioned and reserves as much memory as is required for the simulation as a whole, different kinds of information in the simulation require varying amounts of memory.

The simulation grid geometry and properties are processed into a form more convenient for calculation in the GRID section. For each cell, the model calculates the pore volume, transmissibility in three dimensions and cell centre depth, and creates connections to other cells to or from which fluid may flow. The EDIT section modifies the processed GRID data if required.

The rock and fluid properties are specified in the PROPS section. The term “fluid property” refers to a set of input tables that effectively defines the phase behaviour of each phase. The term “rock property” refers to sets of input tables of relative permeability and capillary pressure versus saturation. Effectively, this defines the connect, critical and maximum saturation of each phase, supplies information for defining the transition zone, and defines the conditions of flow of phases relative to one another. This strongly affects the ratios of produced phases, that is, water cuts and gas oil ratios (GORs). The REGIONS section subdivides the reservoir.

In the SOLUTION section, the initial conditions are defined, often by specifying the oil water contact (OWC) and or Gas Oil Contact (GOC) depths and the pressure at a known depth. The model uses this information in conjunction with much of the information from previous stages to calculate the initial hydrostatic pressure gradients in each zone of the core (reservoir) and allocate the initial saturation of each phase in every grid cell prior to production and injection. This is called initialization.

The SCHEDULE section of the data file is where simulation actually begins. Wells are drilled, perforated and completed, production and injection targets are set up, wells are opened and fluids flow through the reservoir (core), driven by the wells.

The outputs of the simulation and their progress at dates during the simulation are defined in the SUMMARY section. Once the run has finished, the outputs are examined using text editors and post-processors of various degrees of sophistication. Details of each section and keyword description are discussed in Appendix B.

6.4 Relationship between Section and Equation

The flow equation relates different sections in the data file; it is called a well model in simulation. The simulator flow equation is derived from Darcy's law and material balance equation, and solved for each cell and each time-step. In simulation, flow is simulated from one grid block to the next, from a grid block to the well completion, and within the injection and production wells. Fluid flow in each cell in the core is the product of the transmissibility of the rock, the mobility of the fluid and the potential difference between injection and production wells. Transmissibility of the rock is described in geometry, and properties of rock in the GRID and EDIT sections. Mobility is a fluid property. All data and necessary information are put in the PROS, REGIONS and SOLUTION sections. Potential differences between wells are explained in the SCHEDULE section. Figure 6.1 below shows how the sections map to the equations (Schlumberger 2009).

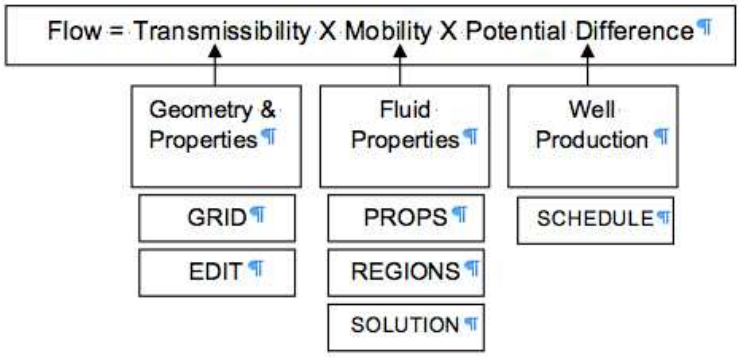

Figure 6.1 Relationship between section and equation

6.5 Governing Equations

The simulation of core-flooding is a form of numerical modelling which can be used to quantify and interpret the physical phenomena of the core-flood. It also has the ability to project future performance. The simulation process involves dividing the core into a number of discrete units in three dimensions and modelling the progression of core and fluid properties through space and time in a series of discrete steps. The equation solved for each cell and each time-step is a combination of Darcy's Law and the material balance equation (Schlumberger 2009). There are several different techniques that can be used to solve the resulting equations. In the black oil model, the finite difference approach is used to solve each equation. It is fully implicit and IMPES (Implicit Pressure, Explicit Saturation). Units of all elements in the equation in this section are expressed in SI unit.

6.5.1 Description of equations

The non-linear residual (Eclipse Technical Description Manual 2011.1 Chapter 23), $R_{fl,}$ for each fluid component in each grid block at each time step is:

$$R_{fl} = \frac{dM}{dt} + F + Q \qquad (6.1)$$

where

dM is the mass per unit surface density, accumulated during the current time step, dt

F is the net flow rate into neighbouring grid blocks

Q is the net flow rate into wells during the time step

R_{fl} is defined for each cell and each fluid in the study.

In the black oil case the fluids are oil, water and gas; however, in this study oil and water are considered.

6.5.2 Variable sets

In order to solve the residual equations, there must be a set of solution variables. The number of independent variables must be equal to the number of residual conditions; the residual equations may then be solved using Newton's method.

In black oil, the primary solution variables X are pressure P and one saturation for a two-phase black oil study. The saturation Sw is chosen to complete the set. For a 2-component black oil system (oil and water), the residual R and the solution X are 2-component vectors in each grid block. By default, the solution procedure is fully implicit.

$$R = \begin{bmatrix} R_o \\ R_w \end{bmatrix} \qquad X = \begin{bmatrix} P_o \\ S_w \end{bmatrix} \tag{6.2}$$

and the Jacobian $J = \frac{dR}{dX}$, takes the form

$$\frac{dR_i}{dX_j} = \begin{bmatrix} \frac{dR_o}{dP_o} & \frac{dR_o}{dS_w} \\ \frac{dR_w}{dP_o} & \frac{dR_w}{dS_w} \end{bmatrix} \tag{6.3}$$

The mass change during the time step, dt, is then proportional to

$$dM = M_{t+dt} - M_t \tag{6.4}$$

with

$$M = PV\begin{bmatrix} \frac{S_o}{B_o} \\ \frac{S_w}{B_w} \end{bmatrix} \qquad (6.5)$$

where

PV is the pore volume

B_o is the oil formation volume factor

B_w is the water formation volume factor

When Sg is zero the solution variable becomes Rs (undersaturated oil) and when So is zero the solution variable becomes Rv (undersaturated gas). Terms in the Jacobian are adjusted in accordance with the change of variable. No approximations are made in evaluating the Jacobian in the black oil model. Great care is taken with derivatives to ensure quadratic convergence of Newton's method.

Hydrocarbon states are:

State 1 Gas only $R_s = 0$, $S_g = 1-S_w$; variables are P_o, S_w, R_v

State 2 Gas and oil only $R_v = R_{v\ sat}$, $R_s = R_{s\ sat}$; variables are P_o, S_w, R_g

State 3 Oil only $R_v = R_{v\ sat}$, $R_s = R_{s\ sat}$; variables are P_o, S_w, $R_{s.}$

The number of cells in each state, together with the number of cells changing state during a Newton iteration, are printed in the summary of each Newton iteration.

6.5.3 Convergence criteria for residual equations

The Newton solver aims to reduce the residuals *R(X)* to zero. In the black oil model the convergence criteria are primarily based on material balance and maximum residual checks on *R*.

6.5.4 Material balance

If the residuals are summed over all cells in the core, the flow term F cancels, because the flow out of one cell is always equal and opposite in sign to the corresponding flow into its neighbouring cell. Thus the sum of the residuals for each phase or component corresponds to the net mass accumulation within the core less the net influx through wells. This is the material balance error. For a two-component system, material balance becomes:

$$\sum_i (R_o)_i = \sum_i \left(\frac{dM_o}{dt} \right)_i + \sum_i (Q_o)_i$$
$$\sum_i (R_w)_i = \sum_i \left(\frac{dM_w}{dt} \right)_i + \sum_i (Q_w)_i \qquad (6.6)$$

where

$\sum_i$ Refers to the sum over all core cells and

$(R_o)_i$ is the oil residual in cell i.

In the black oil model, the material balance errors are converted to meaningful independent numbers by scaling to equivalent field saturation values:

$$MB_o = \overline{B_o} dt \left\{ \frac{\sum_i (R_o)_i}{\sum_i (PV)_i} \right\}$$
$$MB_w = \overline{B_w} dt \left\{ \frac{\sum_i (R_w)_i}{\sum_i (PV)_i} \right\} \qquad (6.7)$$

where

$\overline{B_o}$ is the average oil formation factor, etc.

The numerical values of MBo and MBw are computed after each Newton iteration and the material balance errors are considered sufficiently small if they are all less than 1E-7. MB values are printed out in the summary of each Newton iteration. Conventional material balance accounts in conventional units can also be printed at each report time.

6.5.5 Normalized residuals

Although great care is taken to ensure that material balance errors are unusually small in the black oil model, this is not considered a sufficiently rigorous test of convergence. The second test is obtained by computing the maximum saturation of normalized residuals

$$CNV_o = \overline{B_o} dt.MAX_i \left| \frac{(R_o)_i}{(PV)_i} \right|$$
$$CNV_w = \overline{B_w} dt.MAX_i \left| \frac{(R_w)_i}{(PV)_i} \right| \qquad (6.8)$$

where MAXi is the maximum value over all cells in the core.

By converting each convergence error to an equivalent saturation value, a sensible limit can be put to the CNV numbers, which are considered to have converged if they are all less than 0.001. The convergence criteria can be altered by the TUNING keyword.

6.5.6 Flow

The flow rate into cell *i* from a neighbouring cell *n*, $F_{ni,}$ is

$$F_{ni} = T_{ni} \begin{bmatrix} \frac{k_{ro}}{B_o \mu_o} \\ \frac{k_{rw}}{B_w \mu_w} \end{bmatrix}_u \times \begin{bmatrix} dP_{oni} \\ dP_{wni} \end{bmatrix} \qquad (6.9)$$

where

$$dP_{oni} = P_{on} - P_{oi} - \rho_{oni} G(D_n - D_i)$$
$$dP_{wni} = P_{wn} - P_{wi} - \rho_{wni} G(D_n - D_i) = P_{on} - P_{oi} - \rho_{wni} G(D_n - D_i) - P_{cown} + P_{cowi} \qquad (6.10)$$

where

T_{ni} is the transmissibility between cells n and I,

k_{ro} is the relative permeability of oil

k_{rw} is the relative permeability of water

μ_o is the viscosity of oil

μ_w is the viscosity of water

dP is the potential difference

ρ is the fluid density

ρ_{oni} is the density of oil at the interface between cells n and i

G is the acceleration due to gravity

D is the cell centre depth.

The subscript u indicates that the fluid mobilities are to be evaluated in the upstream cell (cell n if dPni is positive, cell i if dPni is negative). The upstream calculation applies separately for each equation (oil, water and gas) so that, for example, oil may flow from cell i to n while water flows from n to i.

The net flow rate from cell i into neighbouring cells is obtained by summing over the neighbouring cells

$$F_i = \sum_n F_{ni} \tag{6.11}$$

The rate of flow into a production well from cell i is

$$Q_i = -T_{wi}\left(P_{oi} - H_{iw} - P_{bh}\right)\left[\begin{array}{c} \dfrac{k_{ro}}{B_o\mu_o} \\ \dfrac{k_{rw}}{B_w\mu_w} \end{array}\right]_i \tag{6.12}$$

where

T_{wi} is the well connection transmissibility factor

H is the hydrostatic head correction

P_{bh} is the bottom hole pressure

6.5.7 Densities

In the black oil case, densities of oil and gas are computed from surface densities using (ρ_s)

$$\rho_o = \frac{(\rho_{so} + CR_s\rho_{sg})}{B_o} \tag{6.13}$$

with C=1 for metric and laboratory units and C=178.1076 in field units.

The density at the interface between cells n and i is computed as the average of the reservoir densities in cells n and i

$$\rho_{oni} = \frac{(\rho_{on} + \rho_{oi})}{2} \tag{6.14}$$

6.5.8 Newton iteration of the non-linear residual

Given the non-linear residual $R=R_{fl}$ and the solution variables X, we wish to solve the non-linear equation R(X) =0.

Stepwise operation of each iteration of the non-linear equation:

Step 1: Given current solution X, obtain R(X), and then find a correction Δx such that

R(X+Δx)

$$R(X + \Delta x) \approx R(X) + J \cdot \Delta x = 0 \tag{6.15}$$

where

J is the Jacobian $\frac{d}{dX} R(X)$

Step 2: To do this, solve the linear equations

$$J \cdot \Delta x = R(X)$$

or

$$\Delta x = J^{-1} R(X) \qquad (6.16)$$

Step 3: Update the solution vector $X \rightarrow X + \Delta x$

If some measure of convergence has been achieved, exit; if not, repeat.

In the fully implicit case, these equations may be solved for X, using the linear solver to give

$$\Delta x = J^{-1} R'_{fl} \qquad (6.17)$$

6.5.9 Surfactant conservation equation

The distribution of injected surfactant is modelled by solving a conservation equation for surfactant with the water phase. The surfactant concentrations are updated fully-implicitly at the end of each time-step after the oil, water and gas flows have been computed. The surfactant is assumed to exist only in the water phase, and the input to the core as a concentration at a water injector (in the WSURFACT keyword).

6.5.10 Calculation of the capillary number

The capillary number is a dimensionless group that measures the ratio of viscous forces to capillary forces. The capillary number is given by:

$$N_c = \frac{|K \cdot grad\ P|}{ST} C_{unit} \qquad (6.18)$$

$$|K \cdot grad\ P| = \sqrt{(K_x \cdot grad\ P_x)^2 + (K_y \cdot grad\ P_y)^2 + (K_z \cdot grad\ P_z)^2} \qquad (6.19)$$

where

K = permeability

P = potential

ST = interfacial tension (IFT)

C_{unit} = conversion factor depending on the units used.

For cell i

$$K_x \cdot grad\, P_x = 0.5\left[\left(\frac{K_x}{D_x}\right)_{i-1,i} \cdot (P_i - P_{i-1}) + \left(\frac{K_x}{D_x}\right)_{i,i+1} \cdot (P_{i+1} - P_i)\right] \quad (6.20)$$

and similarly for the y and z directions.

The K/D value is calculated in an analogous manner to the transmissibility and depends on how the geometry was specified.

The surface tension is a tabulated function of the surfactant concentration.

6.5.11 Relative Permeability model

The relative permeability model is essentially a transition from immiscible relative permeability curves at low capillary number to miscible relative permeability curves at high capillary number. A table is supplied that describes the transition as function of log10 (capillary number).

The relative permeability used at a value of the miscibility function between the two extremes is calculated in two steps. The first end points of the curve are interpolated and both the immiscible and the miscible curves are scaled to honour these points. Stone II relative permeability model is presented in Appendix C.

6.5.12 Capillary pressure

The water oil capillary pressure will reduce as the concentration of surfactant increases; indeed it is the reduction in the water capillary pressure that gives rise to the reduction in the residual oil saturation. The oil water capillary pressure is taken as:

$$P_{cow} = P_{cow}(S_w)\frac{ST(C_{surf})}{ST(C_{surf}=0)} \tag{6.21}$$

where

$ST(C_{surf})$ = Surface tension at the present surfactant concentration

$ST(C_{surf} = 0)$ = Surface tension at the zero concentration

P_{cow} (S_w) = Capillary pressure from the immiscible curves initially scaled to the interpolated end-points calculated in the relative permeability model.

6.5.13 Water PVT Properties

The surfactant modifies the viscosity of the pure or salted water input using the PVTW or PVTSALT keyword respectively. The surfactant viscosity input as a function of surfactant concentration using the SURFVISE keyword is used to calculate the water-surfactant solution viscosity as follows:

$$\mu_{ws}(C_{surf}, P) = \mu_w(P)\frac{\mu_{surf}(C_{surf})}{\mu_w(P_{ref})} \tag{6.22}$$

If the Brine option is active, Equation 21 becomes a function of salt concentration C_{salt} as well:

$$\mu_{ws}(C_{surf}, P, C_{salt}) = \mu_w(P, C_{salt})\frac{\mu_{surf}(C_{surf})}{\mu_w(P_{ref}, C_{salt-ref})} \tag{6.23}$$

where

μ_{ws} = Viscosity of the water-surfactant mixture

μ_w = Viscosity from the PVTW or PVTSALT keywords

μ_{surf} = Viscosity from the SURFVISC keyword

P_{ref} = Reference pressure in the PVTW or PVTSALT keywords

C_{surf} = Surfactant concentration

C_{salt} = Reference salt concentration in the PVTSALT keywords.

6.5.14 Treatment of adsorption

The adsorption of a surfactant is assumed to be instantaneous, and the quality of adsorption is a function of the surrounding surfactant concentration. Data is supplied as an adsorption isotherm as a function of surfactant concentration in the SURFADS keyword.

The quantity of surfactant adsorption on the rock is given by:

$$M_{AS} = PV_{cell} \cdot \frac{1-\phi}{\phi} \cdot \rho_{mas} \cdot CA\left(C_{surf}\right) \tag{6.24}$$

where

M_{AS} =Mass of adsorbed surfactant

PV_{cell} =Pore volume of the cell

Ø = Porosity

ρ_{mas} = Mass density of the rock in the SURFROCK keyword

$CA(C_{surf})$ = Adsorption isotherm as a function of local surfactant concentration in solution.

6.6 Model assumption

The black oil model is a simplified version of a reservoir simulation that reduces the computation time needed by more complex and rigorous compositional models (Peaceman 1977). The black oil model solves multiphase, multidimensional flow equations for fluid properties that are dependent on pressure. The specific fluxes and concentrations of the conservation equation for each phase are used to determine the flow equation for the water and oil system (Fanchi 2006). The injected surfactant is assumed to only exist in water phase; so surfactant injection is modelled by solving a conservation equation for surfactant within the water phase only. The surfactant concentration is updated at the end of each time-step after the flows of oil and water have been computed (Schlumberger, 2009).

- Isothermal flow and mass transfer within the grid block are instantaneous.

- Fluids have minimal effect on rock properties (e.g. very low grain dissolution, and no gel formation occurs).

Assumptions made to simulate the surfactant model are:

- The water phase has no brine salinity.
- Surfactants only exist in water phase.
- The adsorption of surfactant is instantaneous.

6.7 Modification of Eclipse

The Eclipse simulator was modified to enable it to simulate MEOR and GEOR, as it did not have these options. Two modifications were made: adding the IFT table as a function of the surfactant and alcohol concentration, to replace the existing data file that contained only surfactant concentration; and adding a volumetric sweep efficiency (Ev) term in Eclipse's field oil efficiency (FOE) equation.

6.7.1 Modification one: addition of IFT table

6.7.1.1 The existing Eclipse system

Conventionally in Eclipse, surfactant water solution injected into the core and surfactant concentrations are solved by conservation equations in the water phase. The interfacial tension (IFT) table as a function of surfactant concentration is looked up, then the capillary number is calculated as a function of IFT. The relative permeability of the oil and water phase is interpolated as a function of the capillary number. Water-oil capillary pressure is reduced as a function of the IFT of the surfactant concentration. After that, water viscosity is changed as a function of surfactant concentration, and the surfactant solution adsorbs onto the core. Finally, the wettability of the rock changes as a function of the amount of surfactant adsorbed.

6.7.1.2 Reason for modification

In MEOR, microbes produce bio-products like bio-surfactant and bio-alcohol. These bio-products in combination produce in a solution called nutrient. A surfactant–alcohol solution reduces IFT and increases oil recovery. Similarly, in GEOR a surfactant and alcohol mix is used to reduce IFT and enhance oil production. For this

reason, in GTOR/GEOR green surfactants, alcohol and water in solution are used in place of a surfactant–water solution.

6.7.1.3 Introducing the modification

First, green surfactant, alcohol and water are mixed into solution and injected into the core; then surfactant and alcohol mixture concentration is solved by conservation equation. The IFT table is made a function of the surfactant–alcohol concentration, and the Capillary number calculated as function of IFT. The relative permeability of the oil and water phase is interpolated as a function of the capillary number. Water–oil capillary pressure is reduced as a function of IFT of surfactant–alcohol or surfactant–mixture concentration. After that water viscosity is changed as a function of *surfactant-alcohol* mixture concentration, and surfactant–alcohol solution adsorbs onto core. Finally, the wettability of the rock changes as a function of the amount of *surfactant-alcohol* solution adsorbed.

6.7.2 Modification two: addition of volumetric sweep efficiency (Ev)

6.7.2.1 The exiting Eclipse field oil efficiency (FOE) equation

The oil in place within a grid block is expressed in Eclipse (*Technical Description Manual* 2011, p 819, EQ 54.1) as:

$$Oil\ in\ Place\ (OIP) = \frac{PV \times S_o}{B_o} \tag{6.25}$$

where

PV = pore volume

S_o = oil saturation = 1 - S_w – S_g

S_w = water saturation

S_g = gas saturation = 0

B_o = Oil formation volume factor.

Oil recovery efficiency is calculated as oil efficiency (Eclipse Technical Description Manual 2011, p. 1696). Field oil efficiency is expressed as the keyword FOE and calculated using the equation below:

$$Field\ Oil\ Efficiency\ (FOE) = \frac{OIP_{initial} - OIP_{now}}{OIP_{initial}} \tag{6.26}$$

where

$OIP_{initial}$ = Oil in place at beginning

OIP_{now} = Oil in place at present

Equations 25 and 26 express oil in place and field oil efficiency respectively. Equation 25 can be written at initial and final (after water and/or surfactant flood in core-flood experiment) stages as

$$(OIP)_{initial} = \frac{PV \times S_{oi}}{B_{oi}} \tag{6.27}$$

$$(OIP)_{final\ (after\ water\ /\ surfac\ \ flood)} = \frac{PV \times S_o}{B_o} \tag{6.28}$$

where

PV = Total pore volume of the core

S_{oi} = Oil saturation at initial condition

S_o = Oil saturation at final (after water/surfactant flood)

B_{oi} = Oil formation volume factor at initial condition

B_o = Oil formation volume factor at present (after water/surfactant flood).

Putting the value of EQ 27 and 28 in EQ 25, we get

$$Field\ Oil\ Efficiency\ (FOE) = \frac{\frac{PV \times S_{oi}}{B_{oi}} - \frac{PV \times S_o}{B_o}}{\frac{PV \times S_{oi}}{B_{oi}}} = \frac{\frac{S_{oi}}{B_{oi}} - \frac{S_o}{B_o}}{\frac{S_{oi}}{B_{oi}}} \tag{6.29}$$

Assuming the constant a constant Bo during the flooding life, as pressure and temperature remain constant and used oil is dead oil. So Boi is equal to Bo.

The final form of EQ 29 becomes

$$FOE = \frac{S_{oi} - S_o}{S_{oi}} \tag{6.30}$$

EQ 30 is the final form of FOE equation which is used to calculated field oil recovery efficiency in Eclipse and it does not include volumetric sweep efficiency.

6.7.2.2 The need for modification

Volumetric sweep efficiency is the fraction of the floodable portion of the reservoir swept or contacted by water. It is the product of the areal (E_A) and vertical (E_V) sweep ($E_{VW} = E_A \times E_V$). It is useful to compute the volumetric sweep efficiency of the injected water, as this assists in the management and calculation of future waterflood recovery potential in a mature waterflood. Volumetric sweep efficiency is important because it defines the fraction of the reservoir swept by the injected water (Cob & Marek 1997).

The volumetric sweep efficiency of E_{VW} represents the fraction of the reservoir contacted by the injected water. If the water injection wells are also used as EOR injectors, the EOR injection is likely to sweep the same volume swept by the water. Conversely, ($1-E_{vw}$) defines that portion of the reservoir *not* swept by the injected water, and so identifies that portion of the reservoir where recoverable waterflood oil volumes are likely to exist (Cob & Marek 1997). Mathematical development of volumetric sweep efficiency is discussed in Appendix C.

6.7.2.3 Introducing the modification

Oil recovery by surfactant process can be approximated by the application of a simple material balance (Green & Willhite 1998). Because a favourable mobility ratio is maintained during the process, volumetric sweep efficiency is assumed to be the same as for a waterflood preceding the surfactant process. A constant oil formation volume factor is assumed as pressure and temperature do not change during flood life.

Oil recovery at the end of water flood is given by

$$N_p = \frac{A \times h \times \phi (S_{oi} - S_{orw})}{5.615 \times B_o} \times E_{vw} \tag{6.31}$$

Oil recovery at the end of surfactant flood is given by

$$N_p = \frac{A \times h \times \phi (S_{orw} - S_{orc})}{5.615 \times B_o} \times E_{vw} \tag{6.32}$$

The combined oil recovery at the end of water and surfactant flood is (assuming resaturation of oil in the unswept region)

$$N_p = \frac{A \times h \times \phi (S_{oi} - S_{orc})}{5.615 \times B_o} \times E_{vw} \tag{6.33}$$

Original oil in place is given by

$$N = \frac{A \times h \times \phi \times (S_{oi})}{5.615 \times B_o} \tag{6.34}$$

where

Np = Oil recovered in process, STB

N = Original oil in place, STB

A = Pattern area, ft2

h = Reservoir thickness, ft

Ø = Porosity

Sorw = Residual oil saturation at termination of water flood

Sorc = Residual oil saturation at termination of chemical flood

Soi = Initial oil saturation

Evw = Volumetric sweep efficiency of water flood preceding chemical flood.

B_o = Oil formation volume factor, RB/STB

Oil recovery efficiency (ORE) after water and surfactant flood is given by

$$\frac{N_P}{N} = \frac{\frac{A \times h \times \phi (S_{oi} - S_{orc})}{5.615 B_o} \times E_{vw}}{\frac{A \times h \times \phi \times (S_{oi})}{5.615 B_o}} = \frac{(S_{oi} - S_{orc})}{(S_{oi})} \times E_{vw} \tag{6.35}$$

Oil recovery efficiency can be called field oil efficiency (FOE) and oil saturation at the end of surfactant flood S_{orc} can be written as saturation at present S_o. So Eq 35 becomes

$$FOE = \frac{N_P}{N} = \frac{(S_{oi} - S_o)}{(S_{oi})} \times E_{vw} \tag{6.36}$$

The FOE Equation 30 provided in Eclipse did not include a volumetric sweep, so Equation 36, derived by Green and Willhite (1998), was included to give a better match.

6.7.3 Modification implementation in Eclipse

The first modification was implemented by making the IFT table a function of the surfactant and alcohol concentration; from there, the concentration of the surfactant and alcohol mixture was solved using the conservation equation. The rest of the steps followed Section 6.7.1 of the Eclipse solver.

To implement modification two, first FOE was calculated in Eclipse and put into an Excel sheet. Then E_{vw} was calculated based on laboratory data. At the end, FOE value was multiplied by E_{vw} and put into a different column. Injected PV versus different FOE curves were plotted and compared with laboratory data. Figure 6.2 shows the implementation of modification, showing that after Ev was applied the EOR curve came closer to laboratory EOR than a normal sim curve. A similar characteristic may be observed in the total recovery plot in Figure 6.3.

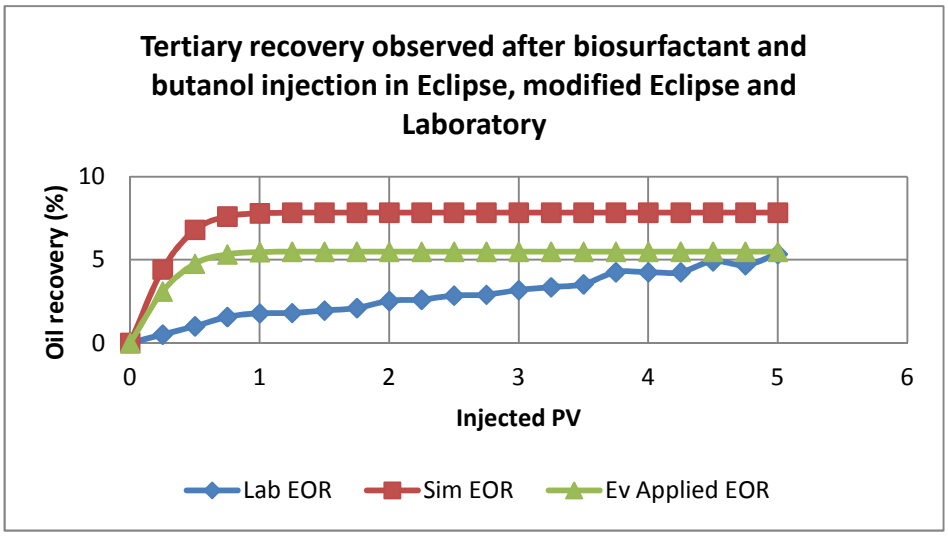

Figure 6.2 Tertiary oil recovery observed after bio-surfactant and butanol injection in Eclipse, modified Eclipse and Laboratory

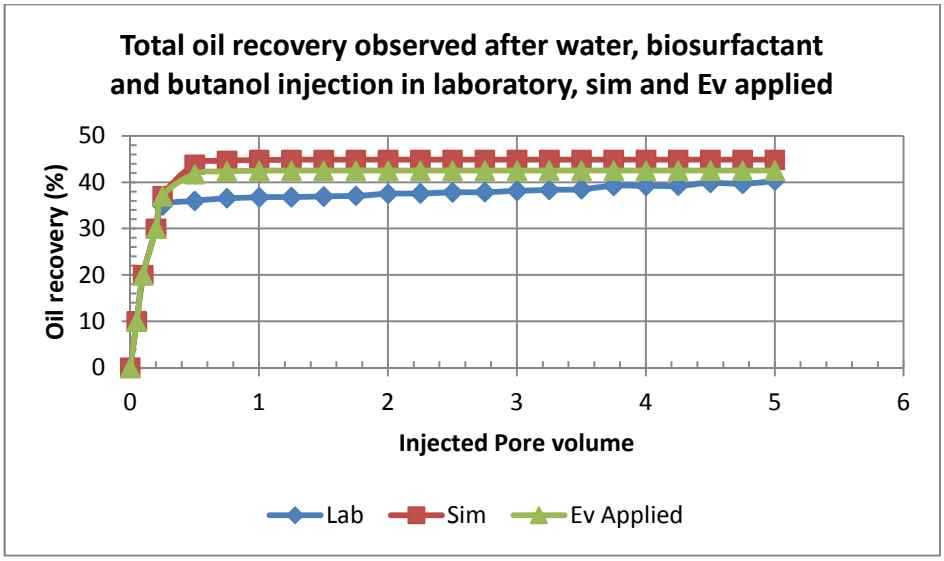

Figure 6.3 Total oil recovery observed after water bio-surfactant and butanol injection in Eclipse, Modified Eclipse, and Laboratory

6.8 Simulation of core-flood experiments

The three green surfactant core-floods described in Chapter Five were simulated; simulation and experimental results were then compared. Simulation basics and input variables are explained below.

6.8.1 Core-flood simulation basics

First, the core is divided into a number of cells, and basic data is provided for each one. Then injection and production wells are positioned with the cells. The required well production or injection rates are specified as functions of time. Finally the equations are solved to give the pressure and saturation for each block as well as the production of each phase from each well.

6.8.2 Input parameters

The simulation model was developed using the block-cantered geometry option, which has the shape of flat-lying “sugar-cubes” arranged in a 3-dimensional volume comprising 1 geological layer with 10 columns of cells in the lateral direction and 1 column of cells in the transverse direction (i.e. 10x1x1). A rectangular core block is presented in Figure 6.4. The main reason for using this geometry is because block-cantered grids tend to be geometrically simpler, thus helping to avoid any

unexpected error and confusion when designing the ECLIPSE simulation file. However, this geometry is still considered highly reliable in representing real field conditions while providing precise results in reservoir simulations.

In the laboratory the core-flood experiments were done using cylindrical cores of Berea sandstone, but in simulation a rectangular core model was taken, keeping the same volume as the cylindrical core. Below is the mathematical evidence that volume was kept the same in both shapes:

Core length = 8.126cm

Diameter = 3.85 cm

Cylindrical core:

Cross sectional Area = $\Pi D^2/4$ = 11.64156 cm2 = 3.412cm×3.412cm

Volume = $\Pi D^2/4 \times L$= 11.64156 cm2×8.126cm=94.6 cm3

Rectangular core:

DY=DZ = 3.412cm

Length = DX=8.126cm

Cross sectional Area = DY×DZ = 3.412cm×3.412cm=11.64156 cm2

Volume = DY×DZ ×L= DY×DZ ×DX =11.64156 cm2×8.126cm=94.6 cm3

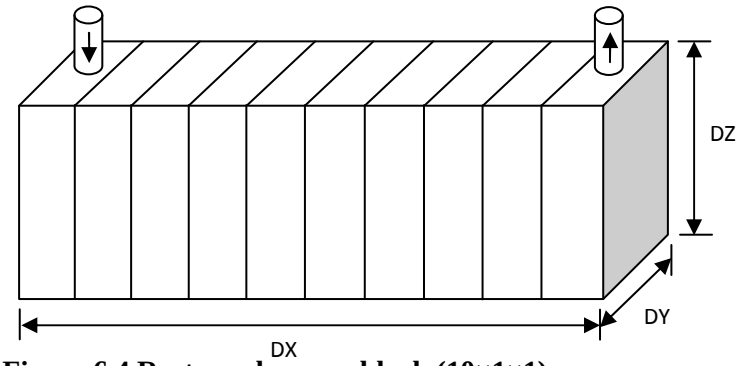

Figure 6.4 Rectangular core block (10×1×1).

In the laboratory, Stag oil was used to do the core-flooding. To replicate the laboratory conditions, the Stag reservoir depth was taken for the simulation. The

reservoir of interest was 680 m below ground level and had one geological layer, represented by the grid block. The grid block thickness was 3.412 cm. The rectangular size of the reservoir model was 3.412 cm wide by 8.126 cm long, represented by 10 columns of cells in the lateral direction and 1 column of cells in the transverse direction.

This simulation considers only one injection well and a single production well. These two wells were located at separate corners at the edge of the core model. This position gave the clearest view of the direction of the surfactant slug, which was expected to flow from the injection well to the production well, sweeping the residual oil in the reservoir before it. Both wells were perforated throughout their core thickness with a wellbore diameter of 4mm.

The reservoir properties used to simulate the effect of surfactants on EOR are based on a medium-wet, under-saturated reservoir. It is assumed that only 2 phases of fluid exist in the reservoir system: oil and water aquifer. The water phase is considered to have zero brine salinity; thus the injected surfactants in this simulation process are not influenced by any ionic interaction with a brine environment.

All three data files use the same reservoir parameters and physical grid dimensions, tabulated in Table 6.1. The only variable is in the surfactant and alcohol mixture (i.e. viscosity, capillary number, surface tension, etc.); the waterflood data file has zero surfactant properties. Tables 6.2 to 6.7 present the input data for the three formulations of the models. Tables 6.2, 6.4 and 6.6 are generated by Eclipse based on three water saturations: initial, at the end of water flood and at the end of surfactant flood. Table 6.3, 6.5 and 6.7 are fluid property data of three formulations. Viscosity and IFT are calculated in the lab and liquid rate is recorded at time of experiment.

E_{vw} was calculated using equation C-2. Free gas saturation (Sg) assumed to zero as core was evaluated and dissolved oxygen was removed from brine. Formation volume factor and average water saturation were assumed within the estimation technique because core flood instrument was broken down at middle of experiment. Required data for calculating those values were not monitored due to that incident.

N_p, S_o, S_{wc} and V_p were taken from Coreflooding experiments and were used to measure E_{vw}. Evw values of three formulations were presented in tables 6.3, 6.5 and 6.7. The Mathematical development of volumetric sweep efficiency is presented in Appendix C.

Table 6.1 Reservoir and simulation model properties.

Model physical dimension	8.126 cm ×3.412 cm ×3.412 cm
Datum pressure	72.41 bar = 1050 psi
Datum depth	680 m
Depth at oil-water contact	690 m
Porosity, Φ	0.20
Horizontal permeability, k_h	Top layer: 470 mD
Vertical permeability, k_v	Top layer: 470 mD
Well/tube diameter (mm)	4.00

Table 6.2 Relative permeability and saturation table of formulation 1 (bio-surfactant and butanol)

S_w	K_{rw}	K_{ro}	S_o
0.18	0.0015	0.67	0.82
0.2	0.003	0.64	0.8
0.22	0.006	0.61	0.78
0.24	0.009	0.58	0.76
0.29	0.02	0.51	0.71
0.39	0.06	0.37	0.61
0.49	0.13	0.24	0.51
0.54	0.16	0.19	0.46

Table 6.3 Fluid property data of formulation 1 (bio-surfactant and butanol)

Oil density (kg/m3)	936
Water density (kg/m3)	1000
Oil Viscosity (cP)	0.47
Water Viscosity (cP)	0.34
Adsorption function	0.00002
Initial IFT (dyne/cm)	27
Final IFT (dyne/cm)	1.8
Liquid rate (cc/min)	100
Volumetric sweep efficiency	0.70

Table 6.4 Relative permeability and saturation table of formulation 2 (APG 264 and butanol)

Sw	Krw	Kro	So
0.22	0.00	0.61	0.78
0.24	0.00	0.58	0.76
0.29	0.02	0.51	0.71
0.39	0.06	0.37	0.61
0.54	0.16	0.19	0.46
0.64	0.24	0.11	0.37
0.70	0.32	0.05	0.30
0.80	0.50	0.01	0.20
0.86	0.63	0.00	0.14

Table 6.5 Fluid property data of formulation 2 (APG 264 and butanol)

Oil density (kg/m3)	936
Water density (kg/m3)	1000
Oil Viscosity (cP)	0.47
Water Viscosity (cP)	0.34
Adsorption function	0.00002
Initial IFT (dyne/cm)	27
Final IFT (dyne/cm)	0.55
Well/tube diameter (mm)	4.00
Liquid rate (cc/min)	100
Volumetric sweep efficiency	1.00

Table 6.6 Relative permeability and saturation table of formulation 3 (APG 264, bio-surfactant and butanol)

Sw	Krw	Kro	So
0.17	0.00	0.68	0.83
0.18	0.00	0.67	0.82
0.20	0.00	0.64	0.80
0.22	0.01	0.61	0.78
0.24	0.01	0.58	0.76
0.29	0.02	0.51	0.71
0.39	0.06	0.37	0.61
0.49	0.13	0.24	0.51
0.54	0.16	0.19	0.46
0.57	0.18	0.16	0.43
0.64	0.24	0.11	0.37
0.70	0.32	0.05	0.30

Table 6.7 Fluid property data of formulation 3 (APG 264, bio-surfactant and butanol)

Oil density (kg/m3)	936
Water density (kg/m3)	1000
Oil Viscosity (cP)	0.47
Water Viscosity (cP)	0.34
Adsorption function	0.00002
Initial IFT (dyne/cm)	27
Final IFT (dyne/cm)	0.41
Liquid rate (cc/min)	100
Volumetric sweep efficiency	1.00

6.9 Results and discussion

Three green surfactant floods were simulated and the results compared with laboratory core-flooding data to verify simulation accuracy. JF-2 bio-surfactant from anionic green surfactants with butanol as a co-surfactant mixture was the model in first formulation. The second formulation was a nonionic surfactant APG and butanol mixture. Last was a mixture of anionic and non-ionic surfactants with a co-surfactant; in this case, APG and JF-2 bio-surfactant blended with butanol. In all three cases, secondary recovery (oil recovery due to water injection) and tertiary recovery (oil recovery due to surfactant and co-surfactant injection) were studied; results are shown in figures below.

6.9.1 Formulation 1: bio-surfactant, butanol and water

A JF-2 bio-surfactant and butanol mixture was the model in this formulation. First fresh water was injected into the core model and then surfactant solutions were injected to see the effect of secondary and tertiary recoveries.

6.9.1.1 Saturation effect

The simulated oil saturation profile after 4PV of waterflooding was compared with the laboratory waterflood data. The input data for the simulation is listed in Tables 6.2 and 6.3; the two solutions are compared in Figure 6.5. The simulation result closely matched the laboratory data apart from the section from 0.8PV to 2.2PV; this

anomaly is due to the simulation input parameter not being properly adjusted. However, there is a perfect match between 2.4PV and 5PV.

There was a 0.31 decrease in oil saturation from 0.82 to 0.51 in the laboratory. To see the other ionic effects in the mixture, salinity was assumed to be zero in simulation. Fresh water was introduced via the injection well. The average oil saturation reduced from 0.79 to 0.51 each grid block, indicating that oil had been displaced.

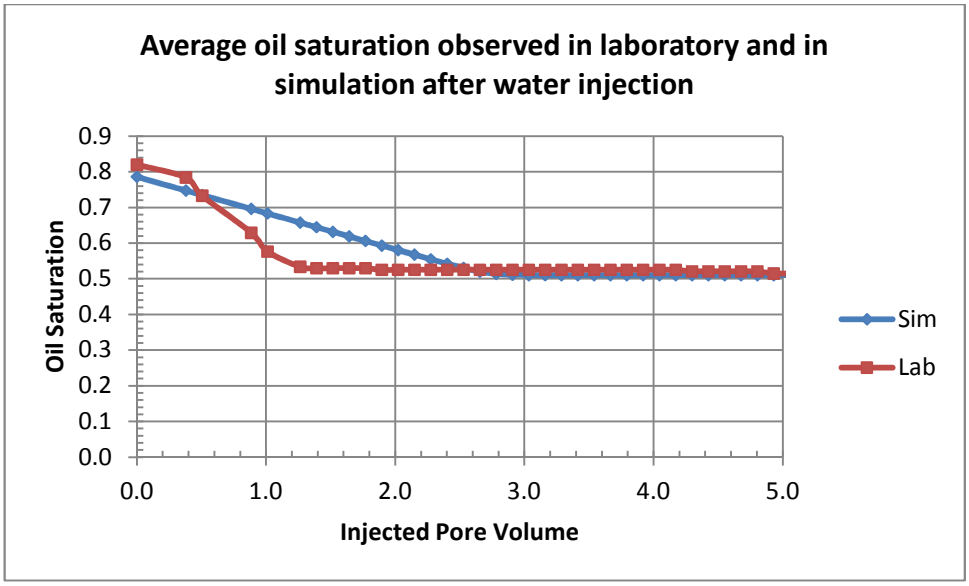

Figure 6.5 Average oil saturation observed in laboratory and simulation after water injection

6.9.1.2 Secondary oil recovery

The 2% NaCl water was injected into a core at a rate of 0.0024 m^3/day until no oil was produced from the core. In the simulation fresh water was introduced via the injection well at a rate of 0.0024 m^3/day. The simulation input data are listed in Tables 6.2 and 6.3; oil recovery is plotted in Figure 6.6. About 35% oil was recovered; in the laboratory about 37 % oil was recovered. The 2 % higher value is because in the laboratory 2 % NaCl was used but in simulation fresh water was used.

The simulated oil recovery curve does not match the laboratory curve from 0.4PV to 3.2PV because the simulation input parameter was not properly adjusted. However, there is a good match between 3.4PV and 5PV.

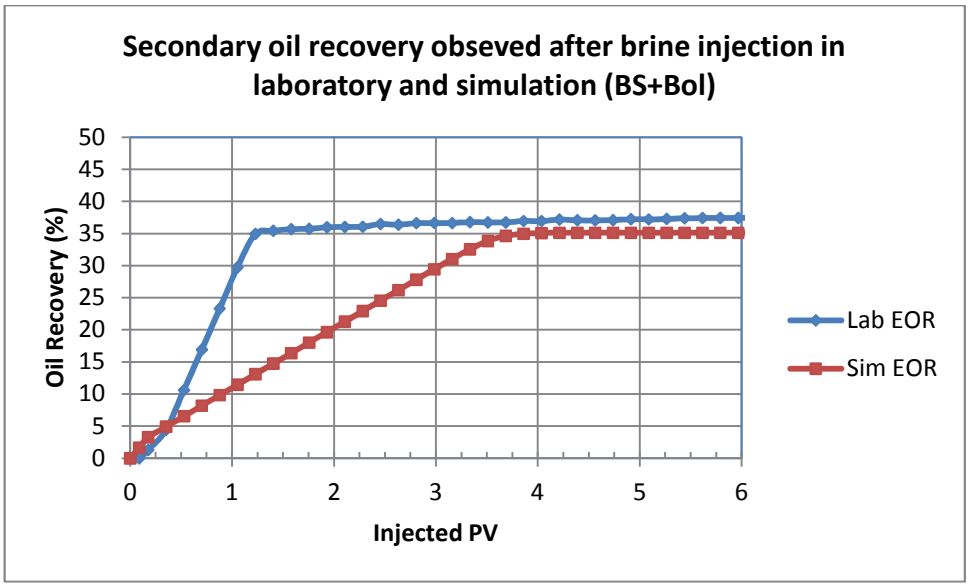

Figure 6.6 Secondary oil recovery observed in laboratory and simulation after brine injection.

6.9.1.3 Tertiary oil recovery

Bacillus mojavensis strain JF-2 bio-surfactant, commonly called JF-2 bio-surfactant, is used in tertiary oil recovery. A solution of 45mg/l JF-2 bio-surfactant and 0.5% butanol was injected into the core to investigate the volume of oil recovery with a bio-surfactant/butanol solution. Input data appear in Tables 6.2 and 6.3; oil recovery is plotted in Figure 6.7. A higher oil recovery is achieved in simulation than in the laboratory core-flood. TOR is about 7.8% in the simulation study, and about 5.4% in the laboratory. Neither of these values is significant compared with other TOR values. Oil production started earlier in the simulation and reached 7.8% with 1PV injection of solution, and remained the same when the injected volume was increased. In the laboratory, the oil production curve rose slowly with an increase of injected volume and reached its highest point of 5.4% with 5PV.

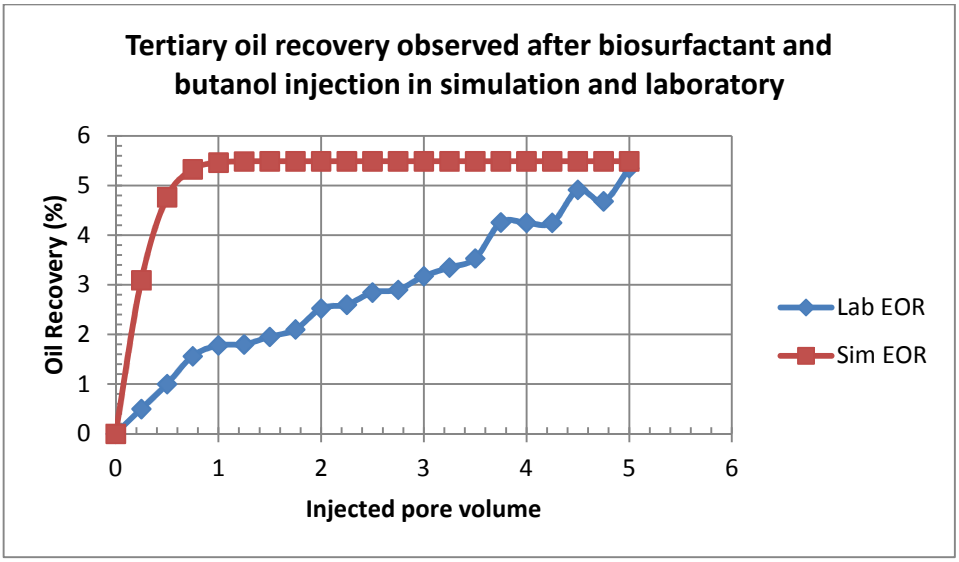

Figure 6.7 Tertiary oil recovery observed in laboratory and simulation after bio-surfactant and butanol injection

6.9.1.4 Total oil recovery

First water, then a bio-surfactant/butanol solution, were injected into the core model, and total oil production was examined. Total recovery profiles of simulation and laboratory are compared in Figure 6.8, which shows that total recoveries were 41% in simulation and 40% in laboratory core-flooding. The results suggest that a bio-surfactant/butanol solution is most likely too weak to mobilize residual oil. The simulation oil recovery profile showed that oil recovery did increase with an increase of surfactant/co-surfactant.

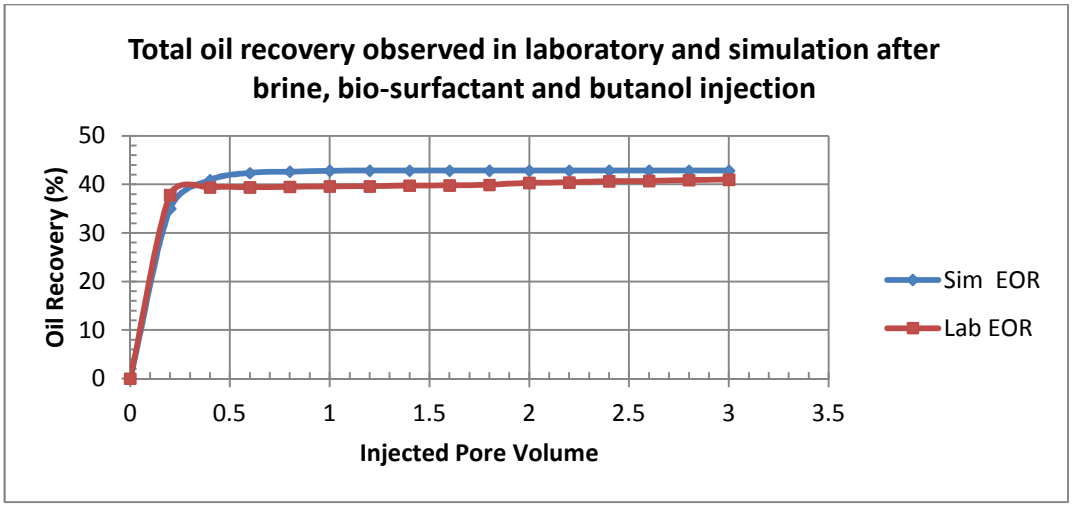

Figure 6.8 Total oil recovery observed in laboratory and simulation after brine, and bio-surfactant and butanol injection

6.9.2 Formulation 2: APG, butanol and water

In the second preparation nonionic surfactant APG and butanol were combined and then passed through the core. Results were examined and compared with laboratory data to determine oil recovery.

6.9.2.1 Saturation effect

The simulated oil saturation plot of water-flood was compared with laboratory data to verify the model in Figure 6.9. Input data for the simulation are listed in Tables 6.4 and 6.5.

There was a good match at the early and later stages of these curves, except between 1 to 3PV. This indicates that the simulation gave better results. Simulated oil saturation decreased from 0.78 to 0.47 in 3PV injection of water and then became constant. There was a 0.29 reduction in oil saturation in the laboratory between .78 and 0.49 in 1.8PV; after that saturation remained unchanged.

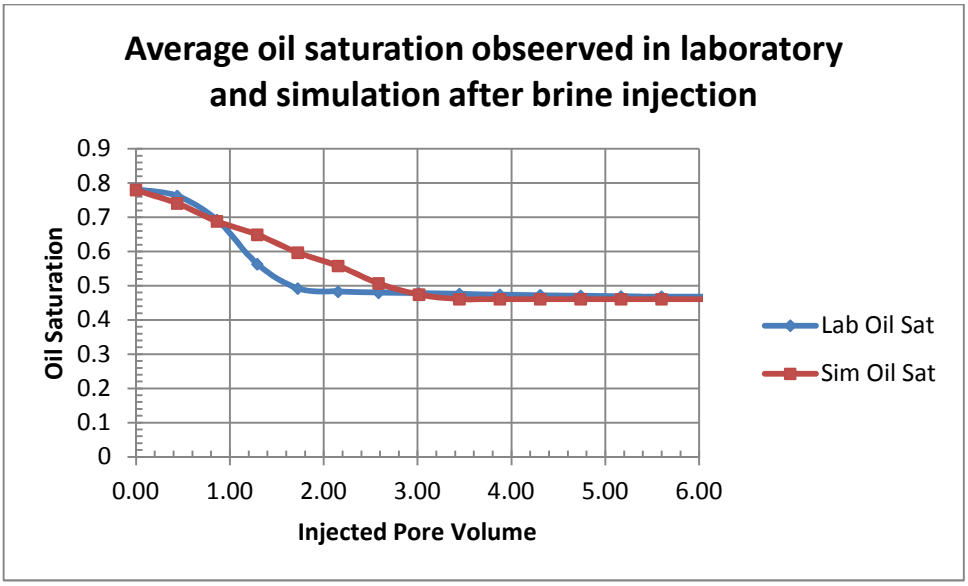

Figure 6.9 Average oil saturation observed in laboratory and simulation after brine injection.

6.9.2.2 Secondary oil recovery

In the simulation fresh water was introduced via the injection well at a rate of 0.0024 m^3/day. The simulation input data are listed in Tables 6.4 and 6.5; output is plotted in Figure 6.10. About 41% oil was recovered; in the laboratory about 40 % was recovered.

The simulated cumulative oil recovery curve went up slowly from 0% to 41% between 0 to 5PV, then remained constant (steady state). The laboratory cumulative oil recovery curve reached 37% at 1.8PV injection of brine. It produced more oil than the simulation at 1.8PV injection, which reached only about 14%.

The simulated oil recovery curve does not match the laboratory curve from 0.5PV to 3.2PV. This is because the simulation input parameter was not properly adjusted. However, there was a perfect match from 5PV onward.

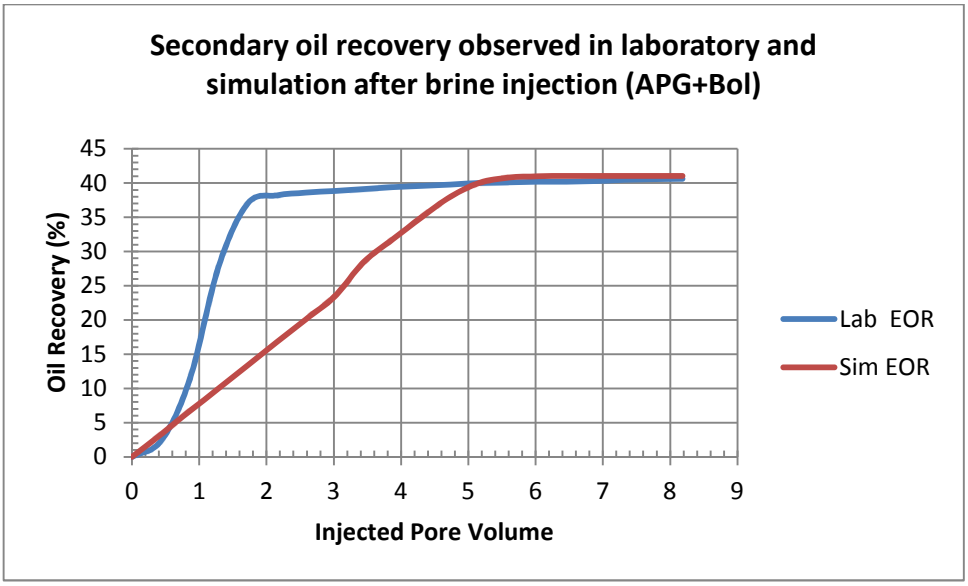

Figure 6.10 Secondary oil recovery observed in laboratory and simulation after brine injection.

6.9.2.3 Tertiary oil recovery

A combination of 0.5% APG and 0.5% Butanol was mixed with fresh water and injected into the core model. Input data are provided in Tables 6.4 and 6.5. Cumulative oil recovery with a surfactant solution was investigated. As shown in Figure 6.11, 41 % tertiary oil was recovered with an injection of 2PV surfactant solution. The same amount of oil was recovered in laboratory core-flooding with a 2PV injection of surfactant solution. The simulated curve differed from the laboratory curve between O and 1PV but became closer at the later stage; at the end they matched. These results suggest that this formulation is more active than a bio-surfactant solution.

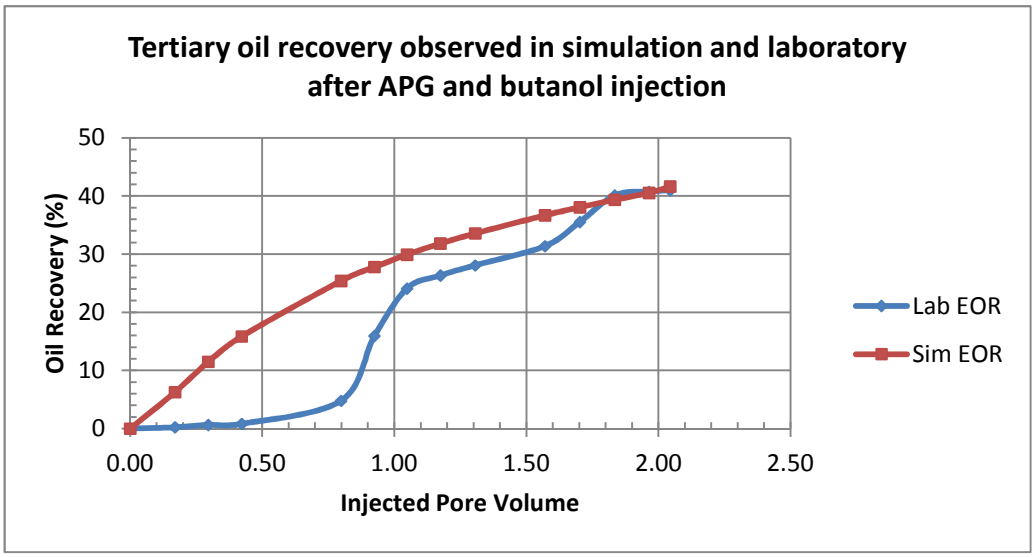

Figure 6.11 Tertiary oil recovery observed in laboratory and simulation after APG 264 and butanol injection

6.9.2.4 Total oil recovery

Total cumulative oil recovery by APG and butanol solution was examined and compared with laboratory core-flooding data. Recovery curves from both methods are plotted in Figure 6.12; the curves match. In the simulation 81% total oil was recovered, and in the laboratory 82%.

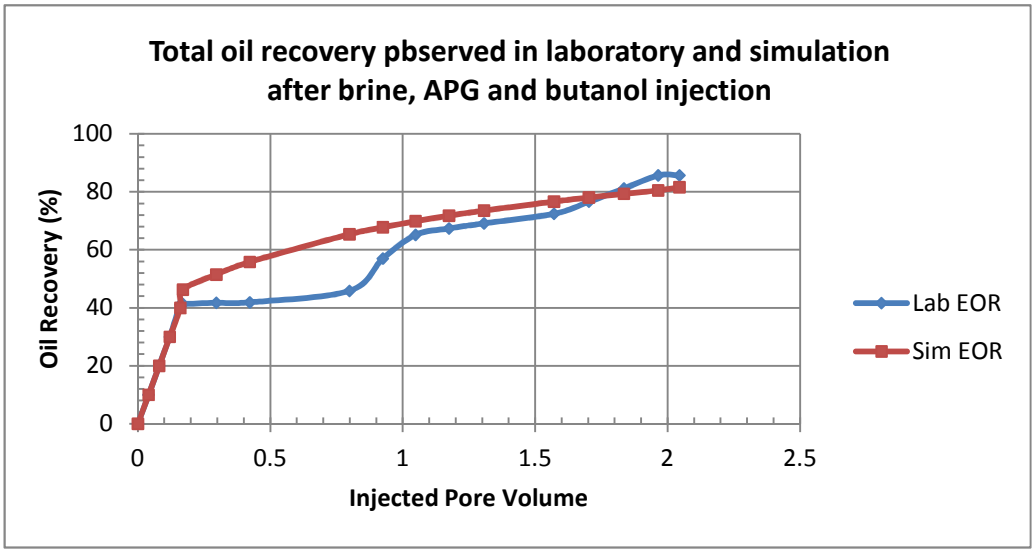

Figure 6.12 Total (secondary and tertiary) oil recovery observed in laboratory and simulation after brine, APG 264 and butanol injection

6.9.3 Formulation 3: APG , bio-surfactant butanol and water

This formulation was a mixture of anionic and non-ionic surfactants with a co-surfactant. In this preparation APG and JF-2 bio-surfactant were blended with butanol. APG, bio-surfactant, butanol and brine, and core properties were discussed in Chapter Three.

6.9.3.1 Saturation effect

The saturation effect of the injection volume of water and surfactant was studied. The simulated oil profile was evaluated against the laboratory oil saturation. Input data for the simulation are listed in Tables 6.6 and 6.7; the two solutions are plotted in Figure 6.13.

Average oil saturation dropped gradually from 0.79 to 0.5 in 4PV injection of water in simulation, then remained steady. Oil production started as saturation went down with the injection of 4PV water; after that oil production stayed constant. This indicates that the injection of water was effective up to 4PV and then had no further effect injection on production. A similar pattern of oil saturation was monitored in core-flooding, with a swift fall from 0.83 to 0.53 with 1.2PV injection. After that it became stable. There was no good match between the two curves from 0.4PV and 3.6PV because of a poor simulator input adjustment.

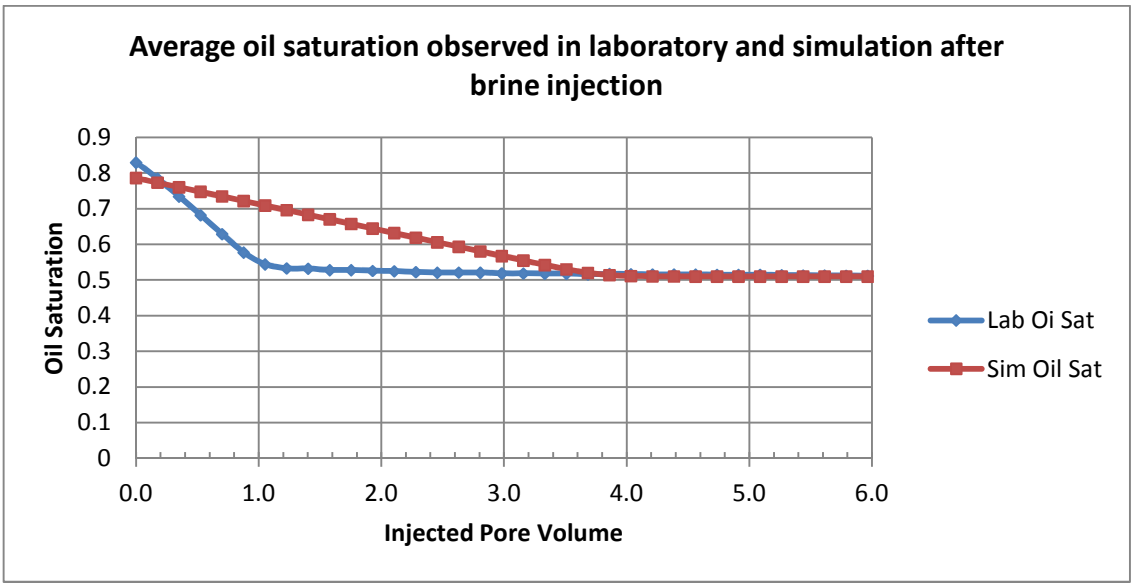

Figure 6.13 Average oil saturation observed in laboratory and simulation after brine injection

6.9.3.2 Secondary oil recovery

Secondary oil recovery curves of both simulation and laboratory are plotted in Figure 6.14; Simulation input data are presented in Tables 6.6 and 6.7. Fresh water was introduced into the core model through the injection well at a rate of 0.0024 m^3/day until oil production became stable. During this time, from 0 to 2.5PV, oil production increased from 0 % to 35 % of original oil in place.. There was steady oil production after 2.5PV injection. In the laboratory there was a rapid increase in oil production to 35 % with 1PV injection, followed by a 2% rise from 35 % to 37 % in 5PV.

There was a 2% difference in cumulative oil recovery between the two methods.

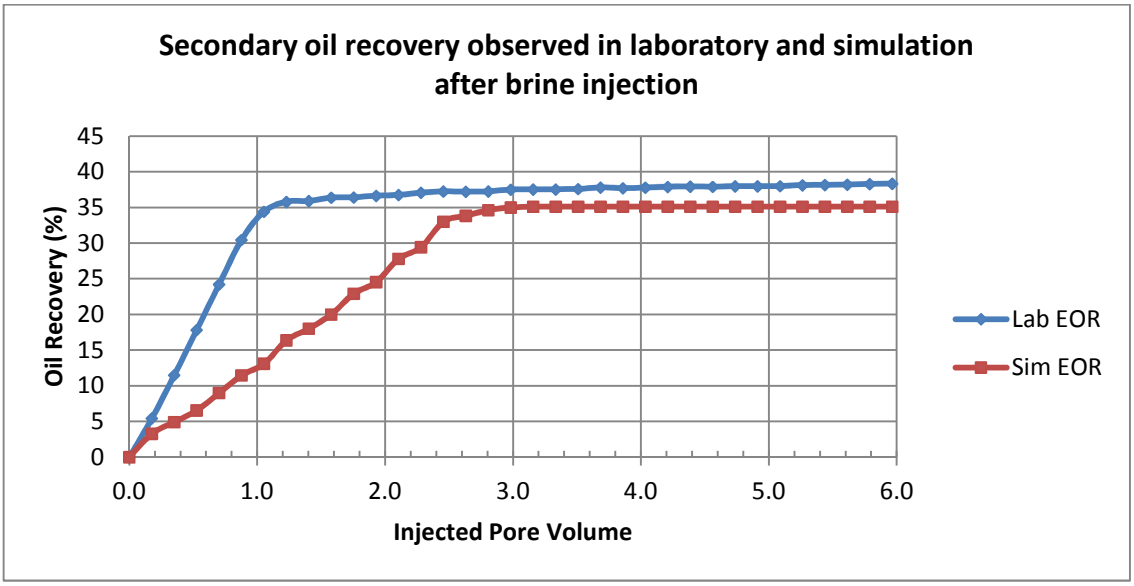

Figure 6.14 Secondary oil recovery observed in laboratory and simulation after brine injection

6.9.3.3 Tertiary recovery

This simulation test explored the effect of anionic and nonionic blends with alcohol on cumulative tertiary oil recovery. An APG, bio-surfactant and butanol combination solution was passed into the model core at a rate of 100 cc/hour. The cumulative tertiary oil recovery is plotted in Figure 6.15; Tables 6.6 and 6.7 show the input data. Nearly 25% of oil was recovered when 4PV of surfactant solution was injected. Oil production went up gradually to 10%, 17%, and 22% with 1PV, 2PV and 3PV injections respectively. However, in the laboratory there was a 25% rise of

cumulative oil with 2.4PV of injection. Oil recovery rose to about 13%, 22% and 25% in 1PV, 2PV and 3PV injections respectively. Results from both methods reveal that an APG and bio-surfactant solution is a promising green surfactant which has a capability to recover substantial tertiary oil.

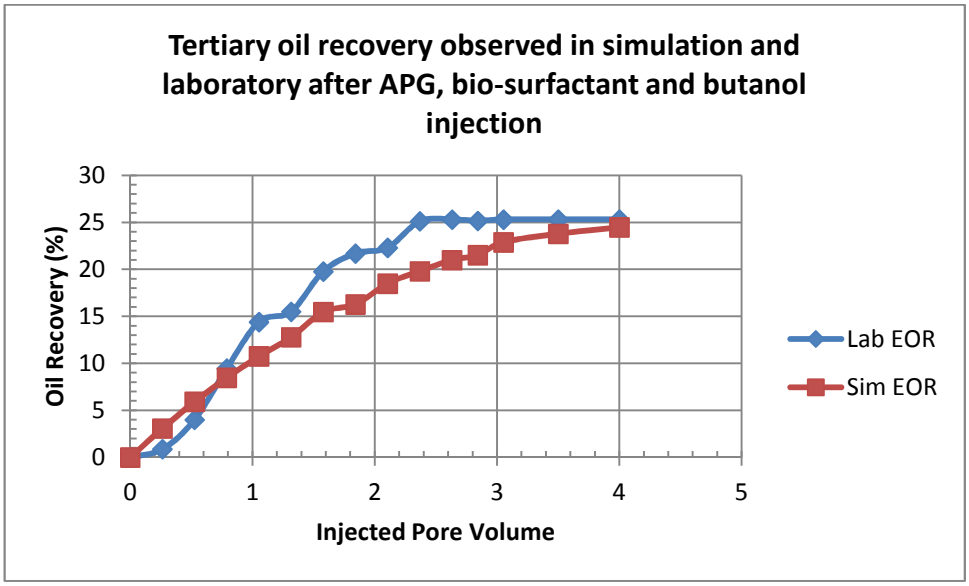

Figure 6.15 Tertiary oil recovery observed in laboratory and simulation after APG 264, bio-surfactant and butanol injection

6.9.3.4 Total oil recovery

This simulation investigated the impact of a solution of water and surfactants on total oil recovery. First water and then an APG, bio-surfactant and butanol solution were injected into the core model. Total cumulative oil production was examined and compared with the laboratory results; total simulated and core-flooded oil recoveries curves are plotted in Figure 6.16. About 60% cumulative oil recovery was found in simulation, and about 64% in core-flooding. The results from both methods suggest that an APG, bio-surfactant and butanol solution is very likely to mobilize a considerable amount of residual oil.

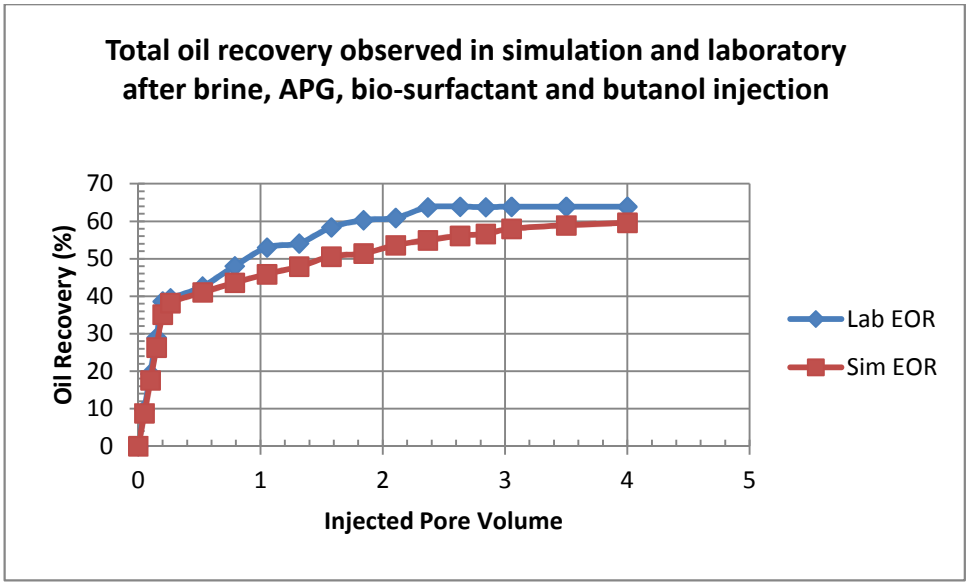

Figure 6.16 Total (secondary and tertiary) oil recovery observed in laboratory and simulation after brine, APG 264, bio-surfactant and butanol injection

6.10 Conclusion

1. The modified Eclipse simulator successfully simulated the effect of secondary and tertiary oil recovery, using water with a green surfactant and alcohol solution, and with a solution of anionic and non-ionic surfactants blended with alcohol. These features were tested by core-flood experiments.

2. A core-flood experiment using bio-surfactant and alcohol on a Berea sandstone core was simulated. Simulated results were higher than experimental results but compared reasonably. The GEOR model could be used to simulate the effect of bio-surfactant and bio-alcohol on MEOR.

3. The simulated tertiary and total oil recoveries of a blended APG and butanol solution were compared with experimental values. Simulated TOR and total recovery were 41% and 81% respectively, while core-flooding TOR and total recovery were 41% and 82% respectively.

4. A simulated core-flood experiment using an APG, bio-surfactant and butanol combination returned simulated outputs with a good match to experimental results. TOR and total recovery values from the simulation were 25% and 60%.

6.11 Recommendations

1. A brine treacle model should be included in simulations to examine the effect of brine salinity on oil recovery.

2. Overburden pressure should be included to see the effect on rock compaction.

3. Microbial reaction should be included in the EOR model to see the real microbial oil recovery.

4. A cylindrical core model should used in place of a rectangular core model to replicate the core.

Chapter 7 A New Method for EOR Green Enhanced Oil Recovery

This chapter discusses the GEOR process used to improve recovery efficiency, primarily through the use of a green surfactant with a low interfacial tension (IFT) with the displaced crude oil. A surfactant is the principal component that causes a system to exhibit low IFT, although this is also affected by the co-surfactant, brine salinity, crude oil composition and reservoir temperature (Green & Willhite 1993). A unique formulation must be developed for each reservoir environment.

This chapter includes a brief induction to GEOR, the classification of EOR, and the differences between GEOR and MEOR, before moving to a discussion of environmental factors and design parameters associated with GEOR. After that theory, design parameters, methodology, and the application of GEOR in Australian oil fields are described. Results are discussed, and conclusions and recommendations presented, at the end of the chapter.

7.1 Introduction

Green enhanced oil recovery (GEOR) is a chemical EOR involving the injection of specific green chemicals (surfactants/alcohols/polymers) that effectively displace oil because of their phase-behaviour properties, which decrease the IFT between the displacing liquid and the oil. In this process, the primary displacing liquid slug is a complex chemical system called a micellar solution, containing green surfactants, co-surfactants, oil, electrolytes and water. The surfactant slug is relatively small, typically 10% PV (Green & Willhite 1993). It may be followed by a mobility buffer, a solution that contains polymer at a concentration of a few hundred mg/l. This polymer solution is often graded in concentration, with the polymer becoming more dilute as more of the solution is injected. The total volume of the polymer solution is typically about 1 PV (Green & Willhite 1993).

In GEOR, either a green polymer or a bio-polymer can be used. This study did not conduct any tests for polymer-surfactant floods, but its procedures are readily adaptable to this method. Maudgalya *et al.'s* (2005) study of experimental and simulation bio-surfactant and polymer floods showed that 40mg/l of bio-surfactant and 1000mg/l polymer could recover 10% to 40% of residual oil when injected

through sandstone cores at typical field rates. His study did not cover green polymer flooding.

Green surfactants are biodegradable and environmental friendly, and are perceived to have great potential for EOR. Green surfactants can be classed in four types based on the ionic charge of the head group, similar to petroleum surfactants: anionic, cationic, non-ionic and zwitterionic. Details of this classification are discussed in 4.3.1. As alcohols are green, they can be subjected to the same conventional classification; see 4.3.2. This study discusses the green chemical-based EOR process.

7.2 Classification of EOR processes

Generally EOR processes (Green & Willhite 1993) can be classified into five main groups: (a) mobility control (b) chemical, (c) miscible, (d) thermal, and (e) others such as MEOR.

(a) Mobility control processes are based mainly on maintaining a favourable mobility ratio by thickening the water with polymers and reducing gas mobility with foams to improve macroscopic (volumetric) displacement efficiency. The design objectives of polymer solutions are to develop a favourable mobility ratio between the injected polymer solution and the displaced oil, and to facilitate a more uniform volumetric sweep of the reservoir both vertically and areally.

(b) In the chemical process, the specific liquid chemicals such as surfactants, polymers and alcohols are injected into the reservoir to decrease IFT by changing phase behaviour, to displace oil and improve microscopic displacement efficiency.

(c) In the miscible process, the fluids (hydrocarbon solvent or carbon dioxide (CO_2)) are directly miscible with the oil or generate miscibility in the reservoir through composition alteration. Phase behaviour is the most important factor in this process.

(d) The thermal process depends on the injection of thermal energy or the in-situ generation of heat to increase oil production. Examples of this process are steam injection or in-situ combustion from air or oxygen injection. This process may be subdivided into hot-water flooding, steam processing and in-situ combustion.

(e) Other processes fall into this catch-all category. Microbial based enhanced oil recovery is an example of one such process.

7.3 Differences between GEOR and MEOR

GEOR is one of the EOR processes where only environmentally friendly chemicals are utilized to enhance oil recovery.

In MEOR, microorganisms produce bio-products which modify the viscosity, density, IFT, wettability and capillarity essential to EOR processes. Oil that is trapped in small pores or dead-end pores after the initial recovery process may be extracted using microorganisms in the microscopic displacement process. In this process microbes can enhance macroscopic displacement by plugging, improving permeability and porosity through acid, and increasing reservoir pressure through gas generation.

MEOR has the potential to compete with other enhanced oil recovery techniques which are thermal-, surfactant- or solvent-based (Leo 1997) because it does not require high energy expenditure or expensive chemicals. In the application of MEOR, indigenous microbes can be directly isolated from oil fields and fed with cheap nutrients with no additional or expensive production processes.

In order to minimise the cost of MEOR and make it competitive with conventional EOR techniques, it is important to select suitable microorganisms that can generate the targeted processes and yield high quantities of by-products useful for EOR using the cheapest nutrients (molasses). The adoption of indigenous microbial flooding is presently believed to be the most economic of the various MEOR methods. There is no microbial development or fermentation at the surface; nor is microbial injection required. The only requirement is the selection of the right nutrients and injection technology that will encourage the growth of indigenous microorganisms under reservoir conditions.

7.4 Environmental factors associated with GEOR

EOR processes are still being developed. The injection of large quantities of chemicals to displace oil in the producing wells may have an adverse environmental impact. Several chemical processes for oil recovery require surface processing of

large quantities of saline water as well as chemical mixtures, which may pollute surface waters and shallow freshwater aquifers. When an oilfield is finally abandoned, large quantities of chemicals used in oil displacement are left in the underground reservoirs, and these too are a potential environmental hazard, depending on the rate of chemical degradation in the subsurface environment (Donaldson 1989b). Questions regarding the environmental consequences of EOR activities should be addressed during the pilot stages of fieldwide commercial implementations of every process.

Chemical flooding and micellar–polymer processes are involved in tertiary oil recovery. Chemical flooding involves the addition of chemicals to the brine prior to injection. Micellar–polymer flooding involves four separate phases of fluid injection: pre-flush, micellar, polymer and post-flood. The injection of fresh water or low-salinity water is done in pre-flush, followed by micellar injection (the micro-emulsion is composed of hydrocarbon, brine, surfactant, alcohol, and electrolytes); polymer is then injected to increase viscosity and assist in the more efficient displacement of the oil bank and micro-emulsion. Brine injection occurs in the post-flush/flood that follows.

Chemical compounds produced with the brine and oil are not a cause for concern because only a small fraction of the injection chemical is eventually produced. The amount of chemical injected in a chemical flood is designed to be approximately equal to the amount of material expected to remain in the petroleum reservoir by adsorption, channelling and dilution. Chemicals dissolved in the produced brines are recycled as part of the brine treatment system and reinjected into the reservoir. Chemicals dissolved in the oil are transported to the refinery to be processed as part of the crude oil. Surplus aqueous fluids are disposed of by injection into a nonproducing brine aquifer, above or below the oil zone, when they cannot be used in the brine-injection program. Micellar-polymer flooding is complex because it injects a large amount of chemicals and environmental concerns are significant.

The major potential (Donaldson *et al.* 1989b,) for environmental problems associated with chemical flooding are: (1) local air pollution by hydrogen sulphide removed from the produced brine during treatment; (2) spills or leaks of chemical additives

during transportation, storage, and processing; (3) health hazards to personnel operating the field from dry chemicals and solutions; (4) leaks from surface storage and treatment ponds for produced brine; (5) leaks from high-pressure pipes transporting mixed chemicals to the wells; (6) underground leaks into shallow aquifers from damaged or corroded wells; (7) production into shallow aquifers from improperly plugged abandoned wells (possible when the pressure of the oil reservoir is raised as a result of EOR activities); (8) production into aquifers above the oil reservoir through an incompetent seal above the reservoir (fracture or fault); (9) subsidence along a fault plane caused by a change of reservoir pressure; (9) subsidence along a fault plane caused by a change of reservoir pressure; and (10) subsidence caused by chemical disaggregation of the oil reservoir rack matrix.

Environmental aspects of EOR technologies undergo a complex governmental approval process for field application. Of most concern are atmospheric emissions, water use, impacts on water quality, waste water effluents, solid wastes, occupational health and safety, physical disturbances and noise.

7.5 Theory

GEOR follows same theory as EOR. The overall oil recovery efficiency (E) (Green & Willhite 1983) of any fluid displacement process is given by the product of the macroscopic displacement (E_D) and microscopic displacement efficiency (E_V).

$$E = E_D \times E_V \tag{8.1}$$

where

E = overall displacement efficiency

E_D = microscopic displacement efficiency expressed as fraction

E_V= macroscopic (volumetric) displacement efficiency expressed as fraction.

The macroscopic displacement efficiency (E_V) relates to the effectiveness of the displacing fluid in contacting the reservoir in a volumetric sense. It is a measure of the areal and vertical displacement of fluids. E_V is reflected in the magnitude of the average residual oil saturation $S_{or\ (avg)}$.The microscopic displacement efficiency (E_D)

relates to the mobilization of oil at the pore scale. It is a measure of how well the displacing fluid mobilizes the residual oil once the fluid has been in contact with the oil. E_V is reflected in the magnitude of the residual oil saturation $S_{or.}$

The capillary and viscous forces that hold residual oil in small and dead-end pores are expressed as a ratio called the capillary number (N_{ca}).

$$N_{ca} = \frac{\mu_w v_w}{\sigma_{ow}} \qquad \textbf{(8.2)}$$

where

μ_w =viscosity

V_w = flux of fluid

σ_{ow}= Interfacial tension of oil and water.

Large changes in capillary number are required for producing the residual oils. Since large changes in viscosity forces are impossible for crude oil except in heavy oil for EOR purposes, the reduction of interfacial tension by surfactants or other means is the only way to achieve a large capillary number.

The efficiency of oil recovery is often dominated by the volumetric sweep efficiency (Craig 1974). One factor resulting in poor volumetric sweep efficiencies is the difference between the mobilities of the oil and aqueous phases. Compared with oil, water moves rapidly through the reservoir. This results in an irregular front with water pushing through the oil and reaching the production well first. The mobility of these two phases is expressed as the mobility ratio

$$M = \frac{k_w \mu_o}{k_o \mu_w} \qquad (8.3)$$

where

μ_w =viscosity of water

μ_o =viscosity of oil

k_w = relative permeability of water in the waterflooded zone

k_o = relative permeability of oil in the saturated zone

M = mobility ratio.

Mobility ratios less than one are favourable and result in uniform displacement of the oil front. Most of the EOR methods such as chemical, polymer, alkaline (caustic) flooding and solvent methods attempt to reduce the surface tension. Thermal methods are applied to reduce the viscosity of the trapped heavy oil. All the methods have both technical and economical limitations which should be evaluated before their application to a specific field.

7.6 Design parameters for GEOR

GEOR is a complex technology and can be justified only when oil prices are relatively high and when residual oil after waterflooding is substantial. The micellar is expensive and the chemical losses can be severe, occurring as a result of adsorption, phase partitioning and trapping. Fingering can take place if mobility is not controlled properly.

Green fluids with useful properties for improving the microscopic and macroscopic displacement efficiency are known or can be developed. These fluids are expensive and practical considerations are given below (Green & Willhite 1993):

(a) Chemical losses

The nature of flow in porous media and rock/fluid interactions lead to the diminished effectiveness of injected fluid slugs. For instance, fluid and fluid mixing cause injected fluid concentrations to change, and physical adsorption causes the loss of certain chemical components. The injected fluid slug size should be large enough to sustain the chemical losses or composition changes and still operate effectively. The cost of the injected fluid and of crude oil are the two most important economic factors controlling the implementation of the GEOR process.

(b) Handling EOR Fluid

Fluids may be corrosive, or need special equipment to be injected. Handling fluids, and their compatibility with physical injection/production systems, need to be considered. GEOR fluids are less toxic and corrosive than conventional EOR fluids.

(c) Availability of Fluid

The availability of fluid is an EOR design parameter. The fluid requirement for a large reservoir is quite considerable, and if the process is widely accepted across the country, volume can become an important limiting factor for EOR application.

(d) Reservoir geology

Reservoir geology and geologic heterogeneities are important factors for success or failure in implementing an EOR process. Processes that are well understood in a laboratory environment and properly designed for reservoir fluids may fail when implemented in the reservoir because of geologic factors, and may lead to unexpected losses of chemicals or bypassing of fluids because of channelling in high-permeability zones or factures. Variations in rock properties may cause irregular fluid movement. These types of factor may cause project failure if they are not well understood and not taken into consideration at the design stage. A number of geological procedures can be used to ensure best implementation of an EOR process, including evaluations of well cores and logs, single-well and well-to-well tracer tests, pressure-transient analysis and seismic surveys.

7.7 Methodology

Enhanced oil recovery processes involve the injection of fluids into a reservoir to supplement the natural energy present in the reservoir and displace the oil to the production well. The injected fluids interact with the reservoir rock/oil system to improve conditions for oil recovery, including lowering IFT, oil swelling and oil viscosity, modifying wettability, and enhancing favourable phase behaviour.

The working principles of GEOR are similar to those of chemical EOR, with the exception that GEOR is environmentally friendly and uses chemicals (surfactants, polymers, and alcohol) that biodegrade rapidly. In GEOR, green surfactants and

alcohol are injected, using a combination of phase behaviour and IFT reduction to displace oil and improve microscopic displacement efficiency (E_D). In some cases, thickening of water with green polymers (if available) may be a part of GEOR (Green and Willhite, 1983), utilized to maintain favourable mobility ratios and improve the magnitude of macroscopic (volumetric) sweep efficiency (E_V) as well as providing the potential to improve both E_V and E_D.

7.7.1 Phase behaviour study

The goal of phase behaviour study is to identify the middle phase micro-emulsion region. Middle phase micro-emulsions can be designed to have low IFT. In this study the role of green surfactant and alcohol on middle phase emulsion was investigated. The effects of changing alcohol and surfactant concentrations on the phase behaviour of brine-surfactant-alcohol systems were examined and discussed in detail in Chapter Two.

7.7.2 IFT measurement

IFT reduction can contribute significantly to oil recovery. Recovery efficiency largely depends on the use of a displacing fluid with a low IFT with the displaced crude oil (Green & Willhite 1983). In this study various IFTs between green surfactant systems and oil were measured. The IFT experiments were: (1) brine and stag crude oil at different temperatures and pressures; (2) green surfactant and alcohol mixture and stag oil at low concentrations and at different temperatures and pressures; and (3) green surfactant and alcohol mixture and Ondina 68 oil at high concentration. Procedures were described in Chapter Three.

7.7.3 Core-flooding test

The goal of core-flooding was to examine the percentage of oil recovery of green surfactant and co-surfactant formulations. Three core-flood experiments were conducted to test the EOR capability of three green surfactant and co-surfactant mixtures: (1) bio-surfactant (anionic) and alcohol; (2) APG 264 (non-ionic) surfactant and alcohol; and (3) bio-surfactant and APG 264 surfactant and alcohol. Experimental methods were discussed in Chapter Five.

In this study an Eclipse reservoir simulator was modified and used to simulate GEOR core-flooding experiments. Three core models for three formulations were simulated to examine the relationship between oil recovery and injected surfactant solutions. In all cases, first fresh water was injected into the core model and then surfactant solutions were injected to see the effect of secondary and tertiary recoveries. JF-2 bio-surfactant with butanol as a co-surfactant mixture was modelled in first formulation. The second formulation was APG 264 and butanol; the last preparation was a mixture of APG 264 and JF-2 bio-surfactant blended with butanol. Details were presented in Chapter Five.

7.8 Application of GEOR in Australian oil fields

GEOR is a green chemical EOR process. This method has wide temperature and salinity tolerance and might have broad application in oil fields as laboratory experiments have proved that temperature and pressure have minor effect on the IFT reduction of an APG and alcohol mixture.

Lyer (2009) at Cognise Company performed salt tolerance efficacy experiments using an APG surfactant (APG 9166 0.8% and 1.2% Hexanol) and found that such a system maintained very low IFT under high salinity (2%–11%) and temperature (20^{o}C–70^{o}C). Table 7.1 shows the pressure, temperature and salinity of North West Shelf oil fields; the average temperature and salinity are 84^{o}C and 35527 mg/l (or 3.5%). Table 7.2 presents the pressure, temperature and salinity of the Gippsland basin oil fields; average temperature and salinity are 91^{o}C and 33210 mg/l (or 3.3%). Based on temperature and salinity tolerance, GEOR might be applicable in a wide range of Australian oil reservoirs.

Table 7.1 North West Shelf oil fields

Field (NWS)	Start-up Year	Operator	Basin	Average Porosity	Average permeability (mD)	Res. Temp.	Res. Press.	Salinity (mg/l)
Stag	1993	Apache	Carnarvon			52	1071	
Wandoo	1991	Mobile	Carnarvon	27.0	3449.89	56	908	33,000
Vincent	1998	Woodside	Carnarvon	34.8	4300	58	1939	36,000
Enfield	1999	Woodside	Carnarvon	29.5	1000	71	2987	33,000
Talisman	1984	Marathon	Carnarvon	19.8	1714	70-98	2881	73,259
Cliff Head	2000	ROC	Perth	10 -18	300/500	73		
Skiddaw	2003	BHPB	Carnarvon			58	1871	
Alkimos	1994	Apache	Carnarvon	21.5	404.18	94	2701	18,500
Tanami	1991	Apache	Carnarvon			87		
Simpson	2001	Apache	Carnarvon			84		
Exeter	2002	Santos	Carnarvon			107	4550	
Mutineer	1998	Santos	Carnarvon	20.83	125.12		4750	34,156
Harrison	2004	BHPB	Carnarvon			71	1620	25,667
Lambert	1974	Woodside	Carnarvon	19.25	438.8	112	4542	44,300
Legendre	1970	Burmah oil	Carnarvon	12.8	174.63	88	2803	35,412
Cossack	1990	Woodside	Carnarvon	16.22	452.46	110	4321	20,000
Griffin	1990	NHPB	Carnarvon	14.7	1249	96	3840	41,493
Wanaea	1992	Woodside	Carnarvon	14.44	197.35	110	4188	20,777
South Pepper		Apache	Carnarvon	18.82	1049	76	2134	58,000
Sage	1999	Apache	Carnarvon			72		43,000
Egret	1973	Woodside	Carnarvon	19.83	100	100	4565	44,277
Novara	1982	ESSO	Carnarvon	21.6	1649.44	56		17,200
Ravensworth	2004	BHPB	Carnarvon	18.52	43.6	74	1917	35,000
North Herald	1983	Mesa Aust	Carnarvon	11.3	0.12	83	1742	35,000
Outtrim	1984	ESSO	Carnarvon	21.46	1978	86	1925	21,000
Nimrod	1996	BHPB	Carnarvon	19.83	1322.14	149	7056	7,500
Dockrell	1973	Woodside	Carnarvon	17.29	157			34,000
Lauda	2005	OMV	Carnarvon			94		

Table 7.2 Gippsland basin oil fields

Field	Year of Set-up	Conductors	Formation	Porosity (%)	Perm. (md)	Res. Press.	Res. Temp (ºC)	Salinity (Kmg/l)
Perch	1968	2	Latrobe N1	27	3000	1795	66	18
Seahorse	1978	subsea well	Latrobe N1	23	300	2054	66	35
Dolphin	1967	2	Latrobe N1	25	4000	1804.7	68	20
Snapper	1968	27	Latrobe N-1	24	1000+	2027	73	20
Tarwhine	1981	subsea well	Latrobe N1	23	100-1000	2008	73	22
West Tuna	1968	48	Latrobe M1	24	800-1000	2006	73	35
Moonfish	1992	snapper platform	Latrobe M2	30	500-3000	2435	79	
Bream	1969	30	Latrobe N-1	22	2900	2770	90	35
Blackback	1975	subsea completion	Latrobe	19	10--5000	4031	90	30
Tuna	1968	30	Latrobe T1	18	500-650	1905	101	35
Kingfish	1967	21	Latrobe M1	21	5000-40000	3318	102	30
West Kingfish	1968	33	Latrobe M1 oil	19	2000	3318	102	40
Whiting	1983	6	Latrobe P 250 E	24	1800	2106	102	25
Batfish	1970		intra-Latrobe Lat, LG	25	100-1000	2373	102	48
Halibut	1967	24	Latrobe M1	22	5000-7000	3430	104	40
Flounder	1968	27	Latrobe T1	21	100-3000	3689	104	33
Cobia	1972	21	Latrobe N-1	22	500-1000	3430	104	40
Fortescue	1978	35	Latrobe FM-1	20	200-5000	3433	104	40
Mackerel	1969	25	Latrobe L1	20	5000	3430	104	37
Angelfish	1985		intra-Latrobe Lat, LT	14		4656	108	48

7.9 Results and Discussion

1. Detailed results of phase behaviour study, IFT measurements, core-flood tests and simulation studies of GEOR are presented in Chapters Two, Three, Four and Five.

2. Although MEOR is relatively cheap and green, it is a slow process. It is not applicable for wide range of pressures and temperatures as bacteria cannot grow in wide range of temperatures. It has been documented that reservoirs suitable for MEOR are typically of low temperature and low salinity, with temperature <90 °C and salinity <10% (Sharma *et al.* 1993; Yakimov *et al.* 1997). The reservoir pressure does not appear to affect the growth of most microorganisms (Sarkar 1989); reservoirs with high temperature and high salinity are therefore regarded as unsuitable for MEOR. The average reservoir temperature of the Gippsland basin oil fields is 91^{o}C, and 13 out of 20 oil fields' reservoir temperatures are above 90^{o}C, which means they are not suitable for MEOR. In the North West Shelf oil fields the average reservoir temperature is 84^{o}C, and 10 out of 26 oil fields are unfavourable for MEOR as their reservoir temperatures are above 90^{o}C. However, our laboratory tests confirm that APG 8166 maintains a steady IFT value between 20^{o}C and 60^{o}C and in pressures from 500psi to 3000psi. In addition, APG 9166 0.8% and 1.2% Hexanol systems maintain very low IFT under high salinity (2%–11%) and temperature (20^{o}C –70^{o}C) (Lyer 2009).

3. Core-flood tests confirm that APG 264 and butanol shows good oil recovery results of about 41.1 % in secondary recovery and 40.8% in tertiary recovery, a total 82 % of initial oil in place (OIIP). Bio-surfactant and butanol produces about 37.8 % secondary oil and 1.7% tertiary oil, a total of about 39.3 % of OIIP.

4. APG 264, bio-surfactant, and butanol produce 24.7% tertiary oil and a total 63.4% of OIIP. This formulation might be applicable in a MEOR environment.

7.10 Conclusion

An APG 264 and butanol formulation in GEOR can be used in the MEOR environment. This formulation can produce more tertiary oil than a bio-surfactant/butanol system and make EOR faster and more effective than MEOR.

7.11 Recommendations

1. An intensive APG, butanol and green polymer study is recommended because the surfactant slug can be followed by a mobility buffer, a solution that contains polymer at a concentration of a few hundred mg/l (Green & Willhite 1993). In GEOR methods either green polymer or bio-polymer can be used. This study did not conduct any tests for polymer-surfactant flooding, but its procedures are suitable for adaptation to such a study.

2. A thorough study of coconut oil in place of molasses as a nutrient in MEOR is recommended because APG surfactants are produced from coconut oil.

Chapter 8 Conclusions and Recommendations

8.1 Conclusions

1. Phase behaviour successfully demonstrates that 0.5% APG and 0.5% to 1.00% of Butanol at 2% NaCl gives stable middle phase micro-emulsion. Blending bio-surfactant (anionic) and APG 264 (non-ionic) surfactant with butanol shows stable middle phase micro-emulsion. However, JF-2 bio-surfactant at concentration 55mg/l and 0.5% butanol combination does not show any middle phase micro-emulsion.

2. Our laboratory experiments confirm that the non-ionic surfactant (APG 264) used at low concentrations with Stag crude oil is more active in the reduction of IFT than anionic surfactant (JF-2 bio-surfactant).

3. Temperature and pressure appear to have little effect on the IFT of non-ionic green APG 8166 surfactant in the temperature range 20–60^{o}C and the pressure range 500–3000psi.

4. To determine the optimum concentration of Bio-surfactant for core flood testing, the IFT values of a bio-surfactant slug and Ondina Oil 15 (Shell) were measured and plotted against bio-surfactant concentration. It was found that at concentrations beyond 40mg/l, IFT values became stable: concentrations between 40pmm and 60mg/l may be optimum for core flood testing. Similarly, the optimum concentration of APG 264 was selected first and then a combination of APG 264 and Butanol concentration was chosen. The optimum concentration of the combination was 0.5% APG 264 and 0.5% Butanol. Finally, anionic and non-ionic surfactants were blended with butanol; the optimum concentration for this formulation was 0.5% APG 264 (non-ionic), 45mg/l bio-surfactant (anionic) and 0.5% butanol.

5. A core flood experiment in Berea sandstone confirmed that a concentration of 0.5% green non-ionic surfactant APG 264 mixed with a concentration of 0.5% butanol could recover 41% of residual oil and 82% of OIIP. A concentration of 45 mg/l (0.045 mg /cm3) JF-2 bio-surfactant mixed with a 5% concentration of butanol concentration recovered only 1.7% of residual oil and 39.5% of OIIP.

6. Blending anionic (45 mg/l bio-surfactant) and non-ionic (0.5% APG 264) surfactants with 0.5% butanol gave approximately 25% incremental oil recovery and

64% of OIIP. This formulation was efficient in terms of recovering additional oil from the core.

7. The modified Eclipse simulator successfully simulated the effects of saturation on waterflooding and secondary and tertiary oil recovery using water and a green surfactant and alcohol solution, and also using anionic and non-ionic surfactants blended with alcohol. These effects were confirmed by the core flood experiments.

8. A simulated coreflooding experiment on a Berea sandstone core using a bio-surfactant and alcohol mixture was simulated. The results were slightly higher than the experimental results, but still compared reasonably. The GEOR model may be utilized to simulate the effect of using a bio-surfactant and bio-alcohol combination for MEOR.

9. The simulated tertiary and total oil recoveries from the APG and butanol blend were compared with the experimentally derived values. The simulated TOR and total recovery were 41% and 81% respectively; the experimental coreflooding TOR and total recovery were 41% and 82%. The simulated results perfectly match with experimental results.

10. The simulated core flood experiment using the APG, bio-surfactant and butanol combination was compared with the coreflooding experiment. The simulated outputs were a good match with the experimental results: TOR values from both the simulation and the experiment were about 25%.

11. GEOR is an environmentally friendly and cost-effective chemical EOR. Its application in environments where MEOR is currently used is likely to produce more tertiary oil and make EOR faster than MEOR.

8.2 **Recommendations**

1. It is recommended that graduated pipettes be used in phase behaviour studies for the better resolution and measurement of solubilised volumes. It was found that a change of 0.1ml during the calculation of the solubilisation ratio had a significant effect on the results; in a sample with a small micro-emulsion volume, a deviation of 0.1ml in the solubilised volume would cause a large error. Further work in this area

should narrowly determine the precise optimal combinations of concentrations being used, to enhance repeatability of the data.

2. Spinning drops are recommended for measuring IFT as pendent drops cannot measure very low values of IFT at the higher concentrations of surfactant.

3. Adsorption parameters for APG surfactants and bio-surfactants need further examination. These parameters are essential for predicting oil recovery during surfactant injection, and in designing appropriate surfactant systems.

4. Particular surfactant performance characteristics should be studied thoroughly for a better understanding of green surfactant behaviour. These include (1) stability at high reservoir temperatures, (2) ultralow IFT and (3) low IFT at high and low salt (TDS) concentrations.

5. It is recommended that in core flood tests, the injection rate should be a standard field rate to replicate field conditions. Rock wettability and end point effective permeability changes during flooding should be investigated. It would be useful to have a better understanding of such changes in order more accurately to simulate mobilized oil flow in reservoirs and so predict oil recovery.

6. Cationic green surfactant characteristics should be investigated further, either in combination with non-ionic or anionic surfactant or both, for optimal recovery rates.

7. It is recommended that the effect of brine salinity be incorporated into further simulations as salinity has an impact on surfactant performance in residual oil recovery.

8. Further studies are needed to examine the combined effect of anionic, non-ionic and green polymers in EOR. In addition, the use of coconut oil in place of molasses in MEOR could be considered because APG surfactants can be produced from coconut oil.

References

Alotaibi, MB & Nasr-El-Din, HA 2009, 'Effect of brine on reservoir fluids interfacial tension', *proceedings of the 2009 SPE EUROPEC/EAGE annual conference and* exhibition, Amsterdam, SPE 121569; DOI 10.2118/149038-MS.

Amphlett, CB, 1964, *Inorganic ion exchanges*, Elsevier, New York.

Barnes, JR, Smit, J, Shpakoff, G, Raney, KH & Puerto, M, 2008, 'Development of surfactants for chemical flooding at difficult reservoir conditions', *proceedings of the SPE/DOE symposium on improved oil recovery*, Tulsa, SPE 113313; DOI 10.2118/155116-PA.

Bedrikovetsky, P, Muhammad, AW, Chang G, Souza, ALS, & Furtado C, 2009, 'Taking advantage of injectivity decline for sweep enhancing during waterflood with horizontal wells', *proceedings of the 2009 SPE European formation damage conference, Scheveningen*, SPE 122844; DOI 10.2118/122844-MS.

Bourrel, M, & Schechter, RS, 1988, *Micro-emulsion and related system,* Marcel Dekker, Inc, New York and Basel.

Carlin, JT, *et al*., 1978, 'Salinity tolerant surfactant oil recovery process', US Patent No. 4,110,229.

Cayias, JL, Schechter, RS, & Wade, WH, 1976, 'Modeling crude oil for low interfacial tension', *SPE Journal,* vol.16, no 6, pp. 351–357.

Cash, RL, Cayias, JL, Fournier, G, MacAllister, DJ, Schares, T, Schechter, RS, & Wade, WH, 1977, 'The application of low interfacial tension scaling rules to binary hydrocarbon mixture', *Journal of Colloid and Interface Science*, vol. 57, pp. 39-44.

Chai, JL, Li, GZ, Zhang, GY, Lu, JJ & Wang, ZN, 2003, 'Studies on the phase behavior of the system APG/alcohol/alkane/H2O with fishlike diagrams', *Colloids and Surfaces A: Physicochemical and Engineering Aspects*, vol. 231, pp. 173–180. Available from: ScienceDirect [31 March 2003].

Cognis, 2009, 'High efficiency, renewable surfactants for enhanced oil recovery' Cognis EOR Surfactant Report, Available from:Denzil.Dmello@cognis.com [Jan 2009]

Cob, WM, & Marek, FJ, 1997, 'Determination of volumetric sweep efficiency in mature waterfloods using production data', *proceedings of the 1997 SPE Annual Technical Conference and Exhibition*, San Antonio, Texas, USA, SPE 38902-MS.

Curbelo, FDS, Santanna, VC, Neto, ELB, Dutra, TV, Dantas, TNC, Neto, AAD & Garnica, AIC, 2006, 'Adsorption of non-ionic surfactants in sandstones', *Colloids and Surfaces A: Physicochemical and Engineering Aspects*, vol. 293, pp. 1–4. Available from: ScienceDirect. [21 March 2010].

Davis, HT, et al., 1983, 'Measurement of interfacial tension' Report DOE/BC/10116-12, US, DOE, Washington, DC.

Doe, PH, & Wade, WH, 1977a, 'Alkyl benzene sulfonates for producing low interfacial tensions between hydrocarbon and water', *Journal of Colloid and Interface Science*, vol. 59 no. 9, pp. 525–531.

Doe, PH, El-Emary, M, Schechter, RS, & Wade, WH, 1977b, 'Linear alkyl benzene sulfonates and low interfacial tensions', *Journal of American Oil Chemists'Society*, vol. 54 no. 12, pp. 570–577.

Donaldson, EC, Chilingarian, GV & Yen, TF, (eds) 1989, *Microbial Enhanced Oil Recovery*, Elsevier, Amsterdam, pp. 1-14.

Donaldson, EC, Chilingarian, GV & Yen, TF, (eds) 1989b, *Enhanced Oil Recovery, II process and operation*, Elsevier, Amsterdam, pp. 495-509.

Donaldson, EC, Thomas, RD & Lorenz, PB, 1969**,** 'Wettability determination and its effect on oil recovery', *SPE Journal*, March, pp. 13–20.

Dongu, AH, Mitsuishi, H, & Yamamoto, RH, 1984**,** 'Numerical simulation of micellar polymer field processes', *proceedings of the SPE Annual Technical Conference*, Houston, TX, SPE 113121.

Dwarakanath, V, Chaturvedi, T, Jackson, A, Malik, T, Siregar, AA & Zhao, P, 2008**,** 'Using co-solvents to provide gradients and improve oil recovery during chemical flooding in a light oil reservoir', *proceedings of the SPE/DOE Symposium on Improved Oil Recovery*, Tulsa, SPE 113965-MS.

Fanchi, JR 2006, *Principles of Applied Reservoir Simulation*, Third edn, Gulf Professional Publishing.

Folmsbee, M, Duncan, K, Han, SO, Nagle, DP, Jennings, E, & McInerney, MJ, 2005, 'Reidentification of Bacillus licheniformis JF-2 as Bacillus mojavensis

strain JF-2' Department of Botany and Microbiology, University of Oklahama, Norman, OK.

Garrett, HE, 1972, *Surface Active Chemicals,* Pergamon, New York.

Gale, WW & Sandvik, EJ, 1973, 'Tertiary surfactant flooding: petroleum sulfonate composition efficiency studies', *SPE Journal,* vol. 13**,** no 4 pp 191–199, SPE 3804-PA.

Guo, C, Wang, S, Liu, H, Feng, L, Song, Y, & Jiang, L, 2009, 'Wettability alteration of polymer surfaces produced by scraping' *Journal of Adhesion Science and Technology,* vol. 22, no 3-4, pp 395-402.

Gjerde, O, Jarosch, HS & Kaarstad, T, 1988, 'Improvement to the Black Oil Simulator', SPE 18612. Available from: SPEelibrary [1989].

Glover, CJ, Puerto, MC, Maerker, JM & Sandvik, EL, 1979**,** 'Surfactant phase behaviour and retention in porous media' *SPE Journal,* vol. 19, pp 183–193.

Graciaa, A, Lachaise, J, Bourrel, M, Osborne-Lee, I, Schechter, RS & Wade, WH, 1987, 'Partitioning of nonionic and anionic surfactant mixtures between oil/microemulsion/water phases', *SPE Reservoir Engineering Journal,* vol. 2**,** pp 305–314.

Green, DW & Willhite, GP, 1998, *Enhanced Oil Recovery,* SPE, Texas.

Hall,AC, 1980, 'Interfacial tensions and phase behavior in systems of petroleum sulfonate/brine/n-alkane', *Journal of Colloid &Surfaces,* vol. 1**,** pp 209–228.

Healy, RN, Reed, RL, & Stenmark, DG, 1976. 'Multiphase Microemulsion Systems', *SPE Journal*, vol. 16, no 3, pp. 146–160, SPE 5565-PA.

Healy, RN, & Reed, RL, 1974. 'Physsicochemical Aspects of Microemulsion Flooding', *SPE Journal*, vol. 14, no 5, pp. 491–501, SPE 4583-PA.

Hendry, P, LI, D, Zabaras, D, Sutherland, T, Wang, X, Ahmed, M, Gong, S, Mitchell, D, Liu, K, Rashid, A, Volk, H & Nicols, C, 2010, 'Designing a microbially enhanced oil recovery (MEOR) strategy for the Bokor oil field', CSIRO Confidential report PR/10-009, p. 60.

Hitzman, DO, Stepp, AK, Dennis DM & Graumann LR, 2003**,** 'Augmenting a microbial selective plugging technique with polymer flooding to increase the efficiency of oil recovery: a search for synergy', Prepared for US Department of Energy Assistant Secretary for Fossil Energy.

Holm, LW & Csaszar, A K, 1962**,** 'Oil recovery by solvents mutually soluble in oil and water', *SPE Journal,* vol. 2**,** pp 129–144.

Iglauer, S, Wu, Y, Shuler, P, Tang, Y & Goddard, WA, 2009, 'Alkyl polyglycoside surfactant-alcohol cosolvent formulations for improved oil recovery'. *Colloids and Surfaces A: Physicochemical and Engineering Aspects,* vol. 339**,** pp. 48–59. Available from: ScienceDirect [1 May 2009].

Iglauer, S, Wu, Y, Shuler, P, Tang, Y & Goddard, WA, 2010, 'New surfactant classes for enhanced oil recovery and their tertiary oil recovery potential', *Journal of Petroleum Science and Engineering,* vol 71**,** pp 23–29. Available from: CattechAUTHORS [24 Dec 2009].

Jones, SC & Dreher, KD, 1976, **'**Cosurfactants in micellar systems used for tertiary oil recovery', *SPE Journal,* vol. 16, no 3**,** pp 161–167.

Kalfoglu, G, 1977, ' Surfactant oil recovery method for use in high temperature formulations containing water having high salinity and hardness', US Patent No. 4,016,932.

Krogh, KA, Halling-Sørensen, B, Mogensen, BB & Vejrup, KV, 2002, 'Environmental properties and effects of nonionic surfactant adjuvants in pesticides: a review', *Journal of Chemosphere,* vol. 50, pp. 871–901. Available from: ScienceDirect. [18 October 2010].

Kremesec, VJ, Raterman, KT, & Taggart, DL, 1988, 'Laboratory evaluation of a crude-oil-sulfonate/Nonionic-cosurfactant micellar Fluid' , *SPE Reservoir Engineering Journal,* vol 3**,** no 3 pp 801–808, SPE 15651-PA.

Kowalewski, E, Rueslatten, I, Steen, KH, Bodtker, G, & Torsater, O, 2006, 'Microbial improved oil recovery – bacterial induced wettability and interfacial tension effects on oil production' , *Journal of Petroleum Science and Engineering,* vol 52**,** pp 275–280.

Koukouni, C, Wade, WH, & Schechter, RS, 1983, 'Phase partitioning of anionic and nonionic surfactant mixtures', *SPE,* vol 23**,** no 2, pp 301–310, SPE 8261-PA.

Kumar, R & Shrivastava, SK, 2000**,** 'Effect of gas relative permeability and mobility ration in reservoir simulation using different methods', *proceedings of the 2000 SPE Asia Pacific Oil and Gas Conference and Exhibition,* Brisbane, SPE 64423; DOI 10.2118/64423-MS.

Leo, G, 1997, 'Paraffin control project' Rocky Mountain Oilfield Testing Centre, FC9544/96PT12.

Levitt, DB, Jackson, AC, Heinson, C, Britton, LN, Malik, T, Dwarakanath V & Pope, GA, 2009, 'Identification and evaluation of high-performance EOR surfactants', *SPE Reservoir Evaluation & Engineering Journal*, vol. 12, pp 243–253.

Lin, S, Minton, MA, Sharma, MM, & Georgiou, G, 1994, 'Structural and immunological characterization of bio-surfactant produced by Bacillus licheniformis JF-2', *Applied Environmental Microbiology*, vol. 60, pp. 31–38.

Malcolm, JD & Elliott, CD, 1980, 'Interfacial tension from height and diameter of a single sessile drop or captive bubble', *The Canadian Journal of Chemical Engineering*, vol. 58, pp. 115–153.

Maudgalya, S, Mclnerney, MJ, Knapp RM, Nagle DP & Folmsbee, MJ, 2004, 'Development of bio-surfactant based microbial enhanced oil recovery procedure', *proceedings of the 2004 SPE/DOE Fourteenth Symposium on Improved Oil Recovery,* Tulsa, SPE 89473.

Maudgalya, S, Mclnerney, MJ, Knapp RM, Nagle DP & Folmsbee, MJ, 2005**,** 'Tertiary oil recovery with microbial bio-surfactant treatment of low-permeability Berea sandstone cores', *proceedings of the SPE conference*, Oklahoma, SPE 94213; DOI 10.2118/94213-MS.

Mclnerney, MJ, Knapp DP, Nagle KE, Duncan, N, Folmsbee, & Maudgalya, S 2003, 'Development of microorganisms with improved transport and biosurfactant activity for enhanced oil recovery' DE-FE-02NT15321, DOE

Mclnerney, MJ, Javaheri, M, & Nagle, KE, 1990, 'Properties of the biosurfactant produced by Bacillus licheniformis strain JF-2' *Journal of Industrial Microbiology,* vol. 5 no 2-3, pp 95–101.

McDiarmid, A, Alexander, I, Ion, A & Thompson, J, 2001, 'Experience of a reservoir water-flood failure and remediation treatment in Stag Reservoir, Australia', *proceedings of the SPE Asia Pacific Improved Oil Recovery*, Kuala Lumpur, SPE 72117; DOI 10.2118/72117-MS.

Morgan, JC, Schechter, RS, & Wade, WH, 1976, 'Recent advances in the study of low interfacial tensions', *proceedings of the 81st National Meeting of AIChE,* Kansas City, Mo.

Mulligan, CN, Yong, RN, & Gibbs, BF, 1999, 'Removal of heavy metals from contaminated soil and sediments using the bio-surfactant surfactin' *Journal of Soil Contamination*, vol. 8 no 2, pp 231–254.

Nelson, RC, 1983**,** 'The Effect of Live Crude on Phase Behaviour and Oil-Recovery Efficiency of Surfactant Flood Systems', *SPE Journal*, vol. 23 no 3, pp 501–10. DOI 10.2118/10677-PA.

Nelson, RC & Pope, GA, 1978, 'Phase relationships in chemical flooding', *SPE* Journal, vol. 18 no. 5, pp 325–338. DOI 10.2118/6773-PA.

Ottewill, RH, 1984 'Introduction', *in Surfactant*, ed. T.F. Tadros, Academic Press, San Francisco. pp. 1–18.

Peaceman, DW, 1977, *Fundamentals of numerical reservoir simulation*, Elsevier Scientific, New York.

Puig, JE, et al, 1979, 'On interfacial tensions measured with Alkyl Aryl surfonate surfactants', *SPE* Journal, pp 71–82.

Ron, EZ & Rosenberg, E, 2001, 'Natural roles of bio-surfactants', *Environmental Microbiology*, vol. 3, pp. 229–236.

Rosen, MJ, 1978, *Surfactants and interfacial phenomena*, John Wiley, New York.

Salager, JL, Bourrel, M, Schechter, RS, & Wade, WH, 1979, 'Mixing rule for optimum phase-behaviou formulaions of surfactant/oil/water system', *SPE Journal*, vol. 19, no 5**,** pp 271–278.

Salimi, H & Bruining, J, 2008, 'Improved prediction of oil recovery from waterflooding fractured reservoirs', *proceedings of the 2008 SPE Annual Technical Conference and Exhibition*, Denver, Colorado, USA, SPE 115361; DOI 10.2118/115361-PA.

Salter, SJ, 1977, 'The influence of type and amount of alcohol on surfactant-oil-brine phase behaavior and properties', *proceedings of the 52nd Annual Technical Conference and Exhibition of SPE*, Denver, Colorado, USA, SPE 6843.

Sarkar, AK, Goursaud JC, Sharma, MM, & Georgiou, G, 1989, 'A critical evaluation of MEOR processes' IN SITU, vol 13(4) pp. 207–237.

Schlumberger 2009, *ECLIPSE technical description manual*.

Schlumberger 2011, *ECLIPSE technical description manual.*

Shabani-Afrapoli, M, Crescente, C, Li, S, Alipour, S, & Torsaeter, O, 2012, 'Simulation study of displacement mechanisms in microbial improved oil

recovery experiment', *proceedings of the SPE EOR Conference at Oil and Gas West Asia*,Muscat, SPE 153323.

Sharma, MM & Georgiou, G, 1993, 'Microbial enhanced oil recovery research', final report, prepared for US Department of Energy, contract No. DE-FG07-89BC14445.

Shahri, HAMGA, 2012, *The impact of permeability heterogeneity on the effectiveness of alkaline surfactant polymer enhanced oil recovery* Ph.D thesis, The University of Western Australia.

Skange, A & Fotland, P, 1990**, '**Effect of pressure and temperature on phase behaviour of microemulsions', *SPE Reservoir Engineering*, vol. 5, pp 601–08.

Tiamiyu, OM, & Boukadi, F, 2011, 'Experimental and simulation study on use of surfactant and de-emulsifier blend additives in steam flood as EOR technique in heavy oil reservoir', *proceedings of the SPE Middle East Oil and Gas Show and Conference*,Manama, SPE 139582.

Temco 2005, *Pendent drop interfacial tension cell (model IFT -10) instruction manual*.

Todd, MR, & Chase, CA, 1979**,** 'A Numerical simulation for predicting chemical flood performance', *proceedings of the SPE Reservoir Simulation Symposium*, Denver, CO, SPE 7689.

von Rybinski, W, Guckenbiehl, B & Tesmann, H, 1998, 'Influence of co-surfactants on microemulsions with alkyl polyglycosides', *Colloids and Surfaces A: Physicochemical and Engineering Aspects*, vol 142**,** pp 333–342.

Wade, WH, Morgan, JC, Jacobson, JK, & Schechter, RS, 1976, 'Low interfacial tensions involving mixtures of surfactants', *SPE Journal*, SPE 6002-PA, vol. 17**,** pp 122–128.

Willhite, GP, Green, DW, Okoye, DM & Looney, MD, 1980**,** 'A study of oil displacement by microemulsion systems mechanisms and phase behavior', *SPE Journal*, vol. 20**,** pp 459–472.

Yakimov, MM, Amro, MM, Bock, M, Boseker, K, Fredrickson, HL, Kessel, DG, & Timmis, KN, 1997, 'The potential of Bacillus licheniformis strains for in situ enhanced oil recovery' *Journal of Petroleum Science and Engineering*, vol 18**,** pp 147–160.

Yu, SY, Akervoll, I, Torsaeter, O, Stensen, JA, Kleppe, J & Midtlyng, SH, 1998**,** 'History matching gas injection processes with in-situ saturation measurements and process hysteresis' *proceedings of the 1998 SPE International Conference* and Exhibition, Beijing, China, SPE 48842; DOI 10.2118/48842-MS.

Nomenclature

B_w	water formation volume factor
B_{wi}	water formation volume factor at initial reservoir pressure
B_o	oil formation volume factor
B_{oi}	oil formation volume factor at initial reservoir pressure
$CA(C_{surf})$	adsorption isotherm as a function of local surfactant concentration in solution
C_{surf}	surfactant concentration
C_{salt}	reference salt concentration in the PVTSALT keywords
D	cell center depth
dP	potential difference
E_{vw}	volumetric sweep efficiency of water flood preceding chemical flood
E	overall displacement efficiency
E_D	microscopic displacement efficiency expressed as fraction
E_V	macroscopic (volumetric) displacement efficiency expressed as fraction
H	hydrostatic head correction
G	acceleration due to gravity
k_{ro}	relative permeability of oil
k_{rw}	relative permeability of water
K	permeability
M	mobility ratio
N_{ca}	capillary number
N	original oil in place
N_p	oil recovered in process
P_{bh}	bottom hole pressure
P	potential
P_{ref}	reference pressure in the PVTW or PVTSALT keywords
PV_{cell}	pore volume of the cell
PV	pore volume
P_{cow} (S_w)	capillary pressure from the immiscible curves initially scaled to the interpolated end-points calculated in the relative permeability model
R_s	solution gas oil ratio

R_{si}	solution gas oil ratio at initial reservoir pressure
S_{wc}	connate or irreducible water saturation
S_o	oil saturation
S_{oi}	oil saturation at initial condition
S_{orw}	residual oil saturation at termination of water flood
S_{orc}	residual oil saturation at termination of chemical flood
S_w	water saturation
S_g	gas saturation
$ST(C_{surf})$	surface tension at the present surfactant concentration
$ST(C_{surf} = 0)$	surface tension at the zero concentration
V_w	flux of fluid
T	temperature
T_{av}	average temperature
T_{sc}	temperature at standard conditions
T_{ni}	transmissibility between cells n and I
T_{wi}	well connection transmissibility factor
V_f	total pore volume
V_w	connate water volume
W_e	cumulative water influx from the aquifer in to the reservoir
W_p	cumulative amount of aquifer water produced, stb
z	gas compressibility factor
z_{av}	average gas compressibility factor
z_i	gas compressibility factor at initial reservoir pressure
γ	specific gravity
ρ	density
ρ_{mas}	mass density of the rock in the SURFROCK keyword
ϕ	porosity
μ_o	oil viscosity
μ_w	water viscosity
μ_{ws}	viscosity of the water-surfactant mixture
σ_{ow}	interfacial tension of oil and water

Appendix A: Formulae for Core-flooding Experiment

A1. Core Pore volume PV (cc) = Final reading on pump (cc) – (Initial reading (cc) + Dead Vol. (cc) + Vol. Of brine collected (cc))

A2. Residual saturation,

$$S_{wr,}S_{or,wf}\,(\%) = \frac{V_W, V_O\,(cc)}{PV\,(cc)} \times 100 \tag{A-1}$$

S_{wr} (%) = Residual water saturation at the end of oil saturation

$S_{or,wf}$ (%) = Residual oil saturation after water flooding

V_w (cc) = Volume of brine remain inside core at the end of oil injection (cc)

V_O (cc) = Volume of oil inside core after water flooding

PV = Pore Volume of core (cc).

A3. Permeability,

$$K_{abs,}K_{W,Eff}\,(mD) = \frac{Q_{Brine} \times \mu_{Brine} \times L_{Core}}{A_{Core} \times \Delta P} \tag{A-2}$$

$$K_{O,Eff}\,(mD) = \frac{Q_{Oil} \times \mu_{Oil} \times L_{Core}}{A_{Core} \times \Delta P} \tag{A-3}$$

K_{abs} (mD) = Absolute permeability of core to brine at 100% saturation

$K_{w,Eff}$ (mD) = Effective permeability of core to brine at residual oil saturation

$K_{o,Eff}$ (mD) = Effective permeability of core to brine at residual oil saturation

Q_{Brine} (cc/hr) = Brine injection flow rate

Q_{oil} (cc/hr) = Oil injection flow rate

μ_{oil} (cP) = Oil viscosity

μ_{Brine}(cP) = Brine viscosity

ΔP (psi) = Pressure drop across the core

L_{core} (cm) = Length of core

A_{core} (cm^2) = Area of cross section of core.

A4. Tertiary Recovery (%)

$$Tertiary\ \text{Recovery}\,(\%) = \frac{V_O\,(cc)}{V_{O,WF}} \times 100 \tag{A-4}$$

$$K_{Surf}, K_{Post}\,(mD) = \frac{Q_{Surfactant,Brine} \times \mu_{Surfactant,Brine} \times L_{Core}}{A_{Core} \times \Delta P} \tag{A-5}$$

V_w (cc) = Volume of brine remaining inside core at the end of oil injection (cc)

V_O (cc) = Volume of oil inside core after water flooding

$Q_{Surfactant}$ (cc/hr) = Surfactant injection flow rate

$\mu_{Postflush}$(cP) = Surfactant viscosity.

Appendix B: Keyword Description

Details of each section and keyword description are discussed below.

B1. RUNSPEC Section

In this section memory is allocated for various components of the simulation sequentially within the main memory area. These components include wells, tabular data, the simulation grid and the solver stack. Another purpose of this section is to specify the basic character of the model and its start date, and to invoke simulation options.

The RUNSPEC section contains the run title, start date, units, various problem dimensions (numbers of blocks, wells, tables, etc.), flags for phases or components present and option switches. It consists of a series of keywords which turn on the various modelling options or contain data (for example problem dimensions). For keywords that have associated data, the data record must be terminated by a slash (/). In this model the following keywords are used:

Table B 1 **Keyword description of RUNSPEC section**

Keyword	Description
TITLE	Title of the simulation.
DIMENS	The basic size of the simulation grid. It is followed by three integers (10 x 1 x 1), specifying the number of cells in X, Y, and Z directions respectively.
OIL	Run contains an oil phase
WATER	Run contains water as an active phase, whose saturation can vary.
SURFACT	The surfactant model is active.
METRIC/LAB	Unit convention: Metric units or Lab units. The LAB convention is intended for use when simulating laboratory-scale experiments. It is based on the original Darcy units, except that the unit of time is an hour rather than a second.
TABDIMS	Table dimension data (2 1 20 20 1 20) contains the following items which describe the sizes of saturation and PVT tables used in the run, and also the number of fluid-in-place regions. The numbers of saturation (SWFN, SOF2 etc.) and PVT (PVTW, PVDO tables entered in the PROPS section are 2 and 1 respectively. The number of saturation nodes in a saturation table is 20. The number of pressure nodes in a PVT table is 20. The number of FIP regions defined using FIPNUM in the REGIONS section is 1. The number of Rs nodes in a oil PVT table is 20.
WELLDIMS	Well dimension data (2 1 1 2) consists of the following items. The maximum number of well in this model is two (2): injector and producer. The maximum number of grid blocks connected to a well is one (1). The maximum number of groups in the model is one. The number of wells

	in a particular local grid refinement is two.
START	Start date (time) of the simulation
NSTACK	This data (8) represents the size of the stack of previous search directions held by the ORTHOMIN linear solver. This may be increased if the linear solver shows a convergence problem.

B2. GRID Section

The main purpose of this section of the model is to provide the information necessary for the calculation of cell pore volume and transmissibility in all directions. This information will be used to calculate the flow of each phase from cell to cell and from time-step to time-step using this equation:

$$PV = V_{cell} \times \phi \times NTG$$

$$T_{(x,y,z)} = \frac{K_{(x,y,z)} \times A_{(x,y,z)} \times NTG}{L_{(x,y,z)}}$$

Model geometry (cell dimensions and depth) and properties are supplied in this section. Cell dimension, permeability and porosity values are given through the keywords DX, DY, and DY, PERMX, PERMY and PERMZ, and PORO. Reservoir tops and RPTGRID are taken into account in this section. Keywords and description are given in the table below.

Table B 2 **Keyword description of GRID section**

Keyword	Description
DX	X-direction grid block size
DY	Y-direction grid block size
DZ	Z-direction grid block size
PERMX	X-direction permeability
PERMY	Y-direction permeability

PERMZ	Z-direction permeability
PORO	Porosity
TOPS	Depth of the top face of each grid block
RPTGRID	Controls on output from GRID section

B3. PROS Section

This section contains the pressure- and saturation-dependent properties of reservoir fluid and rocks. Fluid information includes fluid PVT as a function of pressure, and density or gravity. Required rock properties are relative permeabilities as a function of saturation, capillary pressure as a function of saturation, and rock compressibility as a function of pressure.

Table B 3 **Keyword description of PROS section**

Keyword	Description
SWFN	Water saturation function
SOF2	Oil saturation functions (two phases)
PVTW	Water PVT functions
PVDO	PVT properties of dead oil (no dissolved gas)
ROCK	Rock compressibility.
DENSITY	Fluid density at surface condition
SURFVISC	Surfactant solution viscosity function
SURFADS	Surfactant adsorption functions
SURFST	Water/oil surface tension versus surfactant concentration
SURFCAPD	Surfactant capillary de-saturation functions
SURFROCK	Surfactant rock properties
RPTPROPS	Control on output from PROPS section

B4. REGIONS Section

This section is used to assign variable properties to the reservoir and/or to create useful reports. The REGIONS section divides the reservoir according to variations in reservoir characteristics and reporting purposes.

Table B 4 **Keyword description of REGIONS section**

Keyword	Description
SATNUM	Saturation function region numbers. This keyword should be followed by integer for every grid block in the current input box specifying the saturation function region to which it belongs.
SURFNUM	Surfactant miscible region numbers. This keyword specifies the saturation table numbers used by the model to calculate the relative permeabilities when a high surfactant concentration implies the oil and water are miscible.

B5. SOLUTION Section

This section contains sufficient data to define the initial state (pressure, saturation, compositions) of every grid block in the reservoir. The keywords may be specified in any order.

Table B 5 **Keyword description of SOLUTION section**

Keyword	Description
EQUIL	Equilibration data specification. The keyword sets the contacts and pressures for conventional hydrostatic equilibrium. It contains datum depth, pressure at the datum depth and water-oil contact depth.
RPTSOL	Controls on output from SOLUTION section.

B6. SUMMARY Section

This section specifies a number of variables that are to be written to summary files after each step of the simulation. The graphics post-processor may be used to display the variation of variables in the summary files with time and each other.

Table B 6 Keyword description of SUMMARY section

Keyword	Description
WBHP	Well bottom hole pressure
FWIR	Field water injection rate
FOPR	Field oil production rate
FOPT	Field oil production total
FTPRSUR	Production rate
FTPTSUR	Production total
FTIRSUR	Injection rate
FTITSUR	Injection total
FOE	Field oil recovery efficiency OIL(initial) – OIL(now)/OIP(initial)
FWVIS	Water viscosity average value
BOKR	Oil relative permeability
BVWAT	Water viscosity
BEWV_SUR	Effective water viscosity due to surfactant concentration
BTCASUR	Log (capillary num)
BTCNFSUR	Concentration
BOSAT	Block oil saturation
BWSAT	Block water saturation
BOKR	Block oil relative permeability
BWKR	Block water relative permeability
BWPC	Block water capillary num
WTPRSUR 'OP'	Well production rate
BTADSUR	Block adsorption
RUNSUR	

B7. SCHEDULE Section

This section specifies the operations to be simulated (production and injection control and constraints) and the times at which output reports are required.

Table B 7 **Keyword description of SCHEDULE section**

Keyword	Description
RPTRST	Controls on output to the RESTART
RPTCHED	Controls on output from SCHEDULE section
WELSPECS	General specification data for the well
COMPDAT	Well completion specification data
WCONPROD	Control data for production well
WCONINJE	Control data for injection well
TSTEP	Advances simulator to new report time
END	End

Appendix C: Equations for Eclipse

C1: Stone II Relative permeability model

Eclipse has the option to use either the Stone II three phase relative permeability models or the default model in the surfactant relative permeability model. In this study Stone II three phase relative permeability model was used. Stone II three phase relative permeability model is given below:

$$k_{ro} = (k_{ro})_{S_{wc}} \left[\left(\frac{k_{row}}{(k_{ro})_{S_{wc}}} + k_{rw} \right) \left(\frac{k_{rog}}{(k_{ro})_{S_{wc}}} + k_{rg} \right) - (k_{rw} + k_{rg}) \right] \qquad \text{(C-1)}$$

where

k_{ro} = relative permeability of oil

k_{rg} = relative permeability of gas

k_{rw} = relative permeability of water

$(k_{ro})_{Swc}$ = relative permeability of oil at S_{wc}

k_{row} = oil relative permeability as determined from the oil-water two-phase relative permeability at S_w

k_{rog} =oil relative permeability as determined from the gas-oil two-phase relative permeability at S_g

S_{wc} = connate water saturation

C2. Mathematical development of volumetric sweep efficiency

The technique for estimating volumetric sweep efficiency is applicable in those reservoirs in which the waterflood is initiated when reservoir pressure is above or below the initial bubble point pressure (Cob & Marek 1997). The method is applicable for five spot and regular or irregular pattern waterfloods. The assumptions of the technique are (1) the gas fillup has been achieved in all layers and (2) the oil

remaining within the reservoir is located in the water swept portion of the reservoir or the oil bank portion of the reservoir. Using these assumptions, the final form of the equation for computing volumetric sweep efficiency (E_{vw}) becomes

$$E_{vw} = \frac{\frac{N_p B_o}{V_p} + S_g}{\overline{S_w} - S_{wc}} \qquad \text{(C-2)}$$

where

N_p = oil production since start of waterflooing

S_g = free gas saturation

S_o = oil saturation

S_{wc} = connect water saturation at start of waterflood

V_p = floodable pore volume

$\overline{S_w}$ = average water saturation in the water swept portion of the pore volume

B_o = formation volume factor of oil

Volumetric sweep efficiency can be calculated using equation C-2 when oil production parameters are known. Average water saturation can be obtained from fractional flow analysis.